Biochemical and Pharmacological Studies on Dopamine D1 and D2L Receptors

By

Gordon Yiu Kon Ng

A thesis submitted in conformity with the requirements
for the Degree of Doctor of Philosophy,
Graduate Department of Pharmacology,
University of Toronto

ACKNOWLEDGEMENTS

I would like to extend my sincerest thanks to Dr. Susan R. George who imparted upon me the strength and conviction to succeed. I would also like to express my appreciation to Dr. Brian F. O'Dowd for his encouragement, Dr. Michel Bouvier and Dr. Bernard Mouillac for their guidance, and the many other individuals who led me to the paths of discovery during my thesis research. It should be mentioned that without the unwavering support of my wife, Sherry, and my parents, Kai and Mary, in times of triumph and hardship, this work would not be possible. The research training was supported by a Medical Research Council of Canada Studentship followed in its termination by an Ontario Ministry of Health Research Personnel Development Fellowship.

Biochemical and Pharmacological Studies on Dopamine D1 and D2L Receptors

Doctor of Philosophy, 1996

Gordon Yiu Kon Ng

Department of Pharmacology

University of Toronto

ABSTRACT

D1 and D2L receptors expressed in Sf9 cells were pharmacologically indistinguishable from native receptors, and were shown for the first time to be posttranslationally modified by phosphorylation and palmitoylation. Further, direct evidence now showed the existence of dopamine receptor dimers, in equilibrium with receptor monomers, formed by intermolecular noncovalent interactions involving TM regions. The exposure of D1/cells to dopamine for 15 min resulted in the desensitization of the D1 receptor stimulated adenylyl cyclase system, which was attributed to the increase in phosphorylation and palmitoylation level of the receptor and uncoupling of the receptor from G protein. Following 60 min of agonist exposure, surface D1 receptors, comprising predominantly receptor monomers, were internalized into an intracellular light vesicular membrane fraction. Pretreatment of D1/cells with concanavalin A or sucrose completely blocked agonist-induced D1 receptor internalization without preventing agonist-induced desensitization indicating that these processes were temporally and biochemically distinct mechanisms regulating D1 receptor function. In marked contrast, the D2L receptor coupled adenylyl cyclase system was resistant to agonist-induced desensitization, and dopamine exposure mediated a paradoxical increase in surface D2L receptor density, involving translocation of intracellular receptors and possibly receptor

dimerization. In cells coexpressing D1 and D2L receptors, no modulation of D1 binding in the presence of the D2L receptor, and no modulation of D2L binding in the presence of the D1 receptor, or D1 and D2L receptor heterodimerization was observed. However, in tissues containing both D1 and D2L receptors, selective activation of these receptors resulted in a synergistic adenylyl cyclase response. Under similar conditions, when dopamine was the activator, effector activity was the net effect of D1 receptor stimulation and D2L receptor inhibition. In summary, these findings showed for the first time that D1 and D2L receptors were posttranslationally modified, exist as dimers, and are subject to distinct patterns of regulation upon exposure to dopamine. These processes have not been demonstrated previously, and should prove to be of significant fundamental importance for understanding the function of D1 and D2L and possibly other G protein-coupled receptors.

ABBREVIATIONS

ATP	adenosine triphosphate
B_{max}	maximal binding capacity
cAMP	adenosine 3',5'-cyclic monophosphate
Con A	concanavalin A lectin
Da	Daltons
DNA	deoxyribonucleic acid
DTT	dithiothreitol
EDTA	ethylenediaminetetraacetic acid
G_i	inhibitory guanine nucleotide binding protein
Gpp(NH)p	5'-guanylylimidodiphosphate
GPCR	G protein-coupled receptor
G_s	stimulatory guanine nucleotide binding protein
GRK	G protein-coupled receptor kinase
GTP	guanosine triphosphate
[^{125}I]MAB	7-[^{125}I]iodo-8-hydroxy-3-methyl-1-(4'azidophenyl)-2,3,4,5-tetrahydro-1H-1-benzazepine
[^{125}I]NAPS	N-(p-azido-m-[125I]iodophenethyl)-spiperone
K_D	dissociation constant
K_i	inhibition constant
O.D.	optical density
PKA	cAMP dependent protein kinase

PKC	protein kinase C
R_f	Relative Migration
SDS-PAGE	sodium dodecyl sulfate-polyacrylamide gel electrophoresis
TM	transmembrane
vol	volume
[^{125}I]YM-09151-2	[^{125}I]4-azido-5-YM-09151-2

LIST OF FIGURES

Fig. 1. Rat brain sagittal section showing dopaminergic regions 5

Fig. 2. Schematic model of the proposed membrane topology of a G protein-coupled receptor 8

Fig. 3. Model of the proposed anticlockwise connectivity of TM I -VII of G protein-coupled receptors 9

Fig. 4. Proposed membrane topology, common and unique structural features of dopamine receptors 15

Fig. 5. A proposed scheme for G protein mediated signal transduction. 21

Fig. 6. A schematic diagram summarizing the multiple levels of receptor regulation following agonist activation 25

Fig. 7. A schematic diagram showing the expression of an epitope-tagged D1 receptor in the baculovirus/Sf9 cell system 29

Fig. 8. Pharmacology of expressed c-myc-D1 receptors 55

Fig. 9 Biophysiochemical characterization of the c-myc-D1 receptor. 59

Fig. 10. Agonist-promoted phosphorylation of the c-myc-D1 receptor 66

Fig. 11. Agonist-regulated palmitoylation of the c-myc-D1 receptor. 67

Fig. 12. The effects of 10 μM dopamine treatment on the number of c-myc-D1 receptors in the plasma membrane fraction 71

Fig. 13. Autoradiogram of [^{125}I]MAB photoaffinity labelled membrane preparations electrophoresed on SDS-PAGE 72

Fig. 14. Conventional fluorescence microscopy of agonist-mediated redistribution of cell surface

c-myc-D1 receptors 76

Fig. 15. Confocal microscopy of immunofluorescently labelled nonpermeabilized agonist-treated c-myc-D1/cells 77

Fig. 16. Confocal images of immunofluorescently labelled permeabilized agonist-treated c-myc-D1/cells. 78

Fig. 17. Confocal images of immunofluorescently labelled control Sf9 cells. 79

Fig. 18. Three-dimensional reconstruction of agonist-treated c-myc-D1/cells 82

Fig. 19. Immunoblot of P2 plasma membranes prepared from agonist-treated c-myc D1/cells. 85

Fig. 20. Biochemical separation of agonist-induced c-myc-D1 receptor internalization and desensitization 86

Fig. 21. Radioligand binding studies on membranes from D2L/cells. 89

Fig. 22. Effects of guanine nucleotide treatment on the SDS-PAGE mobility of D2L receptors 92

Fig. 23. Effects of deglycosylation treatments on the SDS-PAGE mobility of D2L receptors. 93

Fig. 24. Biophysical characterization of D2L receptors. 96

Fig. 25. Radioligand detection of D2L receptor monomers and dimers. 98

Fig. 26. Biochemical characterization of D2L receptors. 100

Fig. 27. Pharmacological properties of D2L receptors under basal conditions and following preincubation with dopamine. 102

Fig. 28. Agonist-induced cellular redistribution of D2L receptors as assessed by subcellular fractionation and radioligand binding. 104

Fig. 29. Identification of photolabelled c-myc-D1 and D2L receptor species in plasma membranes and in intracellular light membrane fractions. 105

Fig. 30. Agonist-induced D2L receptor redistribution as assessed by confocal microscopy, immunoblot analysis and radioligand binding. 110

Fig. 31. Clathrin-immunoreactive material in Sf9 cell lysate. 111

Fig. 32. Immunoblot analysis of c-myc-D1 and D2L receptors expressed in isolation and coexpressed in Sf9 cells. 116

Fig. 33. Immunoblot of immunoprecipitated D2L receptors coincubated in the absence or presence of immunoprecipitated c-myc-D1 receptors in detergent. 117

Fig. 34. D1 and D2L receptor coupled adenylyl cyclase activities in D1-D2L/cells 119

Fig. 35. Proposed model illustrating only the intracellular domains of the human 5-HT_{1B} receptor 176

Fig. 36. Saturation isotherms of [^{3}H]5-HT specific binding to membranes from cells expressing 5-HT_{1B} and m5-HT_{1B}. 180

Fig. 37. Effect of guanine nucleotide regulation on [^{3}H]5-HT binding 181

Fig. 38. Pertussis Toxin Assays. 183

Fig. 39. m5-HT_{1B} receptor mediated agonist inhibition of adenylyl cyclase activity. 187

Fig. 40. Biochemical Characterization of m5-HT_{1B} receptor 188

LIST OF TABLES

Table 1. Summary of the biochemical, pharmacological and structural properties of dopamine receptors 16

Table 2. Agonist and antagonist dissociation constants for c-myc-D1 receptors 56

Table 3. Summary of the effects of dopamine exposure on c-myc-D1 receptor and non-receptor stimulation of adenylyl cyclase activity 62

Table 4. Summary of the effects of dopamine exposure on c-myc-D1 receptor radioligand binding 63

Table 5. Dopamine dissociation constants for the human D2L receptor expressed in eukaryotic cell lines. 90

Table 6. Antagonist binding constants for D2L receptors under basal conditions and following preincubation with (-)sulpiride. 109

Table 7. Binding parameters for c-myc-D1 and D2L receptors expressed in isolation and coexpressed in Sf9 cells. 113

Table 8. Dissociation constants for [^{3}H]5-HT in cells expressing m5-HT$_{1B}$ 179

TABLE OF CONTENTS

ABSTRACT i

ACKNOWLEDGEMENTS ii

ABBREVIATIONS vi

LIST OF FIGURES vii

LIST OF TABLES x

1. INTRODUCTION 1

1.1 General Introduction 1

1.2 Brain Dopamine Neuron Pathways 3

1.3 Defining Structural And Biophysiochemical Features Of G Protein-coupled Receptors 6

1.4 Dopamine Receptor Classification 10

1.4.1 Biochemical Classification 10

1.4.2 Pharmacological Classification 10

1.4.2.1 Selective D1-like Receptor Ligands 11

1.4.2.2 Selective D2-like Receptor Ligands 12

1.4.3 Structural Classification 12

1.5 Brain Distribution 17

1.6 D1-D2 Receptor Linkage 17

1.7 G protein Classification, Structure and Function 18

1.8 Receptor-G Protein-Effector Interactions In Hormonal Signaling 19

1.9 Agonist-induced Receptor Desensitization, Phosphorylation And Palmitoylation 22

1.10 The Baculovirus/Sf9 Cell Model 27

2. RATIONALE 30

3. HYPOTHESIS 33

4. RESEARCH OBJECTIVES 34

5. METHODS 35

5.1 Materials 35

5.2 Construction Of Recombinant Receptor Baculoviruses 36

5.3 Cell Culture 37

5.4 Preparation of Cell Membrane Fractions 38

5.5 Protein Determination 39

5.6 Receptor Binding Assays 39

5.7 Adenylyl Cyclase Assay 40

5.8 Endoglycosidase Treatment 40

5.9 SDS-PAGE Electrophoresis 41

5.10 Photoaffinity Labelling 41

5.11 Immunoblot Analysis 42

5.12 Agonist-induced Desensitization Of Expressed Receptors 42

5.13 Treatment of Sf9 Cells with Pertussis Or Cholera Toxin 43

5.14 ADP-Ribosylation of Sf9 Membrane Components by Pertussis Toxin 43

5.15 Solubilization And Immunoprecipitation Of Receptors 43

5.16 Whole Cell Phosphorylation 44

5.17 Whole Cell Palmitoylation 44

5.18 Soluble Binding And Determination Of Specific Activity Of [^{3}H]palmitic Acid Or ^{32}P Labelled Receptors 45

5.19 Immunocytochemical Fluorescence Labelling of Receptors in Fixed Cells 46

5.20 Microscopy of Immunofluorescently Labelled Cells 46

5.21 Three-dimensional Reconstruction of Immunofluorescently Labelled Cells ... 47

5.22 Coincubated of Immunoprecipitated C-myc D1 Receptors and D2L Receptors in Detergent Solution 48

5.23 Biophysiochemical Characterization of Receptor Dimers 49

5.24 Statistics 50

6. RESULTS 51

6.1 Establishing and Validating the Baculovirus/Sf9 Cell Model System: Pharmacological and Biochemical Characterization of the Serotonin 5-HT$_{1B}$ Receptor 51

6.2 Pharmacological And Biochemical Characterization of D1 Receptors 52

6.2.1 Ligand Binding Profile of D1 Receptors 52

6.2.2 D1 Receptor Coupling to Endogenous Adenylyl Cyclase 53

6.2.3 Biochemical Characterization of the c-myc-D1 Receptor 57

6.2.4 Agonist-induced Desensitization Of c-myc-D1 Receptor Stimulated Adenylyl Cyclase Activity 60

6.2.5 Agonist-induced c-myc-D1 Receptor Uncoupling From G Protein and Reduction in Cell Surface Receptor Binding 61

6.2.6 Agonist-induced Phosphorylation of the c-myc-D1 Receptor 64

6.2.7 Agonist-induced Palmitoylation of the c-myc-D1 Receptor 64

6.2.8 Agonist-induced c-myc-D1 Receptor Redistribution As Assessed by Radioligand Binding on Plasma and Light Vesicular Membrane Fractions 68

6.2.9 Agonist-induced c-myc-D1 Receptor Internalization As Assessed By Photoaffinity Labelling 69

6.2.10 Agonist-induced Redistribution of Surface c-myc-D1 Receptors in Whole Cells As Assessed by Immunocytochemical Labelling and Conventional Fluorescence Microscopy 73

6.2.11 Agonist-induced c-myc-D1 Receptor Redistribution in Whole Cells As Assessed by Immunocytochemical Labelling and Confocal Fluorescence Microscopy 73

6.2.12 Three-dimensional Assessment of c-myc-D1 Receptor Distribution in Whole Cells 80

6.2.13 Agonist-induced c-myc-D1 Receptor Internalization As Assessed by

Immunoblot Analysis 83

6.2.14 Inhibition of Agonist-induced c-myc-D1 Receptor Internalization by Concanavalin A Does Not Prevent Desensitization 83

6.3 Pharmacological and Biochemical Characterization of the D2L Receptor 87

6.3.1 Ligand Binding Properties of Expressed D2L Receptors 87

6.3.2 D2L Receptor Coupling with Endogenous G Proteins 88

6.3.3 Identification of Multiple D2L Receptor Species 91

6.3.4 Biophysical Properties of Dopamine Receptor Dimers 94

6.3.5 Ligand Binding Properties of D2L Receptor Monomer and Dimer 97

6.3.6 Phosphorylation and Palmitoylation of the D2L Receptor 99

6.3.7 Pharmacological Characterization of D2L Receptors Under Basal Conditions and Following Varying Periods of Dopamine Exposure 101

6.3.8 Agonist-induced Cellular Redistribution of D2L Receptors As Assessed by Subcellular Fractionation and Radioligand Binding 103

6.3.9 Agonist-induced Redistribution of Cellular D1 and D2L Receptors As Assessed by Photoaffinity Labelling 106

6.3.10 Localization of D2L Receptors in Whole Cells by Immunocytochemical Fluorescent Staining 106

6.3.11 Agonist-induced Increase in Cell Surface D2L Receptor Monomer and Dimer 107

6.3.13 Antagonist-induced increase in cell surface D2L receptor density 108

6.3.14 Clathrin-like Immunoreactive Material and Dopamine Receptor Subtype

Sorting 108

6.4 Pharmacological Characterization of Coexpressed D1 and D2L Receptors .. 112

6.4.1 Binding Properties of D1 and D2L Receptors Are Not Altered in the Presence of the Receptor Subtype 112

6.4.2 Absence of D1-D2L Receptor Heterodimerization in Living Cells Coexpresssing the Receptor Subtypes 114

6.4.3 Absence of D1-D2L Receptor Heterodimerization in Detergent Solution 114

6.4.4 D1-D2L Receptor Linkage Downstream the Level of the Receptor 118

7. DISCUSSION 120

7.1 Biochemical and Pharmacological Properties of the D1 Receptor 121

7.1.1 Pharmacology of D1 Receptors 121

7.1.2 Biophysiochemical Properties of D1 receptors 122

7.1.3 Agonist-induced Desensitization of D1 receptors 122

7.1.4 Agonist-induced Redistribution of D1 Receptors 124

7.2 Biochemical and Pharmacological Properties of D2L Receptors 126

7.2.1 Pharmacological Characterization of D2L receptor Monomers and Dimers 126

7.2.2 Biophysiochemical Properties of D2L Dimers 127

7.2.3 Differential Regulation Of The D2L Receptor Coupled Adenylyl Cyclase System Following Agonist Exposure 131

7.2.4 Agonist-induced Redistribution of D2L Receptors 132

7.3 Mechanistic Basis Of Dopamine Receptor-subtype Specific Redistribution ... 133

7.4 Pharmacological Properties of Coexpressed D1 and D2L Receptors 135

8. SUMMARY AND COMMENTARY 137

9. REFERENCES 144

10. APPENDIX

Biochemical Characterization of the Serotonin 5-HT_{1B} Receptor in Sf9 Cells: Phosphorylation, Palmitoylation and Adenylyl Cyclase Inhibition 172

10.1 Summary 172

10.2 Introduction 174

10.3 Results 177

10.3.1 Pharmacological Characterization of Expressed 5-HT_{1B} Receptors ... 177

10.3.2 Pertussis toxin-mediated [^{32}P]ADP-ribosylation of membrane components from Sf9 cells 182

10.3.3 Pertussis toxin sensitivity of Sf9 cells and effect on [^{32}P]ADP-ribosylation 182

10.3.4 Effect of Pertussis Toxin on the Binding of [^{3}H]5-HT 184

10.3.5 m5-HT_{1B} Receptor Coupling to Endogenous Adenylyl Cyclase 184

10.3.6 Biochemical characterization of the m5-HT_{1B} receptor 185

10.4 Discussion 189

1. INTRODUCTION

1.1 General Introduction

Communication in the brain is centred on the electrochemical messages delivered within networks of neurons. The chemical component of the message is a neurotransmitter that binds to membrane spanning receptors to perpetuate the chain of signals. No role other than the propagation of the chemical message conveyed by the neurotransmitter is more important in receptor function. The neurotransmitter dopamine has wide but discrete localization in the mammalian brain (Fig. 1). Dopamine containing neurons comprise two major ascending mesencephalic projections with cell bodies located in the substantia nigra and ventral tegmental area of the mid brain (Lindvall and Borklund, 1983). Dopamine has been shown to play an important role in posture and motor control, and in generating emotions such as feelings of well-being, pleasure and euphoria. Thus, aberrations in dopamine neurotransmission have been implicated in neuropsychiatric diseases such as schizophrenia, Huntington's disease and Tourette's syndrome (reviewed by Seeman and Niznik, 1990). However to date, no clear link has yet emerged, although it is well known that drugs that target dopamine receptors alleviate symptoms of these disorders. Molecular cloning has identified the genes for 5 distinct dopamine receptors, categorized as D1-like, including D1 and D5 receptors, or D2-like, comprising D2, D3 and D4 receptors (reviewed by O'Dowd, 1993). All dopamine receptors belong to the family of G protein-coupled receptors (GPCRs) that have seven highly conserved membrane spanning regions which are linked by intracellular and extracellular loops (reviewed by Probst et al., 1992) (Fig. 2, 3). Dopamine receptors differ most in the homology and size of the hydrophilic intracellular domains. For instance, D1 and D5 receptors have a shorter third intracellular loop and a longer carboxyl tail compared to D2, D3, and

D4 receptors (Fig. 4). The third intracellular loop and carboxyl tail have been shown for other structurally related receptors to be involved with G protein interaction, and contain consensus sites for phosphorylation by regulatory kinases. Additionally, in the carboxyl tail of GPCRs are cysteine residues that are putative sites for palmitoylation which may play a role in the functional coupling of some receptors (reviewed by Bouvier et al., 1994). It was therefore of great interest to determine whether dopamine receptors were biochemically modified in this manner. Moreover, very little was known about the regulation of dopamine receptors following activation by agonist at the molecular level. For instance what happens from the time agonist binds the receptor, turning on the signal, to the time the signal is turned off. It has been shown that agonist activation of other GPCRs lead to a decrease in receptor responsiveness to subsequent agonist stimulation, an adaptive process collectively termed desensitization. Agonist-induced desensitization has been most extensively characterized for the β-adrenergic receptor, and shown to involve several distinct mechanisms: rapid functional uncoupling, involving the phosphorylation and palmitoylation of the receptor; rapid receptor sequestration or internalization; and longer-term receptor down-regulation (reviewed by Benovic et al., 1988, Perkins et al., 1990, and Dohlman et al., 1991). The challenge was to identify whether dopamine receptors are posttranslationally modified and regulated in a manner similar to β-adrenergic receptors believed to be a prototyical model for all GPCRs. To date, our current understanding about dopamine receptor mediated hormonal signalling at the molecular level derive from a few limited studies (reviewed by Sibley and Monsma, 1992). Studies in tissues are difficult given the presence of other related receptor subtypes, and the limited amount of receptors available for detailed analysis. More significantly, the difficulty in purifying these receptors and the lack of cell lines able to express biologically active receptors have hampered our understanding of the

structure and function of these important brain proteins. Such mechanistic studies are essential for understanding normal and aberrant functioning of dopamine receptors upon activation by their cognate hormone. Our goal was to experimentally determine the biology of the D1 receptor, which is prototypic of the D1-like receptors, and the D2L receptor, which is prototypic of the D2-like receptors, at the molecular level. For this purpose, we expressed recombinant D1 and D2L receptors in the baculovirus/Sf9 insect cell system. Others have shown that expression of other GPCRs in this foster cell line yields sufficient quantities of biologically and immunoreactive protein for detailed studies (George et al., 1989, Parker et al., 1991, Mouillac et al., 1992, Richardson and Hosey, 1992, Vasudevan et al., 1992, Oker-Blom et al., 1993, Mills et al., 1993, Mulheron et al., 1994). Our methods included a variety of molecular, biochemical and advanced imaging techniques never applied to the investigation of such receptors. To study the D1 receptor, the D1 receptor was c-myc epitope-tagged which allowed the identification and purification of the receptor by a monoclonal antibody raised against c-myc. In the case of the D2L receptor, a receptor-specific antibody directed against amino acid residues of the third intracellular loop would enable its immunological identification and purification. These original approaches have enabled us for the first time to purify D1 and D2L receptors for detailed biochemical and pharmacological analysis. In this thesis research, we provide first direct evidence to show that D1 and D2L receptors undergo distinct patterns of regulation, involving receptor dimers, following agonist exposure. These studies constitute a fundamental advance in our understanding of the biology of D1 and D2L receptors and possibly other GPCRs.

1.2 Brain Dopamine Neuron Pathways

Dopamine, a catcholamine neurotransmitter, exhibits a wide but distinct distribution in the

mammalian brain (Fig. 1). Based on anatomical measurements of dopamine content, two major ascending mesencephalic projections have been identified with neuron cell bodies located in the substantia nigra and ventral tegmental area (Lindvall and Bjorklund, 1983, Fuxe et al., 1978). The nigrostriatal pathway has projections terminating in the nucleus accumbens and caudate nucleus of the striatum, and is mainly involved in posture and motor control. For instance, striatal dopamine receptors are targets and mediators of antipsychotic drug-induced Parkinsonism and tardive dyskinesia (reviewed by Seeman and Niznik, 1990). The mesolimbic pathway is anatomically and functionally distinct from the nigrostriatal system. Mesolimbic neuronal projections terminate in such areas as the globus pallidus, olfactory tubercle, septum, amygdala, and cortex. The mesolimbic system has been implicated in generating feelings of well-being, pleasure, and euphoria associated with the rewarding properties of drugs of abuse since lesioning of these neurons or administration of drugs with antagonistic activity at dopamine receptors would reduced the self-adminstration of these drugs (Imperato and DiChiara, 1988). For these reasons, dopamine has been identified in some laboratories as the neural substrate of reward for drugs of abuse (Bozarth, 1986). Dopamine's diverse biological activities can be explained both by the wide distribution of dopamine and the multiplicity of dopamine receptors.

1.3 Defining Structural And Biophysiochemical Features Of G Protein-coupled Receptors

All dopamine receptors belong to the superfamily of cell surface receptors referred to as G protein-coupled receptors (GPCRs) (reviewed by Probst et al., 1992). Based on hydropathy analysis, all GPCRs are thought to share a similar topological motif consisting of seven hydrophobic α-helical domains that span the lipid bilayer connected by extracellular and intracellular loops (Fig. 2). The similar topology is probably indicative of a common mode of receptor self-assembly, ligand binding and ligand-induced signal transduction. The seven transmembrane (TM I-VII) helices of GPCRs are thought to be sequentially arranged in anticlockwise fashion, thus forming a very tightly packed TM core or pocket for ligand binding (reviewed by Baldwin, 1993). Mutagenesis studies have suggested that the proper folding of GPCR monomers involves intramolecular interactions between TM 1 and TM VII (Kobilka et al., 1988, Suryanarayana et al., 1992). The results of these studies suggested that TM regions contain not only the structural determinants for ligand binding, but also binding sites that mediate specific interactions between TM segments of receptor proteins essential for receptor self-assembly (Fig. 3). Comparison of the primary structure of GPCRs shows that the greatest similarity exist in the transmembrane domains, whereas greatest differences are found within the N- and C-terminal regions and the cytoplasmic third loop connecting transmembrane domains V and VI. For instance, D1 and D5 receptors have a shorter third intracellular loop and a longer carboxyl tail compared to D2, D3, and D4 receptors (Fig. 4). These structural distinctions are predicted to distinguish the G proteins and signalling pathways activated by the various receptors as well as differences in the regulation of these receptors.

The third intracellular loop and carboxyl tail of G protein-coupled receptors are believed to be most important in G protein interaction, and contain consensus serine and threonine residues for

phosphorylation by various intracellular kinases such as protein kinase A, receptor specific kinase and protein kinase C (Fig. 2). Protein phosphorylation by regulatory kinases is a common mechanism by which receptor activity is regulated in a cell such as following activation by agonist (Lefkowitz et al., 1990). Under basal conditions, receptor phosphorylation in the absence of agonist may determine receptor cycling (Orti et al., 1989) and/or the intrinsic or constitutive properties of receptors. Additionally, comparison of the primary sequence among GPCRs reveals one or two cysteine residues within the carboxyl tail believed to be putative site(s) for palmitoylation which occurs through the thioesterification of cysteine residues (Fig. 2) (reviewed by Bouvier et al., 1994). The sensitivity of the palmitate labeling of GPCR to neutral hydroxylamine treatment supports the attachment of the fatty acid through a thioester link. Because of the hydrophobic nature of the palmitate residues, it has been proposed that palmitoylation may anchor part of the carboxyl tail of GPCRs to the plasma membrane to form a fourth intracellular loop which may play a role in G protein coupling and regulating the access of phosphorylating kinases to the receptor. These ideas are supported by site-directed mutagenesis studies of the β_2-adrenergic receptor which showed that when Cys-341 was substituted with Gly-341 this resulted in a decreased ability of the receptor to couple to G_s and to stimulate adenylyl cyclase activity (O'Dowd et al., 1989). Subsequent studies showed that the functional uncoupling of this receptor was accompanied by an increase in the basal phosphorylation of the receptor indicating that dynamic receptor palmitoylation could play an important role in governing the activity of GPCRs (Moffet et al., 1993). Whether the same is true for other GPCRs that are palmitoylated remains to be shown. The challenge, however, has been to determine which features are shared among GPCRs because of conservation of function, and which divergent features represent structural adaptations to new functions.

Fig. 2. Schematic model of the proposed membrane topology of a G protein-coupled receptor. The extracellular amino (NH_2), and intracellular carboxy (COOH) termini, putative palmitoylation («) and phosphorylation (P) sites of the receptor, areas of interaction with G protein (Gα), glycosylation sites (Y), and the transmembrane spanning domains (numbered I-VII) are indicated.

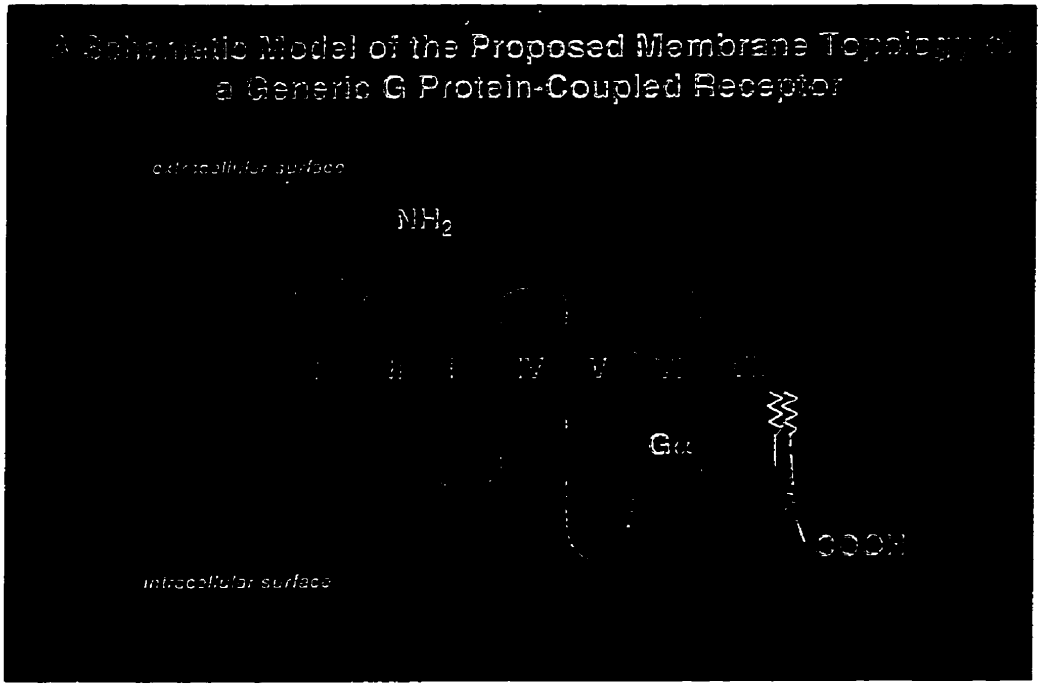
A Schematic Model of the Proposed Membrane Topology of a Generic G Protein-Coupled Receptor
extracellular surface
NH_2
G_{α}
COOH
intracellular surface

Fig. 3. Model of the proposed anticlockwise connectivity of TM I -VII of G protein-coupled receptors. The seven cylinders represent TM I-VII, whereas the solid circles mark extramembranous receptor sequences. TM I and VII are thought to interact and mediate the self-assembly of receptors, whereas the third cytoplasmic loop (i3) is thought to act as a linker sequence between two structural receptor subunits (one containing TM I-V and the other containing TM V-VII. The figure was adapted from Maggio et al., 1993.

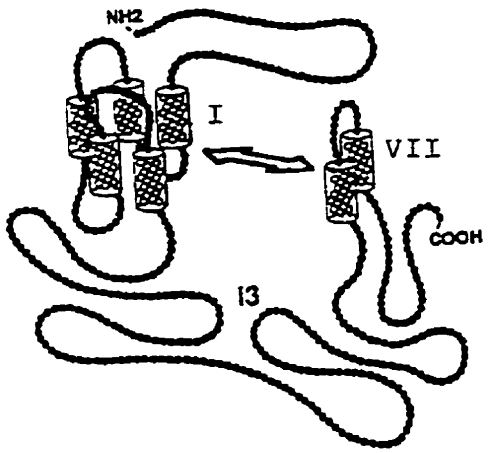
NH2
I
VII
COOH
13

1.4 Dopamine Receptor Classification

1.4.1 Biochemical Classification

In the late 1970's dopamine receptors were classified into D1 and D2 receptors to explain the electrophysiological, biochemical and pharmacological behavior of dopamine receptor agonist and antagonists (Spano and Trabucchi, 1978, Kebabian and Calne, 1979). Molecular cloning has since revealed a heterogeneity of dopamine receptors classified now as D1-like or D2-like. Classically, D1-like receptors, such as D1 receptor and subtype D5 receptor, couple to the stimulatory guanine nucleotide protein G_s to mediate dopamine stimulation of adenylyl cyclase (Kebabian and Calne, 1979, Sunahara et al., 1990, 1991). In contrast, D2-like receptors which include the D2 isoforms: designated D2Long (D2L) and D2Short (D2S), and subtypes D3 receptor and D4 receptor interact with the inhibitory guanine nucleotide protein $G_{i/o}$ to mediate dopamine inhibition of adenylyl cyclase activity (Clement-Cormier et al., 1974, Seeman, 1977, Bunzow et al., 1988, O'Malley et al., 1990, Todd et al., 1989, Dal Toso et al., 1989, Sokoloff et al., 1990, Van Tol et al., 1991, Tang et al., 1994). Recently, it has also been shown that D1 receptors are linked to the increase, and D2 receptors to the decrease in membrane-bound enzyme phospholipase C activities (Mahan et al., 1990, Liu et al., 1992, and reviewed by Casey and Gilman, 1988, Neer and Clapham, 1988). More complete understanding of the molecular events of how each receptor subtype mediates hormonal signalling will ultimately have a tremendous impact on our understanding of the biology of these receptors and on the development of receptor subtype-specific pharmaceuticals.

1.4.2 Pharmacological Classification

Radioligand binding assays provide an operational means of quantifying and measuring a receptor's affinity for ligands, and have been used traditionally for the identification of receptors

based on a pharmacological rank order of ligand binding affinities. Thus a receptor with the following rank order of catecholamine binding: dopamine> serotonin> noradrenalin> isoproterenol would be classified as a dopamine receptor. However ligands are not specific, and under many conditions ligands show nonselective pharmacology and bind many related receptor subtypes. As a result, previous radioligand binding studies failed to identify the heterogeneity in dopamine receptor subtypes in tissues until the recent application of molecular cloning techniques. This multiplicity of receptor subtypes and/or low abundance of some of these receptors make precise pharmacological analysis of a given receptor subtype impossible unless an extremely selective ligand is available. Further, whether a ligand behaves as antagonist or partial agonist or other seems a current concern as factors such as receptor density and the characteristics of the cell line in which the receptor is expressed can affect the determination of intrinsic activity (reviewed by Hoyer and Boddeke, 1993). Thus the pharmacological characterization of receptors in tissues could potentially be an uncertain exercise.

1.4.2.1 Selective D1-like Receptor Ligands

SKF-38393 represents the first selective D1-like receptor ligand to be characterized, binding to D1-like receptors as a partial agonist with a $K_i \leq 1$ nM (Setler et al., 1978). SCH-23390 has emerged as a D1-like selective antagonist shown to inhibit dopamine stimulated adenylyl cyclase activity in brain tissue (Iorio et al., 1983), and bind D1-like receptors with high affinity at pM concentration (Billard et al., 1984, Sunahara et al., 1991). It should also be noted that type 1 and 2 serotonin receptors (Hess et al., 1986) can also be detected with SCH-23390, but with low affinity and at high μM concentrations. Although ligands are lacking to discriminate receptor subtypes within the D1-like family, there are ligands better able to distinguish between D1-like and D2-like

receptor families.

1.4.2.2 Selective D2-like Receptor Ligands

Selective D2-like receptor agonist activity was demonstrated for the ergot derivative bromocriptine (Kebabian et al., 1978), whereas D2-like antagonist activity is characteristic of neuroleptic drugs (Seeman, 1987). (-)Sulpiride, a substituted benzamide, has been used as a selective D2-like receptor antagonist but its lower affinity for the receptor than spiperone has limited its wide application. Spiperone, a butyrophenone, has emerged as the ligand of choice for the D2-like receptors due to its high affinity and low non-specific binding to other catecholamine receptors (Leyson et al., 1978). However, a significant drawback to spiperone's universal application is that it shows similar affinities for D2, D3 and D4 receptors. Unfortunately, few selective ligands for D2-like receptor subtypes have been identified. The atypical neuroleptic clozapine has been identified as a relatively selective D4 receptor antagonist (Van Tol et al., 1991), and better affinity of 7-OHDPAT for D3 receptors (Sokoloff et al., 1990) has made this the ligand of choice for identifying these receptors. It is apparent that the successful design of selective ligands for dopamine receptors will need to evolve from a rational drug design program based on the new understanding of receptor structure and function at the molecular level.

1.4.3 Structural Classification

There seems to be evolutionary pressure to retain certain structural differences between D1-like and D2-like receptors (reviewed by O'Dowd, 1993). For instance, the genes for the D1-like, D1 and D5, receptors are intronless, that is they do not have intervening nucleotide sequences that interrupt the coding sequences (Sunahara et al., 1990, 1991). Pseudogenes related to the D5 receptor, termed ψD5-1 and ψD5-2, believed to encode truncated receptors are similarly intronless

(Nguyen et al., 1991). In contrast, genes encoding D2-like receptors such as the D2 receptor (Bunzow et al., 1988) and closely related D3 (Sokoloff et al., 1990) and D4 (Van Tol et al., 1991) receptors have their coding sequences separated by introns. The D2 gene encodes two isoforms of the D2 receptor, that arise through alternative splicing of the primary mRNA transcript, designated D2L and D2S that differ only by the insertion of a 29 amino acid sequence in the third intracellular loop (Dal Toso et al., 1989, Giros et al., 1989, Grandy et al., 1989, Monsma et al., 1989, Selbie et al., 1989, Chio et al., 1990, O'Dowd et al., 1990, O'Malley et al., 1990, Rao et al., 1990). Similarly, the D3 gene encode multiple receptor species generated by alternative splicing of receptor mRNA giving rise to D3Long (D3L) and D3Short (D3S) isoforms, and truncated receptors (Fishburn et al., 1993, Giros et al., 1991, Snyder et al., 1991, Nagai et al., 1993, Schmauss et al., 1993). Although mRNA splice variants have not been found for the D4 gene, multiple variants of the D4 receptor arise via gene polymorphism (Van Tol et al., 1992). Presently, receptor isoforms and variants of the D2-like family cannot be differentiated pharmacologically and the elucidation of their function(s) are the subject of much research.

Structural similarities between D1-like and D2-like receptors at the primary amino acid level are also strictly conserved throughout evolution. The amino acid sequences of these receptors show that all dopamine receptors have seven highly conserved membrane (TM) spanning regions characteristic of all GPCRs (Fig. 2). The high degree of conservation of this structural arrangement suggests that TM regions may play key roles in dopamine receptor folding and/or receptor function. The dopamine receptors however differ markedly in the homology and size of hydrophilic intracellular domains. D1 and D5 receptors have a shorter intracellular third loop and a longer carboxyl tail as compared to D2, D3 and D4 receptors (Fig. 3). These intracellular regions contain

putative serine and threonine residues for phosphorylation by regulating kinase(s) suggesting that structural differences in these regions may confer functional differences among dopamine receptors. For instance, it has been reported that D1-like receptors show higher affinity for dopamine than D2-like receptors, the basis of which is as yet unclear.

Fig. 4. Proposed membrane topology, common and unique structural features of dopamine receptors. The schematic shows the proposed membrane topology of a c-myc epitope-tagged D1 receptor (left panel) and the D2 receptor (right panel). The extracellular amino (NH_2), and intracellular carboxy (COOH) termini, putative palmitoylation («) and phosphorylation (P) sites of the receptor, areas of interaction with G protein (Gα), glycosylation sites (Y), and the transmembrane spanning domains (numbered I-VII) are indicated.

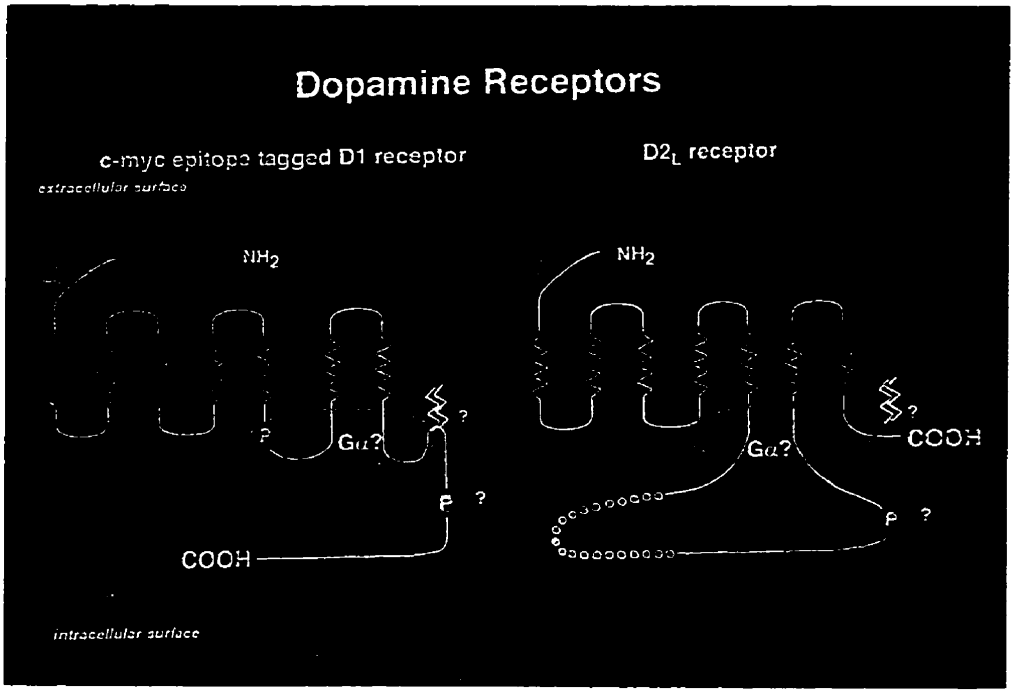
Dopamine Receptors
c-myc epitope tagged D1 receptor
extracellular surface
NH2
Gα?
?
?
?
COOH
intracellular surface
D2L receptor
NH2
Gα?
?
?
COOH

Table 1. Summary of the biochemical, pharmacological and structural properties of dopamine receptors. The second messenger response, selective receptor antagonists and agonists, percentage amino acid (aa) identity, the gene structure and chromosome localization of dopamine receptors are summarized.

Receptor Type	Receptor Subtype	Second Messenger	Antagonist /Agonist	% aa Identity	Gene Structure	Chromosome
D1-like	D1	↑cAMP, ↑IP_3, ↑Ca^{+2}	SCH-23390 /SKF-38393	100	intronless	5
	D5	↑cAMP	SCH-23390 /SKF-38393	55	intronless	4
D2-like	D2	↓cAMP, ↓IP_3, ↓Ca^{+2}, Na^+/H^+	eticlopride /quinpirole	100	intron	11
	D3	↓cAMP	clozapine /7-OHDPAT	50	intron	3
	D4	↓cAMP	clozapine /quinpirole	37	intron	11

1.5 Brain Distribution

Receptor radioligand binding analysis has shown that D1-like and D2-like receptors have distinct but overlapping distributions in the brain (Bouthenet et al., 1987, 1991, Mansour et al., 1990). Highest densities are found in the striatum (caudate-putamen, nucleus accumbens), olfactory tubercle, and substantia nigra with lower densities in the cortex, hippocampus and limbic brain regions. At the cellular level, D1-like and D2-like receptors have been identified on synaptic nerve terminals, and there is evidence that D1 and D2 receptors are colocalized in certain neuronal populations (Surmeier et al., 1992). The cloning of the genes for the D1 and D2 receptors and their subtypes has enabled the anatomical localization and mapping of receptor subtype mRNAs using specific oligonucleotides probes. Northern blot analysis and *in situ* hybridization histochemistry have shown that the distributions of D1 and D2 receptor mRNAs parallel the distribution patterns of D1-like and D2-like receptor proteins. Although little is known about D3, D4, and D5 receptor proteins, their mRNAs are present in highest levels in limbic regions suggesting a greater role for these receptors in the regulation of emotional states (Bouthenet et al., 1987, Wamsley et al., 1989, Mansour et al., 1990, Sokoloff et al., 1990, Sunahara et al., 1991). These mapping studies also indicate a pre-synaptic localization of D2-like receptors where they may function as autoreceptors regulating the synthesis and/or release of dopamine (Starke et al., 1989, Sokoloff et al., 1990). Thus the distributions of dopamine receptor mRNAs and receptor proteins reveal the different activities, organization and possibly functions of the brain dopamine receptor systems.

1.6 D1-D2 Receptor Linkage

The actions of indirect dopamine agonists such as apomorphine and amphetamine to induce hyperactivity and stereotyped behaviour that could be blocked by dopamine receptor antagonists

prompted the greater clarification of the functional roles of D1 and D2 receptors. Behavioural studies have consistently shown that D1 agonists behave as D2 and/or exerted a qualitative and quantitative cooperative control of D2-mediated motor activity (Star and Star, 1989). In humans, these two receptors can enhance each other's actions in functions including body motion (Gershanik et al., 1983) and neuron firing (Walters et al., 1987). Collectively, these and other data gave rise to concepts of behavioural cooperative/synergistic D1-D2 interactions. Biochemical and electrophysiological studies have also shown a functional balance and possibly synergistic interaction between D1 receptors and D2 receptors (Walters et al., 1987, Piomelli et al., 1991), and it has also been suggested that a D1-D2 link is reduced in brains of schizophrenics (Seeman et al., 1989). However to date, the mechanisms underlying the linkage between D1-D2 receptor systems remain a matter of speculation.

1.7 G protein Classification, Structure and Function

In the early 1980s, the role of guanine nucleotide-binding proteins (G proteins) as the transducing element in receptor signalling was identified (reviewed by Casey and Gilman, 1988). G proteins exist as heterotrimeric complexes of α and β γ dimer subunits, and are normally associated with the plasma membrane. To date, at least 21 G protein α subunits, 4 β subunits, and 6 γ subunits have been identified, and increasing evidence show that these proteins play a far greater role beyond just the activation of adenylyl cyclase (reviewed by Clapham and Neer, 1993). The best characterized G_α subunits are G_s, a polypeptide of ~45 kDa, which stimulates adenylyl cyclase activity and Ca^{+2} channels, and G_i, a polypeptide of ~41 kDa, which inhibits adenylyl cyclase activity, but also shown to activate phospholipase C and A2 and K^+ channels (reviewed by Casey and Gilman, 1988, Clapham and Neer, 1993). The discovery of bacterial cholera toxin and bacterial

islet activating protein or pertussis toxin were the most important findings in understanding post-receptor mechanisms. Both toxins are enzymes which can covalently modify the G_α proteins by the addition of an ADP-ribose group. Whereas cholera toxin results in the uncoupling of receptor-G_s protein interactions, pertussis toxin has been used to uncouple receptor-G_i/G_o protein interactions. The biochemical characterization of $G_{\beta\gamma}$ dimers is less well understood. Although $\beta\gamma$ subunits are also heterogeneous, this heterogeneity owes in large part to the stable combinations of similar β subunits with different γ subunits. The combinations may be functionally different. Recently, $G_{\beta\gamma}$ dimers have been shown to directly activate adenylyl cyclase, mediate receptor trafficking, and participate in G protein-coupled receptor kinase (GRK) phosphorylation of GPCRs (reviewed by Lefkowitz, 1993, Clapham and Neer, 1993, Milligan, 1993). Thus, G proteins seem to play a much bigger role in transducing receptor signalling than previously predicted.

1.8 Receptor-G Protein-Effector Interactions In Hormonal Signaling

Much of our current thinking about G protein-coupled receptor signalling is based on the idea of the ternary complex model involving freely mobile receptors, G proteins and effectors in which the specificity of their interaction derives from the three-dimensional structure at the protein-protein interface (De Lean et al., 1980). This concept arose in part from an effort to account for the heterogeneity of agonist binding to the β_2-adrenergic receptor. Agonist competition of radiolabelled antagonist binding are described as biphasic, "shallow" in appearance reflecting (1) a high-affinity state of the receptor, a guanine nucleotide- and sodium-sensitive receptor-G protein complex, and (2) a low-affinity state of the receptor, a guanine nucleotide- and sodium-insensitive receptor, free from G proteins. A population of receptors then comprise a mixture of uncoupled receptors and G protein-coupled receptors. According to the model, hormonal signalling is widely held to occur via

a transient complex between the receptor and G protein whereby guanine nucleotides act via G proteins to effect an interconversion from higher to lower affinity of the receptor-G protein complex for hormone. Upon hormone binding to the G protein-coupled receptor, the agonist-bound receptor, in high affinity state, is believed to undergo isomerization into an active conformation. This results in receptor activation of (stimulatory or inhibitory) heterotrimeric $G_{\alpha\beta\gamma}$ proteins (reviewed by Clapham and Neer, 1993) which invokes the exchange of GDP on G_α for GTP. Concomitantly, the receptor loses affinity for the ligand and reverts to the low-affinity state. Consequently, G_α -GTP and $G_{\beta\gamma}$ dissociate to transmit the receptor-generated signal. Separate G_α -GTP and $G_{\beta\gamma}$ subunits in turn independently activate an effector molecule such as adenylyl cyclase, a family of membrane-bound enzymes, resulting in the generation of the second messenger. These reactions are terminated when G_α-GTP is rapidly inactivated by GTPase converting the GTP to GDP. G_α -GDP now reassociates with free $G_{\beta\gamma}$ dimer and subsequently interacts with the unliganded receptor to start the cycle over again. Antagonists in contrast may exhibit the opposite preference of agonist or bind to either the coupled or uncoupled form of the receptor with equal affinity (Costa et al., 1992, Chidiac et al., 1994). A schematic representation of receptor/G protein/adenylyl cyclase interactions is summarized in Fig. 5.

Fig. 5. A proposed scheme for G protein mediated signal transduction. Schematic diagram showing the cycle of receptor/G protein/effector action upon hormone binding. (a) Receptor and G-protein complex and effector. (b) Binding of agonist (A) to receptor and association of receptor and G-proteins. (c) Dissociation of receptor and G-proteins and activation of effector pathway. Figure was adpated from Neer and Clapham, 1988.

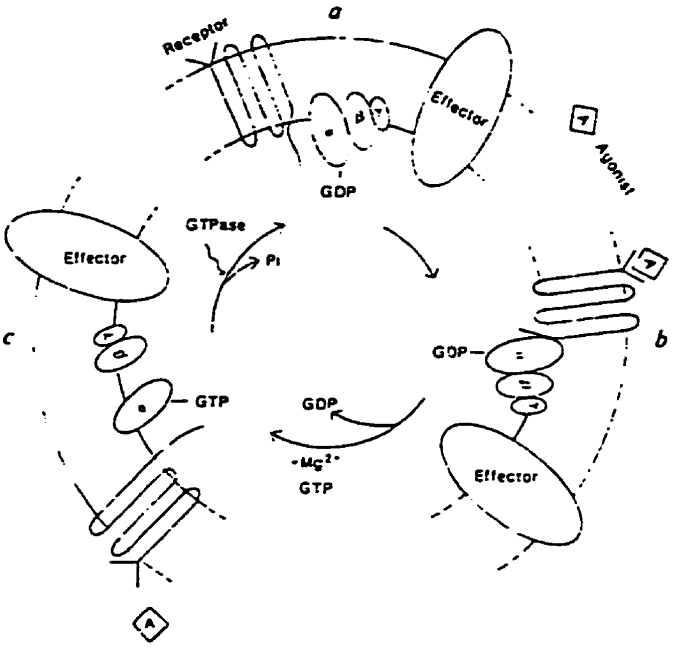
a
Receptor
Effector
Agonist
GDP
GTPase
Pi
Effector
c
GTP
GDP
$-Mg^{2+}$
GTP
GDP
b
Effector
A

1.9 Agonist-induced Receptor Desensitization, Phosphorylation And Palmitoylation

A common property of receptor mediated hormonal signalling is the ability to undergo negative regulation to prevent sensory overload of the signal-response system. This adaptation is collectively referred to as desensitization which may be termed homologous, leading to the reduced responsiveness to the original stimulus, or heterologous leading to a decrease in responsiveness as a result of the stimulus acting through other systems. To date, very little is known about the molecular mechanisms from the time agonist binds to dopamine receptors, turning on the signal, to the time the signal is turned off. Agonist-induced desensitization has been most extensively characterized for the structurally related β_2-adrenergic receptor expressed in various heterologous cell lines (Fig. 6) (reviewed by Benovic et al., 1988, Perkins et al., 1990, Dohlman et al., 1991).

A model of the homologous desensitization of the β_2-adrenergic receptor proposes that high concentrations of agonist are required to activate receptors invoking phosphorylation of the intracellular third loop of the receptor by cAMP-dependent protein kinase (PKA) and phosphorylation of the receptor C-terminal by substrate-dependent G protein-coupled receptor kinase (GRK). It has been proposed that phosphorylation changes the net charge of the receptor thus disrupting receptor-G protein coupling. Further studies have shown that agonist-induced desensitization is accompanied by increased turnover rate of the palmitoylation of the receptor (reviewed by Bouvier et al., 1994). Palmitoylation of the β_2-adrenergic receptor is believed to participate in G_s coupling and stimulation of adenylyl cyclase activity. Mutant β -adrenergic receptors, lacking Cys-341 for palmitoylation, are thought unable to attach the receptor C-terminal to the plasma membrane. Consequently, these receptors exhibit increased constitutive phosphorylation which could be responsible for the functional uncoupling of the receptors. It has

been proposed then that palmitoylation of the receptor, and generation of a fourth intracellular loop, govern the accessibility of regulatory kinases such as GRK to C-terminal receptor phosphorylation sites contributing to the development of agonist-induced desensitization.

In the heterologous desensitization of the β_2-adrenergic receptor, it has been proposed that this process involves phosphorylation of the receptor by PKA as a consequence of elevated intracellular cAMP. This type of desensitization occurs following exposure of cells to agonist at nM levels that result in fractional occupany of the receptor pool, but maximal stimulation of cAMP and PKA. The end result is similar with the functional uncoupling of the receptor. The precise role of palmitoylation in this process remains unknown.

Two other distinct processes occur concomitantly with agonist-induced desensitization that serve to regulate cell surface β_2-adrenergic receptor density following agonist exposure: rapid receptor sequestration or internalization, and longer term receptor down-regulation. Agonist-induced rapid sequestration occurs biochemically separate from desensitization, and not requiring receptor phosphorylation. It is believed that sequestration may be responsible for delivering desensitized receptors to intracellular vesicles where agonist and phosphate groups from desensitized receptors are removed, and reactivated receptors are recycled back to the cell surface. This process has been termed resensitization. Longer-term agonist exposure, involving PKA mediated receptor phosphorylation, results in receptor down-regulation which is defined as a net loss of total receptors in the cell presumably due to negative feedback resulting in altered stability and reduced levels of receptor synthesis. Although the β_2-adrenergic receptor system has been a valuable model upon which theories of cell signalling have been proposed, these mechanisms may not be universal for all GPCRs. Given the well-known roles dopamine

receptors may have in the brain in the generation of mood, emotion, reward, motor control, and endocrine functions, it was of interest to determine the molecular events underlying the regulation of dopamine receptor-linked signalling.

Fig. 6. A schematic diagram summarizing the multiple levels of receptor regulation following agonist activation. The biochemical processes involved in the agonist-induced functional uncoupling (desensitization) of the receptor coupled G protein/ effector system may include phosphorylation (P) and palmitoylation (<) of the receptor. Sequestration (internalization), down-regulation (receptor degradation) and receptor recycling have also been shown to regulate receptor activity.

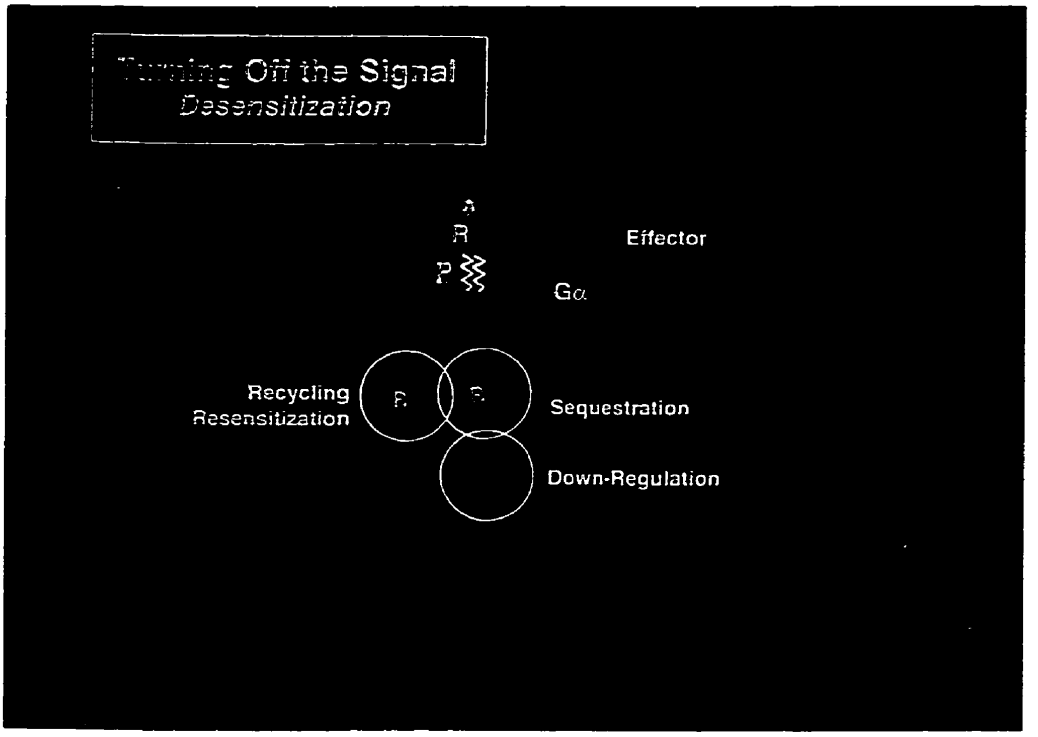
Turning Off the Signal
Desensitization
R
P
Effector
Gα
Recycling
Resensitization
Sequestration
Down-Regulation

1.9 Receptor Dimers

A prevailing view of GPCR signalling in cells includes freely mobile receptors and random collisions with G proteins with great specificity at the sites of protein-protein interaction (De Lean et al., 1980). A better understanding of signalling via single transmembrane spanning receptors such as the tyrosine kinase receptors and growth factor receptors raises the possibility of a specific organization of GPCRs into multimers.

A critical mechanism needed for signal transduction to occur for tyrosine kinase receptors is the dimerization of receptor monomers (reviewed by Schlessinger et al., 1986). Dimerization has been suggested to generate the close contact needed for high affinity ligand binding. It has been shown that dimers of epidermal growth factor receptor isolated from cell lysates exhibited higher affinity for ligand than monomers (Boni-Schnetzler and Pilch, 1987), and chemical cross-linking has shown epidermal growth factor induced dimerization of epidermal growth factor receptors (Fanger et al., 1986). Another example is the interleukin 2 receptor that exists as a heterocomplex of at least two peptides of 75 and 55 kDa (Tsudo et al., 1986). The heterocomplex is the only form of the receptor that is able to bind interleukin 2 with high affinity and transduce a mitogenic signal (Robb et al., 1987). Receptor self-aggregation is thought to be criticial for the major histocompatibility antigens and the CD4 antigen (Kaufman et al., 1984, Maddon et al., 1985), receptors for fibronectin and vitronectin (Argraves et al., 1986, Pytela et al., 1985), platelet glycoprotein IIb/IIIa (Charo et al., 1986), the low density lipoprotein and poly (Ig) receptors (Yamamoto et al., 1984, Mostov et al., 1984), and transferrin and insulin receptors (McClelland et al., 1984, Ebina et al., 1985). Recent evidence suggests that GPCR signalling systems may be more highly organized than previously anticipated.

Radioligand binding and radiation inactivation studies have suggested that GPCRs exist as higher molecular weight forms (Venter and Fraser, 1983, Wregget and Wells, 1995). Receptor dimers for muscarinic M1 and M2 receptors (Parker et al., 1991), the human serotonin 5-HT_{1B} receptor (Ng et al., 1993), and the metabotropic glutamate receptor (Pickering et al., 1993) have been suggested, and support the radioligand binding studies described for the histamine receptor (Sinkins and Wells, 1993, Sinkins et al., 1993). A possible mechanism of GPCR signal transduction, for which there is increasing circumstantial evidence, might involve dimerization. The demonstration of GPCR dimers should prove to be a fundamental advance in our current understanding of the biology of these important receptors that represent greater than 80% of all known receptors (reviewed by Probst et al., 1992).

1.10 The Baculovirus/Sf9 Cell Model

The recombinant *Autographa californica* nuclear polyhedrosis virus (AcNPV) baculovirus/ *Spodoptera frugiperda* (Sf9) insect cell model is an eukaryotic expression system that performs all common mammalian protein posttranslational modifications (reviewed by Luckow and Summers, 1988). For instance, Sf9 cells are able to produce truncated high-mannose type glycomoieties and sustain thiopalmitoylation which may be required for the correct folding and targeting of proteins such as GPCRs to the plasma membrane. AcNPV baculoviruses are host-specific insect viruses commonly used with Sf9 cells which originate from the oviduct of *Spodoptera frugiperda*, the fall army worm. Sf9 cells can be grown as monolayer or suspension culture at 27° C in normal atmosphere, and not requiring extensive culture conditions and facilities. The strong promoter of the abundantly expressed matrix protein (polyhedrin) is generally used for the expression of foreign DNA, and the host-specificity of the recombinant baculovirus makes this an attractive model for the

investigation of foreign genes (Fig. 7). Recombinant virus is obtained by homologous recombination after cotransfection of host cells with viral DNA and a transfer vector, which contains the powerful polyhedrin promoter and the foreign cDNA insert. The high efficiency of virus infection, insuring high expression of foreign genes, has also helped make the baculovirus/Sf9 expression system popular. Most importantly, this model has been proven highly suitable to generate a number of recombinant eukaryotic (glyco)proteins such as GPCRs for detailed functional studies.

Fig. 7. A schematic diagram showing the expression of an epitope-tagged D1 receptor in the baculovirus/Sf9 cell system. The human D1 receptor cDNA is linked to a c-myc nucleotide sequence and inserted into the baculovirus transfer vector, and through the process of homologous recombination with wild-type baculovirus DNA, results in a recombinant baculovirus DNA encoding an epitope-tagged D1 receptor.

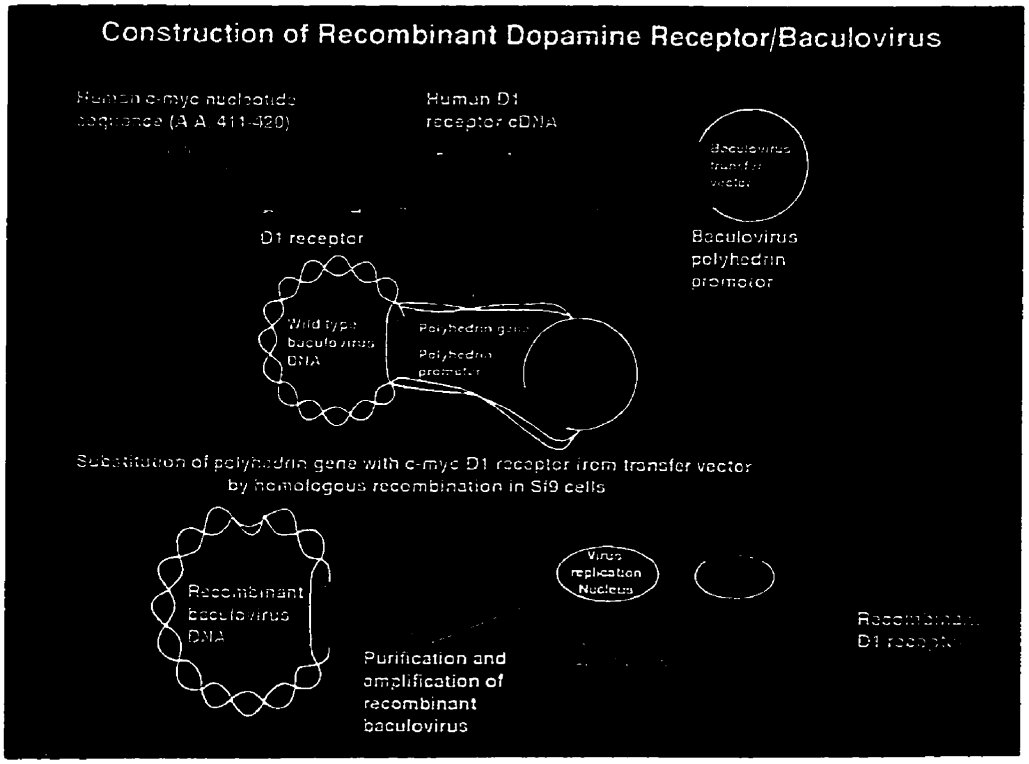
Construction of Recombinant Dopamine Receptor/Baculovirus
Human c-myc nucleotide sequence (A A 411-420)
Human D1 receptor cDNA
Baculovirus transfer vector
D1 receptor
Baculovirus polyhedrin promotor
Wild type baculovirus DNA
Polyhedrin gene
Polyhedrin promotor
Substitution of polyhedrin gene with c-myc D1 receptor from transfer vector by homologous recombination in Si9 cells
Recombinant baculovirus DNA
Virus replication Nucleus
Purification and amplification of recombinant baculovirus

2. RATIONALE

Aberrations in dopaminergic function have been implicated in a number of neuropsychiatric, mood and endocrine diseases. Disorders of movement, and alcohol and drug abuse have also been associated with this important neurotransmitter system. Despite numerous genetic and biochemical studies associating dopamine receptors with these illnesses, no clear link has yet emerged. The challenge now is to identify the physiological processes of dopamine receptors at the mechanistic and fundamental level, which will be extremely valuable for understanding and developing hypotheses concerning receptor-ligand and receptor-effector interactions as they may relate in normal and pathological states. Additionally, this greater understanding of the molecular biology of dopamine receptors holds the promise of the creation of new receptor-subtype specific drugs with greater efficacy and lower incidence of unwanted side-effects. We therefore perceive a great need and potential for the understanding, diagnosis and treatment of CNS-dopaminergic disorders.

Molecular cloning has revealed a heterogeneity of dopamine receptors, and although the similarity of their sequences has made the cloning of related genes/cDNAs easier, it has made the separation of receptors and correlation of receptor and function an uncertain exercise in tissues. Heterologous expression systems have been shown to be of significant usefulness for the study of cloned GPCRs. To better understand the biology of different dopamine receptor subtypes, cloned receptors have been expressed in various foster cell lines for detailed functional studies. However, yet another obstacle has been an inability to purify these receptors. Additionally, not all cell lines are capable of expressing dopamine receptors in sufficient levels and with appropriate coupling to down-stream effector systems. In vitro expression of membrane glycoproteins in general, and hence of functional protein, is not easily realized in many heterologous systems probably due to the need

for posttranslational modifications which govern the correct membrane insertion and correct folding of receptors including the formation of disulfide bonds. The recombinant *Autographa californica* nuclear polyhedrosis virus (AcNPV) baculovirus/ *Spodoptera frugiperda* Sf9 insect cell model has all these desired qualities, and has been chosen by some investigators for the study of a wide spectrum of proteins. Taking advantage of the remarkable similarity in processing pathways used by the Sf9 insect cells and by mammalian cells, others have shown that a number of G protein-coupled receptors such as β_2-adrenergic (Mouillac et al., 1992), muscarinic (Parker et al., 1991, Richardson and Hosey, 1992, Vasudevan et al., 1992), α_2-C4 adrenergic (Oker-Blom et al., 1993) and serotonin 5-HT_{1A} (Mulheron et al., 1994) receptors expressed in Sf9 cells were biologically and immunologically active, and functionally coupled to endogenous G proteins. Further, Sf9 cells are able to sustain thiopalmitoylation (Kloc et al., 1991), and expressed β_2-adrenergic (Mouillac et al., 1992) and muscarinic (Richardson and Hosey, 1992) receptors were shown to undergo desensitization and posttranslational modifications. The establishment of the Sf9 model system for the expression of dopamine receptors should prove tremendously useful towards the elucidation of the molecular biology of these important brain proteins.

For the purposes of establishing and validating the suitability of the baculovirus/Sf9 model, we expressed the structurally related serotonin 5-HT_{1B} receptor for pharmacological and biophysiochemical analysis. Like dopamine receptors, it too is a complex glycoprotein that requires membrane translocation and possibly several posttranslational modifications (palmitoylation, phosphorylation, disulfide bridge formation) in order to fulfill all its structural and functional properties. Thus, the successful expression and characterization of this receptor should not only permit us to establish and validate the suitability of the model system, but will increase our poor

understanding of the important family of serotonin receptors. An additional aim was to show that expressed receptors in Sf9 cells were immunoreactive, since the strategy chosen to study D1 receptor biology was to express a recombinant c-myc epitope-tagged D1 receptor so that specific antibodies directed against the c-myc epitope in the amino terminal domain of the receptor would enable its identification by immunoblotting and purification by immunoprecipitation. Lastly, it was critical to establish that the monoclonal antibody show high signal to low noise background in the Sf9 cells. Thus, the strategy chosen was to express and pharmacologically and biophysiochemically characterize a c-myc epitope-tagged 5-HT_{1B} receptor prior to conducting more extensive studies on the biology of dopamine receptors.

In summary, the ability to express receptors in isolation and in the absence of related receptor subtypes may enable the identification of receptor subtype-specific biochemical and functional processes nearly impossible to identify in tissues. The levels of protein expression in the Sf9 cells add only to the confidence of the experimental results, and the evidence is convincing that processes observed in Sf9 cells may occur in cells endogenously expressing dopamine receptors. Thus, we chose this model system for the study of dopamine D1 receptors, prototypic of D1-like receptors, and D2L receptors, prototypic of D2-like receptors.

3. HYPOTHESIS

I. Posttranslational modifications of proteins are common mechanisms by which GPCR activity is modulated. D1 and D2L receptors are candidate targets of phosphorylation and palmitoylation.

II. It is commonly believed that GPCRs exist in monovalent form to mediate biological activities. The involvement of receptor dimers and receptor cross-talk in these processes have been suggested, but direct evidence has been lacking to support these claims. D1 and D2L receptors exist as dimers and participate in receptor cross-talk.

III. Receptor-G protein coupled systems show waning of receptor responsiveness following sustained stimulation by agonist. D1 and D2L receptor coupled adenylyl cyclase systems are subject to agonist-induced patterns of regulation.

4. RESEARCH OBJECTIVES

The overall goal was to elucidate the pharmacological and biochemical properties distinguishing dopamine D1 and D2L receptor transmembrane signalling at the molecular level. These investigations should further our understanding of normal physiological processes, and may have considerable clinical importance for the understanding and treatment of dopamine-based CNS diseases.

Specific goals were:

1. Establish and validate a model system for the study of G protein-coupled receptors.
2. Expression, biophysicochemical and pharmacological characterization of D1 and D2L receptors.
3. To delineate the mechanisms of regulation for D1 receptor-stimulated adenylyl cyclase and D2L receptor-inhibited adenylyl cyclase systems.

5. METHODS

5.1 Materials

Cell culture materials such as Grace's supplemented medium, fetal bovine serum, gentamycin sulfate, and fungizone were purchased from Gibco (Toronto, Ont). Radiolabelled compounds such as [^{3}H]SCH-23390, [^{125}I]SCH-23982, [^{125}I][3methyl-2-(4'-azidophenyl)-2,3,,5-tetrahydro-2H-3-benzazepine] ([^{125}I]IMAB), [^{3}H]spiperone, [^{3}H]YM-09151-2, Carrier-free ^{32}P, [^{3}H]palmitic acid, [^{3}H]cAMP, [α^{32}P]ATP, [^{3}H-9,10]-palmitic acid, [^{125}I]N-p-azidophenethylspiperone ([^{125}I]NAPS) and [^{125}I]4-azido-5-YM-09151-2 ([^{125}I]YM-09151-2) were obtained from Du Pont-New England Nuclear (Boston, MA). Receptor ligands were purchased from Research Biochemicals Inc. (Natick, MA) unless indicated. Glycopeptidase F (PNGase F) was from Boehringer Mannheim. All other laboratory chemicals such as Gpp(NH)p, ATP, GTP, cAMP, phosphoenol pyruvate, myokinase, anti-mouse and anti-rabbit IgG agarose, leupeptin, benzamidine, and soybean trypsin inhibitor were from Sigma Chemical Co (St. Louis, MO). Immunologicals such as anti-mouse IgG FITC (fluorescein-5-isothiocyanate) conjugate, anti-mouse IgG alkaline phosphatase conjugate and anti-rabbit IgG alkaline phosphatase conjugate were purchased from BioRad (Toronto, Ont). Digitonin was purchased from Gallard-Schlessinger (Carle Place, NY, USA). The mouse monoclonal antibody anti-c-myc (9E10), and the AL-26 polyclonal D2 antibody were gifts from Dr. J. Park, Massachusetts General Hospital, USA and Dr. M.R. Brann, Departments of Pharmacology and Psychiatry, University of Vermont, Vermont, USA respectively. Partially purified G_i/G_o was supplied by Jean Labreque (BioSignal, Montreal, QC). Recombinant receptor baculoviruses were prepared by Dr. M. Dennis and M. Caron (BioSignal, Montreal, QC). All other chemicals and materials for gel electrophoresis were of analytical grade and purchased from commercial sources.

The human D2L receptor as from Dr. O. Civelli (Portland, OR, USA). *Spodoptera frugiperda* (Sf9 cells) were from ATCC (Rockville, MD, USA).

5.2 Construction Of Recombinant Receptor Baculoviruses

The plasmid vector Sp65 containing the human dopamine D1 receptor on an *EcoR*I genomic fragment was digested with *EcoRI/Nco*l. This digestion removed a fragment comprising 5'-non-coding sequences plus a portion of the N-terminal coding segment up to the unique *Nco*l site. The resulting *NcoI/EcoR*I fragment was isolated by agarose gel electrophoresis. To reconstitute the complete D1 receptor coding sequence, two complementary oligonucleotides were synthesized which encoded the missing N-terminal sequence, plus an *Xba*l site 5 nucleotides upstream of the initiator ATG, with *EcoR*I and *Nco*l sites at the 5' and 3' extremities, respectively. The two oligonucleotides were annealed and subcloned into the *EcoRI/Nco*l site of the D1 receptor-Sp65. The resulting plasmid was digested with *XbaI/EcoR*I and the fragment containing the reconstituted D1 receptor coding sequence was isolated and 5'-protruding ends filled in with Klenow DNA polymerase. This fragment was then subcloned by blunt-end ligation into the filled-in *Nhe*l site of pJVETLZ, a modified baculovirus transfer vector (Vialard et al., 1990) containing the gene for beta-galactosidase. The c-myc-D1 receptor fusion was constructed in a similar manner. Two complementary oligonucleotides were synthesized which encoded the N-terminal sequence of D_1 receptor up to the *Nco*l site, fused at the N-terminus to an 11 amino acid sequence corresponding to residues 411-421 (Glu-Gln-Lys-Leu-Ile-Ser-Glu-Glu-Asp-Leu-Asn) of human c-myc protein (Evan et al., 1985) and an initiator ATG codon. The oligonucleotides, flanked by EcoRI and *Nco*l sites were annealed and cloned into the EcoRI/Ncol site of D1-Sp65. The fragment containing the c-myc-D_1 receptor fusion was recovered by digestion with *EcoR*I, filled-in with Klenow DNA

polymerase and subcloned into the *Nhe*I site of pJVETLZ by blunt-end ligation. Similar procedures were employed to construct the recombinant baculovirus encoding theD2L receptor.

A cDNA clone encoding the long form of the human D2 receptor (D2L) was extracted from the pZem 3 vector with *Dra*III and *Kpn*I. The resulting fragment was blunt ended and isolated by electrophoresis on soft agarose. The transfer vector pJVETLZ New was digested with *Nhe*I and blunt ended. The cDNA fragment coding for the D2L receptor was inserted into this vector by blunt-end ligation and the orientation verified by sequencing.

Transfer of recombinant baculovirus encoding the D1 receptor, c-myc-D1 receptor, or D2L receptor into the AcNPV genome was achieved by co-transfection of plasmid and wild-type viral DNA in Sf9 cells using the calcium phosphate precipitation procedure. Purification of recombinant D1 and D2L viruses was carried out as described (Vialard et al., 1990), and stocks of the purified recombinant viruses were amplified in Sf9 cells.

5.3 Cell Culture

Sf9 cells were grown in monolayer or suspension culture essentially as described by Summers and Smith (1987) in supplemented Grace's insect media at 27 °C. Pluronic F-68, a cell protective agent, was added to improve cell viability in suspension cultures since Sf9 cells are very sensitive to mechanical shear. Cells at a density of 1-2 x 10^6/ml were infected with the appropriate recombinant virus at a multiplicity of infection of 2-5 and harvested at 24 or 48-h post-infection for D1/Sf9 cells or 72 h post-infection for D2L/Sf9 cells. Typically, viral infections were performed in one-third of the final volume to a final cell density of 2 x 10^6 cells/ml. Cell viability at these times were ~90% (trypan blue-negative) as determined by trypan blue staining. To minimize variations in recombinant baculovirus infection efficiencies among batches of cultures, the same recombinant

virus stock was used in all experiments for a study.

5.4 Preparation of Cell Membrane Fractions

The preparation of membranes was done at 4°C. Cells were centrifuged at 100xg for 7 min and pelleted. Cells were then washed twice with PBS and centrifuged at 100xg for 7 min (X2) and resuspended in 10 ml of buffer A: 5 mM Tris-HCl, 2 mM EDTA buffer containing the protease inhibitors: 10 μg/ml benzamidine, 5 μg/ml leupeptin, and 5 μg/ml soybean trypsin inhibitor (pH 7.4 at 4°C). The cell suspension was then polytroned, two bursts at maximum setting for 15 seconds and homogenates were centrifuged at 100xg for 7 min to pellet unbroken cells and nuclei, and supernatant was collected. The resulting pellet was homogenized a second time in 10 ml of buffer A, centrifuged as described above and supernatant fractions saved. The pooled S1 supernatant was centrifuged at high speed (27 000xg for 20 min) washed once with buffer A, centrifuged again at high speed and resuspended in buffer A, and stored at -80°C or resuspended in buffer B: 75 mM Tris-HCl, 12.5 mM $MgCl_2$, 2 mM EDTA, pH 7.4 and assayed immediately for adenylyl cyclase activity. Alternatively, the S1 supernatant was used to prepare a cell surface plasma membrane fraction or an intracellular light vesicular membrane fraction that exhibits a lower density than that of the plasma membrane (Waldo et al., 1983, Hertel et al., 1990). This was done by layering the S1 supernatant on top of a 35% sucrose cushion which was then subjected to centrifugation at 150 000 x g for 90 min at 4 °C. As reported by Lohse et al. (1990), the 0-35% interface contains the light vesicular membrane fraction believed to contain sequestered β_2-adrenergic receptors, whereas the plasma membrane fraction containing surface receptors sediments at the bottom of the sucrose cushion. Plasma and light membrane fractions were resuspended in buffer A and centrifuged at 200,000 x g for 60 min. Pelleted membranes were

resuspended in buffer A and stored at -70 °C or resuspended in the appropriate buffers for immediate use in various assays.

5.5 Protein Determination

Protein content was determined by the method of Bradford (BioRad). A standard protein concentration curve was made with bovine serum albumin (BSA). Protein concentration in the test sample was determined from the standard curve which was a plot of absorbance at 595 nm measured using a Hitachi model U-2000 spectrophotometer against concentration.

5.6 Receptor Binding Assays

Saturation binding experiments were performed with ~25 μg P2 membrane protein unless indicated and used to determine receptor densities (B_{max}) and affinities for ligands (K_D). Saturation experiments for the D1 receptor were done with increasing concentrations of [^{3}H]SCH-23390 (10-4000 pM, final concentration) whereas increasing concentrations of [^{3}H]spiperone (1-2000 pM, final concentration) were used for the D2L receptor. Each concentration was examined in duplicate and incubated for 2 hours at 22°C in a total volume of 1 mL binding buffer C: 50 mM Tris-HCl, 5 mM EDTA, 1.5 mM $CaCl_2$, 5 mM $MgCl_2$, 5 mM KCl, 120 mM NaCl buffer with protease inhibitors. Nonspecific binding for [^{3}H]SCH-23390 and [^{3}H]spiperone was defined as binding that was not displaced by 1 μM (+)-butaclamol. Competition experiments were done in triplicate without Gpp(NH)p or GTPγS (used at 100-150 μM where indicated) with increasing concentrations of agonists (10^{-12}-10^{-3} M) or antagonists. Tubes were incubated for 2 h at 22°C in a final volume of 1 ml with binding buffer C as described, with NaCl for antagonists, without NaCl and with ascorbic acid for agonists. The concentration of radioligand used in the competition assays was approximately equivalent to its K_D. Bound ligand was isolated by rapid filtration through a Brandel

48-well cell harvester using Whatman GF/C filters. Filters were washed with 10 ml of cold 50 mM Tris-HCl buffer (pH 7.4) and placed in glass vials with 5 ml of Universol scintillation fluid and counted for tritium. Data were analysed by nonlinear least-squares regression using the computer-fitting program INPLOT version 3.0 GraphPad (San Diego).

5.7 Adenylyl Cyclase Assay

Adenylyl cyclase assays were conducted essentially as described (Salomon et al., 1974). The assay mix contained 0.02 ml of membrane suspension (10-25 μg of protein), 0.012 mM ATP, 0.1 mM cAMP, 0.053 mM GTP, 2.7 mM phosphoenolpyruvate, 0.2 units of pyruvate kinase, 1 unit of myokinase and 0.13 μCi of [^{32}P]ATP in a final volume of 0.05 ml. Enzyme activities were determined in duplicate or triplicate assay tubes containing 10^{-3} - 10^{9} M dopamine or 100 μM forskolin or 10 mM sodium fluoride and incubated at 37°C for 30 mins. For inhibitory receptors such as the D2L receptor, adenylyl cyclase activity mix contained 100 μM forskolin. Inhibition of adenylyl cyclase assays was determine following incubation at 27°C for 20 mins. Reactions were stopped by the addition of 1 ml of an ice-cold solution containing 0.4 mM ATP, 0.3 mM cAMP and [^{3}H]cAMP (25000 cpm). Antagonist inhibition of dopamine stimulated cyclase was performed with 10^{-4}-10^{-12} M SCH-23390 in the presence of 10 μM dopamine. cAMP was isolated by sequential column chromatography using Dowex cation exchange resin and aluminum oxide. Data were analysed by computer fitted nonlinear least-squares regression.

5.8 Endoglycosidase Treatment

PNGase F has a broad specificity against sulfated and nonsulfated high-mannose type glycans including complex type N-linked glycans. Photoaffinity labelled P2 membranes (~25 μg) from receptor expressing cells were washed twice in PBS containing 2.5 mM EDTA, and

preincubated for 1 h at 22 °C with 0.5% SDS and 100 mM 2-mercaptoethanol. 1.25% Nonidet P-40, and glycopeptidase F (PNGase F) (up to 60 U/ml, final concentration) were added to samples with a final concentration of 0.3% SDS and incubated for a minimum of 12 h at 37 °C.

5.9 SDS-PAGE Electrophoresis

Sodium dodecyl sulfate 10-12% polyacrylamide gel electrophoresis (SDS-PAGE) was performed as described by Laemmli, 1970. Membranes were solubilized in SDS sample buffer consisting of 50 mM Tris-HCl pH 6.5, 10% SDS, 10% glycerol, and 0.003% bromophenol blue with or without 10% 2-mercaptoethanol. Molecular mass (Da) of receptors was determined graphically by plotting the log molecular weight of known protein standards versus the R_F (relative migration) of these proteins. The apparent molecular mass of proteins was estimated by determining the R_F (from the centre of the band) and interpolating this value onto the standard curve.

5.10 Photoaffinity Labelling

P2 membranes were resuspended in buffer D: PBS, 5 mM EDTA, pH 7.4 with protease inhibitors and incubated in the dark with photoactive ligands at K_D concentrations in a final volume of 10 ml for 3 h at 22°C. D1 receptors were identified by 7-[^{125}I]iodo-8-hydroxy-3-methyl-1-(4'azidophenyl)-2,3,4,5-tetrahydro-1H-1-benzazepine ([^{125}I]IMAB), whereas D2L receptors were labelled by [^{125}I]N-p-azidophenethylspiperone ([^{125}I]NAPS) and [^{125}I]4-azido-5-YM-09151-2 ([^{125}I]YM-09151-2). The membranes were centrifuged at 27 000xg for 20 min and resuspended in buffer D with 0.5% bovine serum albumin and recentrifuged. The pellet was washed in buffer D, centrifuged at 27 000xg for 20 min and resuspended in 1 ml of buffer D and exposed on ice to 360 nm ultraviolet light at 2 inches from the source for 10 min. Photolabelled membranes were washed in buffer D and pelleted membranes were solubilized in SDS sample buffer, electrophoresed, blotted

onto nitrocellulose and exposed to Kodak XAR film with an intensifying screen at -70°C as described above.

5.11 Immunoblot Analysis

Membranes from cells infected with recombinant virus or with wild type baculovirus were prepared, electrophoresed, and blotted on to nitrocellulose as described. The blots were washed in TBS for 10 min, blocked with 3% skim milk powder in TBS buffer for 30 min, washed for 10 min and incubated for 1 h at 22°C with the mouse monoclonal antibody (9E10) directed against the c-myc epitope of the c-myc-D1 receptor, or with the AL-26 polyclonal antibody against a 120 amino acid sequence (nt 661-1020) in the third intracellular loop of the human D2 receptor. Primary antibodies were diluted 1/1000 in TBS containing 1% skim milk powder. Blots were then treated with 0.05% Tween 20 in TBS for 30 min and binding of the primary antibody was detected after incubation for 1 h at 22°C with goat anti-mouse or goat anti-rabbit IgG alkaline phosphatase conjugate diluted 1/1000 in TBS containing 1% skim milk powder. Blots were then rinsed in 150 mM NaCl, 50 mM Tris-HCl pH 7.5 before developing with BCIP/NBT (5-bromo-4-chloro-3-indolyl phosphate/nitroblue terazolium) substrate.

5.12 Agonist-induced Desensitization Of Expressed Receptors

Sf9 cells (25 ml culture with a cell density of 10^6 cells/ml) were infected with recombinant virus and cultured up to 48 h post-infection, the last 18 h in serum free media. Prior to harvesting, cells were preincubated with 10 μM dopamine and 5 mM ascorbic acid for various periods. To determine whether the effects observed after agonist exposure were agonist-specific, cells were pretreated with 100 μM receptor antagonist 15 min prior to incubation with 10 μM dopamine. The incubations were stopped by washing with PBS. To biochemically assess the contribution of

receptor-mediated internalization on desensitization, cells were preincubated for 45 min with concanavalin A prepared in PBS (0.25 mg/ml, final concentration) or sucrose prepared in PBS (0.5 M, final concentration) before dopamine treatment. In all cases, controls for treatment conditions were receptor expressing cells from the same batch treated with vehicle and performed in parallel.

5.13 Treatment of Sf9 Cells with Pertussis Or Cholera Toxin

Pertussis or cholera toxin (1 μg/ml) were preactivated at 30°C for 20 min with 20 mM DTT and added to a suspension cell culture infected with recombinant virus and incubated for 20 hours prior to harvesting of cells at the 48-h (D1/Sf9 cells) or 72-h (D2L/Sf9 cells) post-infection time point.

5.14 ADP-Ribosylation of Sf9 Membrane Components by Pertussis Toxin

The ADP-ribosylation experiments were performed essentially as described (Ribeiro-Neto et al., 1985) with minor modifications. Pertussis toxin (20μg/mL) was preactivated as described and added to a tube containing 100 μg of membrane protein, 10 mM Tris-HCl pH 7.4, 25 mM DTT, 0.5 mM EDTA, 1 mM ATP, 0.1 mM GTP, 10 μM NAD^+, 5 μl protease inhibitor cocktail and 50 μCi [^{32}P]NAD^+ in a final volume of 50 μl and incubated at 37°C for 60 min. Reactions were stopped by adding SDS sample buffer and samples boiled before SDS-PAGE analysis. Control samples were incubated in the absence of pertussis toxin or utilized 1-2.5 pmol of partially purified solubilized bovine brain G_i/G_o in place of Sf9 membrane protein. The number of pmol of ADP-ribosylated protein was calculated by excising the ~41 kDa band from the gel for liquid scintillation counting.

5.15 Solubilization And Immunoprecipitation Of Receptors

Membranes were prepared by sonication in buffer A as described. The pellet was resuspended and stirred at 4°C for 2 h in 2 ml of freshly prepared solubilization buffer consisting of 100 mM NaCl, 10 mM Tris-HCl pH 7.4, 2% digitonin, and 5 mM EDTA with protease inhibitors. The homogenate was centrifuged at 27 000xg for 20 min and the solubilized fraction was washed and concentrated in Centriprep 30 four times with 10 ml cold buffer C: 100 mM NaCl, 10 mM Tris-HCl pH 7.4 with protease inhibitors. The washed fraction was precleared with 1/20 normal rabbit serum and protein A-Sepharose beads for 2 h on ice. Solubilized receptors were immunoprecipitated with the mouse monoclonal 9E10 antibody (D1 receptor) or rabbit AL-26 polyclonal antibody (D2 receptor) at a 1/37 dilution in buffer C for 2 h on ice, and agitated gently overnight at 4°C with 1/40 dilution of agarose fixed goat anti-primary IgG. The immunoprecipitate was washed 6 times with 5 volumes cold buffer C for 20 min, solubilized in SDS sample buffer, sonicated and electrophoresed on SDS-PAGE as described.

5.16 Whole Cell Phosphorylation

Sf9 cells (25 ml culture) expressing recombinant receptors were incubated for 18 h in serum free media. Carrier-free ^{32}P (0.5 mCi/ml) was then added and equilibrated at 22°C for 90 mins at 48 h post-infection. Desensitization experiments were done as described above and reactions were terminated by centrifugation at 100xg, and the cells washed twice with PBS before membrane preparation, solubilization and immunoprecipitation as described.

5.17 Whole Cell Palmitoylation

Sf9 cells (25 ml culture) expressing c-myc-dopamine D_1 receptors were cultured for 18 h prior to the labelling experiment in serum free media. Following this period, cells were resuspended in Grace's insect media supplemented with 1% fetal bovine serum for 1 h at 27°C. [^{3}H]palmitic acid

was dissolved in dimethyl sulfoxide (0.05 ml) and added to the suspension culture (0.2 mCi/ml) for 4 h at 48 h post-infection. Palmitic acid labelling and desensitization experiments were terminated by centrifugation at 100xg and cells washed twice with cold PBS and receptors prepared as described above. The nature of the chemical linkage between the receptor and the palmitate was determined by incubation of immunoprecipitated [^{3}H]palmitoylated receptors with 1.0 M hydroxylamine pH 10.0 for 12 h at 22°C. Following electrophoresis, the gels were fixed and treated with Enlightning fluid (NEN) for 30 min, dried and exposed to Kodak X-AR film at -70°C.

5.18 Soluble Binding And Determination Of Specific Activity Of [^{3}H]palmitic Acid Or ^{32}P Labelled Receptors

The amount of solubilized receptor immunoprecipitated and loaded in each lane of a gel was determined by radioligand binding with, in the case of the D1 receptor, the antagonist [^{125}I]SCH-23982. Aliquots were taken before and after immunoprecipitation experiments and incubated with [^{125}I]SCH-23982, 4 nM final concentration, for 2 h at 22°C in a total volume of 1 ml binding buffer: 100 mM NaCl, 10 mM Tris-HCl, 0.05% digitonin, 2 mM EDTA with protease inhibitors, pH 7.4. Following the incubation period, the binding preparation was loaded onto a Sephadex G-25 column (Pharmacia) and ligand bound receptor was separated from free ligand by elution. The eluate was counted in a gamma counter for determination of the amount (pM) of receptor immunoprecipitated. In the same experiments, the activity of [^{3}H]palmitate or [^{32}P] labelled receptors, expressed in Ci, was determined by cutting out the ~48 kDa band from the gels and dissolving the gel slice in scintillation fluid before counting in a scintillation counter. The specific activity of metabolically labelled receptors is reported as Ci/mole of receptor. 1 μm (+)-butaclamol was used to define specific binding.

5.19 Immunocytochemical Fluorescence Labelling of Receptors in Fixed Cells

Immunofluorescence labelling was carried out in aliquots of cells from a suspension culture at a concentration of 1.5 x 10^6/ml. Cells were fixed in freshly prepared 4% paraformaldehyde in PBS, pH 7.3 for 15 min in microtubes, pelleted in a Mini Spin Microfuge (Bio/Can Scientific; Mississauga, ON) at a speed of 300 rpm for 10 sec. The supernatant was removed and the cells were washed in PBS and re-suspended. Cells were permeabilized with methanol at -70 °C for 3 min to allow labelling of intracellularly located receptors. Samples were next incubated with a blocking solution of 1% bovine serum albumin and 5% goat serum to reduce nonspecific staining. Cells were incubated with primary antibody for 60 min. This was followed by incubation with an FITC-secondary anti-primary antibody for 60 min. After final PBS rinses totalling 30 min, all liquid was removed from the microtubes and the cells were resuspended in the mounting media Mowiol-88 (Hoechst; Montreal, QC) with 2.5% 1,4-diazobicyclo-octane (DABCO; Sigma, MO) added to reduce photobleaching. The drop of liquid containing the labelled cells was placed on a slide protected by a coverslip and allowed to polymerize overnight. Alternatively, slides were cover slipped with Fluoromount®.

5.20 Microscopy of Immunofluorescently Labelled Cells

Fluorescently labelled Sf9 cells were examined under conventional microscopy and with greater detail with a BioRad MRC600 confocal microscope with a krypton-argon ion laser light source equipped with a Nikon Optiphot upright microscope (Bio-Rad; Mississauga, ON). Using a 60(X), 1.4 NA Nikon Planaphochromat objective lens, a multiple series of sections was collected at incremental steps of 1.5 μm steps with a minimum of five multiple passes for a smoothing effect using a technique of distributed averaging which eliminates the uneven effects of photobleaching

while stepping through the z-axis. In brief, sequential images for a single cell were collected. During the second pass the stage was returned to its original position, the frame buffer loaded with previously stored first image, and another image was collected and averaged with the first one. This was repeated for all the individual sections and resulted in an even distribution of any bleaching artifacts throughout the entire cell's volume. All collected images were averaged with an identical number of passes. Settings such as neutral density filter, gain, pinhole size, and background level were maintained at identical values during the imaging of all samples to allow subsequent direct comparison. The intensity range was 0-255 gray levels and care was taken not to saturate the maximal range. The staining pattern of receptor expressing cells not found in control wild-type baculovirus infected cells were defined as follows: 1. Surface, if labelling appeared as a even or broken ring of fluorescence on the cell periphery. 2. Internal, if labelling appeared as pockets of label in the perinuclear area. 3. Unclassified, if staining occurred in nucleus and included ruptured, unstained or dead cells. This classification of a population of cells was done twice, independently by 2 investigators, and the number of cells with a particular staining pattern was expressed as a percentage of the total number of cells examined.

5.21 Three-dimensional Reconstruction of Immunofluorescently Labelled Cells

A Silicon Graphics workstation was used with a high-speed proprietary graphics processor (ISG Technologies; Mississauga, ON). Three-dimensional reconstruction was carried out on a series of confocal sections representing many cells. Briefly, reconstruction consisted of conversion of two-dimensional pixels of selected intensities into arrays of three-dimensional voxels used to create an object. Identification of objects consisted of selection of pixels representative of the staining pattern and was carried out by density segmentation, using an identical range of values in each section of

a stack of sequential sections representing a single cell. In this study, the brightest pixels were outlined with an automatic contouring algorithm and converted into three-dimensional voxels. Next, pixels of intensity value just above background noise level were selected to outline the cell body. Finally, manual tracing around the edge of the space in the centre of each permeabilized cell from which all label was excluded represented the nucleus. Each three-dimensional array of voxels defining a selected range of intensities visually represented a component of the original image. The final reconstruction were interactively rotated, outer membrane cut away, and appropriate orientations found that visually best described the receptor distribution indicated by the numerical data.

5.22 Coincubation of Immunoprecipitated C-myc D1 Receptors and D2L Receptors in Detergent Solution

P2 membranes from Sf9 cells expressing the D2L receptor and c-myc epitope-tagged D1 receptor were prepare and solubilized by stirring in 100 mM NaCl, 10 mM Tris-HCl pH 7.4, 2% digitonin, and 5 mM EDTA with protease inhibitors at 4°C for 8 h. The homogenate was centrifuged at 27 000xg for 20 min and the solubilized fraction was washed and concentrated in Centriprep 30 four times with 10 ml cold buffer D: 100 mM NaCl, 10 mM Tris-HCl pH 7.4 with protease inhibitors. The washed fraction was precleared with 1/20 normal rabbit serum and protein A-Sepharose beads for 2 h on ice. The solubilized receptors were immunoprecipitated with the mouse monoclonal 9E10 c-myc D1 antibody or the rabbit AL-26 D2 antibody at a 1/37 dilution in buffer D for 2 h on ice, and agitated gently overnight at 4°C with 1/40 dilution of agarose fixed goat anti-mouse IgG. The immunoprecipitate was washed 6 times with 5 vol cold buffer D for 20 min, solubilized in SDS sample buffer or in buffer E (100 mM NaCl, 10 mM Tris-HCl pH 7.4, 2 mM

EDTA and 0.5% digitonin with 5 mg/ml leupeptin, 10 mg/ml benzamidine and 5 mg/ml soybean trypsin inhibitor) at 37 °C for 1 h. Samples were sonicated to free receptors from resin and following centrifugation the supernatant was subjected SDS-PAGE and immunoblot analysis as described.

5.23 Biophysicochemical Characterization of Receptor Dimers

The human D2L receptor, c-myc epitope-tagged human D1 receptor, and c-myc epitope-tagged human 5-HT_{1B} receptor were expressed in Sf9 cells and immunoprecipitated for assays as previously described. 3 pmol of receptors, as determined by soluble binding assay were prepared in buffer F (100 mM NaCl, 10 mM Tris-HCl pH 7.4, 2 mM EDTA and 0.5% digitonin with 5 mg/ml leupeptin, 10 mg/ml benzamidine and 5 mg/ml soybean trypsin inhibitor), and incubated with 1.6 μg/μl (final concentration) of peptide (unless otherwise indicated). All peptides were freshly prepared in buffer F with 10% DMSO. SDS buffer (50 mM Tris-HCl, pH 6.5/12% SDS/10% 2-mercaptoethanol/10% (vol/vol) glycerol/0.003% bromophenol blue) was added to the samples to make a total assay volume of 30 μl, and incubated at 37 °C for 30 min prior to SDS-PAGE and immunoblot analysis. Peptide sequences are as follows:

D2-TM VI peptide (aa 375-394: H-LAIVLGVFIICWLPFFI THI-NH_2),

D2-TM VII (aa 407-426: H-LYSAFTWLGYVNSAVNPIIY-NH_2),

D2-C III_A peptide (aa 244-263: H-CTHPEDMKLCTVIMKSNGSF-NH_2),

D2-C III_B peptide (aa 284-303: H-LSSTSPPERTRYSPIPPSHH-NH_2),

β_2-AR-TM VI peptide (aa 276-296: NH_2 -GIIMGTFTLCWLPFFIVNIVH-COOH),

D1-C-$tail_A$ peptide (aa 369-383: NH_2-MFSSHHEPRGSISKE-COOH), and

D1-C-$tail_B$ peptide (aa 416-431: NH_2-SPALSVILDYDTDVS-COOH).

Peptides were synthesized by Chiron Mimotopes, Victoria, Australia. Receptor temperature stability studies were performed with 1.5 pmol of immunoprecipitated D2L receptors. Receptors were prepared in buffer A and incubated at 23, 37, 65, and 90 °C for 30 min with SDS buffer at a final volume of 30 µl, and subjected to SDS-PAGE and immunoblot analysis. Receptor pH-stability experiments were performed with 1.5 pmol of immunoprecipitated D2L receptors prepared in buffer A. Receptors were treated with H_2O, or 0.1 N tartaric acid (final concentration), or 0.1 N HCL (final concentration), or 0.1% glacial acetic acid (final concentration). Samples were then incubated at 37 °C for 30 min with SDS buffer at a final volume of 30 µl, and subjected to SDS-PAGE and immunoblot analysis.

5.24 Statistics

Ligand binding data were analysed and K_D and B_{max} values were determined by the weighted nonlinear-least squares curve-fitting program GraphPAD Inplot version 3.0 (GraphPAD Software, San Diego, CA). Unless indicated otherwise, the statistical significance of the differences between groups was measured using a paired student's t test using GraphPAD Instat version 3.0 (GraphPAD Software, San Diego, CA). A probability of $P < 0.01$ at the 99% and $P < 0.05$ at the 95% confidence limits respectively was considered to represent a significant difference.

6. RESULTS

6.1 Establishing and Validating the Baculovirus/Sf9 Cell Model System: Pharmacological and Biochemical Characterization of the Serotonin 5-HT_{1B} Receptor

To establish and validate the baculovirus/Sf9 cell model for the detailed study of dopamine receptors, we have expressed the structurally related 5-HT_{1B} receptor. The strategy employed was to c-myc epitope-tag the 5-HT_{1B} receptor which should provide a means to detect receptors by immunoblot analysis and purify receptors by immunoprecipitation using a monoclonal antibody, 9E10, specific for the c-myc epitope. Detailed reporting of the 5-HT_{1B} receptor results, and a thorough discussion of these data is provided in the APPENDIX. A brief summary is given now.

Saturation binding was first conducted to assess whether recombinant receptors were expressed and biologically active. Indeed, c-myc-5-HT_{1B} receptors showed saturable binding for [^{3}H]5-HT with specific activities reaching 1-5 pmol/mg of protein at 72 h post-infection. Additionally, a desirable high signal to noise ratio was achieved which prompted the critical examination of the pharmacology of the expressed receptors. The data showed that c-myc-5-HT_{1B} receptors bound agonists and antagonists with a rank order of potency characteristic of a classical 5-HT_{1B} receptor pharmacological profile. Additionally, agonist binding to expressed receptors was sensitive to guanine nucleotides and bacterial toxins, suggesting receptor coupling to endogenous G proteins. Receptor mediated agonist inhibition of adenylyl cyclase activity supported this interpretation providing direct evidence of intact G protein/effector pathways in the cell line. Immunoblots of membranes prepared from c-myc-5-HT_{1B}/cells revealed major bands of ~44 and ~90 kDa suggesting the presence of receptor monomers and dimers. Indeed, [^{125}I]MAB photoaffinity labelling experiments confirmed that these species were active ligand

binding receptors indicating for the first time existence of serotonin receptor dimers. It was of significance to further determine the presence of phosphorylating and palmitoylating enzymes in the Sf9 cells since the phosphorylation and palmitoylation of other receptors, in many cases, is associated with desensitization. Indeed, c-myc-5-HT_{1B} receptor monomer and dimer isolated by immunoprecipitation from whole cells were shown to be posttranslationally modified by phosphorylation and palmitoylation. Collectively, these studies led us to believe that dopamine receptors could also be expressed successfully in Sf9 cells with the appropriate biologically and immunoreactive activity for detailed functional studies.

6.2 Pharmacological And Biochemical Characterization of D1 Receptors

6.2.1 Ligand Binding Profile of D1 Receptors

To determine whether recombinant D1 receptors expressed in Sf9 cells exhibited similar binding patterns as the human D1 receptor in neuronal tissue, binding of the D1 receptor selective antagonist [^{3}H]SCH-23390 was assessed. ^{3}[H]SCH-23390 bound in a specific and saturable manner to the expressed receptors, and receptor densities up to 33 pmol per mg of protein were detected at 48 h post-infection. K_D values of the ligand for the D1 receptor and the c-myc-D1 receptor were not significantly different ($P>0.05$) and were 574.2 ± 33.0 pM ($n=7$) and 696.9 ± 20.9 pM ($n=7$) respectively, and nearly identical to the K_D value of the ligand for the D1 receptor in human caudate tissue (Seeman, 1987). No specific [^{3}H]SCH-23390 binding was detected in cells infected with the wild-type baculovirus (data not shown), and nonspecific binding represented $\sim 15\%$ of total binding at 4000 pM concentration of [^{3}H]SCH-23390.

To define whether the expressed receptors exhibited D1 receptor pharmacology,

catecholamine agonists and dopaminergic antagonists were used to compete for [^{3}H]SCH-23390 binding. Agonist displacements were observed with the rank order of potency: dopamine > SKF-38393 > (-)-noradrenaline > serotonin > isoproterenol. Binding constants for the agonist-detected high and low affinity receptor states and the relative proportions of sites in each state are indicated in Table 2. The K_D value for the selective β -adrenergic receptor agonist, isoproterenol is not shown because it did not displace [^{3}H]SCH-23390 binding at concentrations below 1 mM. As shown in Fig. 8A, the displacement curve for dopamine was shallow and statistically best fitted to a two affinity state model ($P<0.05$) using the computer program GraphPad INPLOT. When the binding was determined in the presence of the non-hydrolyzable GTP analogue Gpp(NH)p, the curve became steeper and was best fitted to a single affinity state ($P<0.05$). Such a guanine nucleotide-sensitive high-affinity state of the receptor suggested the presence of receptors functionally coupled to endogenous G-proteins in Sf9 cells. Inhibition of [^{3}H]SCH-23390 binding by antagonists was concentration dependent and monophasic, corresponding to a single affinity form of the receptor recognized by antagonists. The following rank order of antagonist potency was determined: SCH-23390 > (+)-butaclamol > haloperidol with K_D values listed in Table 2. The above data indicated that the expressed D1 receptors were pharmacologically similar to human neuronal D1 receptor (Seeman and Niznik, 1988).

6.2.2 D1 Receptor Coupling to Endogenous Adenylyl Cyclase

Fig. 8B, shows agonist mediated c-myc-D1 receptor stimulation of adenylyl cyclase activity and antagonist SCH-23390 inhibition of 10 μM dopamine stimulated adenylyl cyclase activity. The mean EC_{50} for dopamine stimulated adenylyl cyclase was 153.0 ± 8.8 nM (n=3) and the IC_{50} for SCH-23390 inhibition of dopamine stimulated adenylyl cyclase activity was

65.9±41.2 nM (n=2). Dopamine induced a maximal 3.5 fold increase in adenylyl cyclase activity from basal values (Table 3). No dopamine stimulated adenylyl cyclase activity was detected in cells infected with the wild-type baculovirus (data not shown).

Fig. 8. Pharmacology of expressed c-myc-D1 receptors. (A) Effect of Gpp(NH)p on the affinity of c-myc-dopamine D_1 receptor for dopamine at 24 h post-infection. Membranes were incubated with ~600 pM [^{3}H]SCH-23390 and increasing concentrations (10^{-1} - 10^{-10} M) of dopamine in the absence (o) or presence (▲) of 150 μM Gpp(NH)p as described in methods. The data were analysed by GraphPad INPLOT and fitted statistically for one and two sites. K_D values of the dopamine detected affinity states for this fit are indicated and the results shown are representative of three independent experiments. (B) Effect of increasing concentrations of dopamine to stimulate adenylyl cyclase activity and, inset, effect of increasing concentrations of SCH-23390 to inhibit 10 μM dopamine stimulated adenylyl cyclase activity. Adenylyl cyclase activity was measured in membranes derived from cells expressing c-myc-D1 receptors at 48 h post-infection and are expressed as pmol of cAMP produced/min/mg of protein. The data were analysed using nonlinear least squares regression and the results shown are representative of 2 or 3 independent experiments. *Reproduced, with permission, from Ng et al., Desensitization, phosphorylation and palmitoylation of the human dopamine D1 receptor, Eur. J. Pharmacol. Mol. Pharmacol. Sect. 267, 7-16, 1994.*

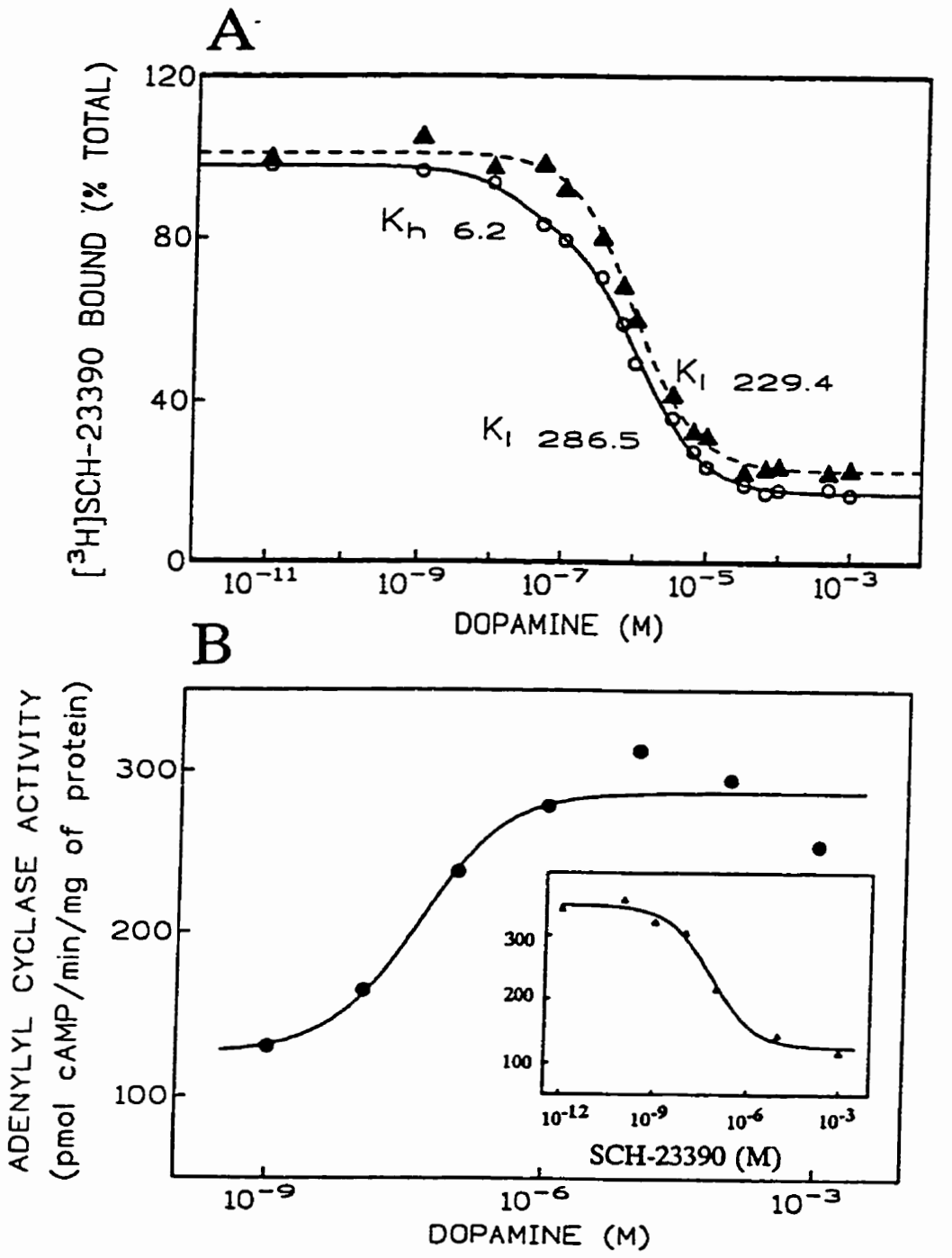
A
120
80
40
0
[3H]SCH-23390 BOUND (% TOTAL)
Kh 6.2
KI 229.4
KI 286.5
10-11
10-9
10-7
10-5
10-3
DOPAMINE (M)
B
300
200
100
ADENYLYL CYCLASE ACTIVITY
(pmol cAMP/min/mg of protein)
10-9
10-6
10-3
DOPAMINE (M)
300
200
100
10-12
10-9
10-6
10-3
SCH-23390 (M)

Table 2. Agonist and antagonist dissociation constants for c-myc-D1 receptors. Membranes prepared from Sf9 cells at 24 h post-infection were incubated with varying concentrations (10^{-11} - 10^{-3} M) of catecholamine agonists or dopamine receptor antagonists in the presence of ~600 pM [^{3}H]SCH-23390 as described in methods. Nonspecific binding was defined by 1 μM (+)-butaclamol. Data was analysed by GraphPad INPLOT and fitted statistically to the best of either one or two sites. Data are expressed as either the mean $\pm$ SEM when n=3 or as the mean $\pm$ SD when n=2.

	K_D (nM)		Proportions (%)		
	D_{1high}	D_{1low}	D_{1high}	D_{1low}	n
Agonists					
Dopamine	9.0±3.5	470.0±36.4	29.6±13.4	70.4±13.4	3
SKF-38393	98.2±36.2	375.0±115.0	57.3±8.6	42.7±8.6	2
(-)-Noradrenaline	1590.0±659.0	2,877.0±2850.0	53.5±5.1	46.5±5.1	2
Serotonin		39,700.0±1560.0			2
Antagonists	K_i (nM)				
SCH-23390	0.28±0.01				3
(+)-butaclamol	2.47±0.76				3
Haloperidol	166.0±27.6				3

6.2.3 Biochemical Characterization of the c-myc-D1 Receptor

To further characterize the c-myc-D1 receptor species expressed in Sf9 cells, photolabelling experiments were carried out with the D1 receptor selective ligand [^{125}I]MAB (Fig. 9A). Upon exposure to UV light, [^{125}I]MAB photolabelled a major band at ~48 kDa in membranes from cells expressing D1 receptors (lane 2). Labelling was completely blocked by incubation in 1 μM of the dopamine receptor antagonist (+)-butaclamol (lane 3), and was absent as expected in membranes from cells infected with the wild-type baculovirus (lane 1).

The selectivity and sensitivity of the monoclonal 9E10 antibody for the c-myc epitope of the c-myc-D1 receptor, was confirmed by immunoblot analysis (Fig. 9B). The antibody revealed the presence of three groups of immunoreactive bands in the range of 43-50 kDA, 86-100 kDa and above 200 kDa. The series of immunoreactive material in the 43-50 kDa range comigrated with the major photolabelled ligand binding species of the c-myc-D1 receptor seen in lane 2 of Fig. 9A. The immunoreactive bands at 43-50 kDa appears to represent the unglycosylated D1 receptor monomer as deduced from the predicted molecular mass of the D1 receptor. The additional immunoreactive species at ~90 and > 200 kDa (lane 2) were poorly labelled by [^{125}I]MAB and may represent improperly folded or denatured forms of the receptor. Alternatively, they may suggest dimers and oligomers of the D1 receptor. Similar results were obtained for the β_2-adrenergic receptor expressed in Sf9 cells (Mouillac et al., 1992). No immunoreactive material was observed in cells infected with the wild-type baculovirus (lane 1) or cells expressing untagged D1 receptor (lane 3) demonstrating the specificity of the 9E10 antibody for the c-myc epitope of the c-myc-D1 receptor. Moreover, the 9E10 antibody immunoprecipitated more than 80% of the dopamine receptor binding activity expressed in the

Sf9 cells.

Following metabolic labelling of c-myc-D1/cells with ^{32}P, c-myc-D1 receptor was immunoprecipitated using the 9E10 antibody. As shown in Fig. 9C, autoradiography of an SDS-PAGE of the immunoprecipitated material revealed a major phosphorylated band in the range of 43-50 kDa (lane 2) corresponding to the mobility of the photolabelled receptor (Fig. 9A, lane 2). No phosphorylated proteins were immunoprecipitated using the 9E10 antibody from Sf9 cells infected with the wild-type of baculovirus (lane 1). The relatively high concentration of phosphate in Grace's medium may account for the low specific activity of ^{32}P labelling, but the data clearly demonstrate that the immunoprecipitated c-myc-D1 receptor is phosphorylated in the Sf9 cells.

Following metabolic labelling of the c-myc-D1/cells with [^{3}H]palmitic acid, c-myc-D1 receptor was immunoprecipitated with the 9E10 antibody. Fluorograph of an SDS-PAGE of the immunoprecipitated material revealed the presence of a radiolabelled band migrating at the expected molecular weight (43-50 kDa) (Fig. 9D, lane 2) which was absent in Sf9 cells infected with the wild-type baculovirus (lane 1).

In these experiments the 9E10 antibody could immunoprecipitate with 80 ± 5 % efficiency, as much as 2-5 pmol of receptor from a 25 ml culture as determined by radioligand binding. These receptor levels were sufficient to study the extent of post-translational modifications.

Fig. 9 Biophysicochemical characterization of the c-myc-D1 receptor. (A) Identification of photolabelled c-myc-D1 receptors in Sf9 membranes. Membranes derived from c-myc-D1 receptor-baculovirus infected cells at 48 h post-infection were photolabelled with [^{125}I]MAB and visualized by autoradiography. Lane 1, membranes from cells infected with wild-type baculovirus. Lane 2, photoincorporation of [^{125}I]MAB upon photolysis in the absence and lane 3, in the presence of 1 μM (+)-butaclamol. The amount of membrane protein used for each labelling condition was 250 μg protein and in membranes from cells expressing c-myc-D1 receptors. This contained 10 pmol receptor. The autoradiogram shown is from a 7-day exposure. Three independent experiments were done to determine the specificity of the photolabel and the molecular weight of the photolabelled species identified by an arrow. (B) Identification of immunoreactive c-myc-D1 receptors in Sf9 membranes. Membranes (100 μg protein) were prepared at 48 h post-infection from cells infected with the wild type baculovirus (lane 1) or from cells expressing c-myc-D1 receptors (lane 2) or D1 receptors (lane 3). Membranes were solubilized in SDS buffer, electrophoresed, and electroblotted onto nitrocellulose as described in methods. Immunoreactivity was revealed with a goat anti-mouse IgG conjugated to alkaline phosphatase. The blot is representative of three independent experiments. (C) Phosphorylation of c-myc-D1 receptor. The figure shows an autoradiogram (3 day exposure) of 9E10 immunoprecipitated c-myc-D1 receptors solubilized from membranes prepared from Sf9 cells infected with wild type baculovirus (lane 1) or expressing c-myc-D1 receptors (lane 2) prelabelled with carrier free ^{32}P. The ~48 kDa immunoprecipitated radiolabelled band is identified and the result shown is representative of three independent experiments. (D) Palmitoylation of c-myc-D1 receptor. The figure shows a fluorograph (1 month exposure) of immunoprecipitated sample from cells prelabelled with [^{3}H]palmitic acid infected with the wild-type baculovirus (lane 1) or expressing c-myc-D1 receptors (lane 2). The radiolabelled band identified is representative of 3 different experiments. *Reproduced, with permission, from Ng et al., Desensitization, phosphorylation and palmitoylation of the human dopamine D1 receptor, Eur. J. Pharmacol. Mol. Pharmacol. Sect. 267, 7-16, 1994.*

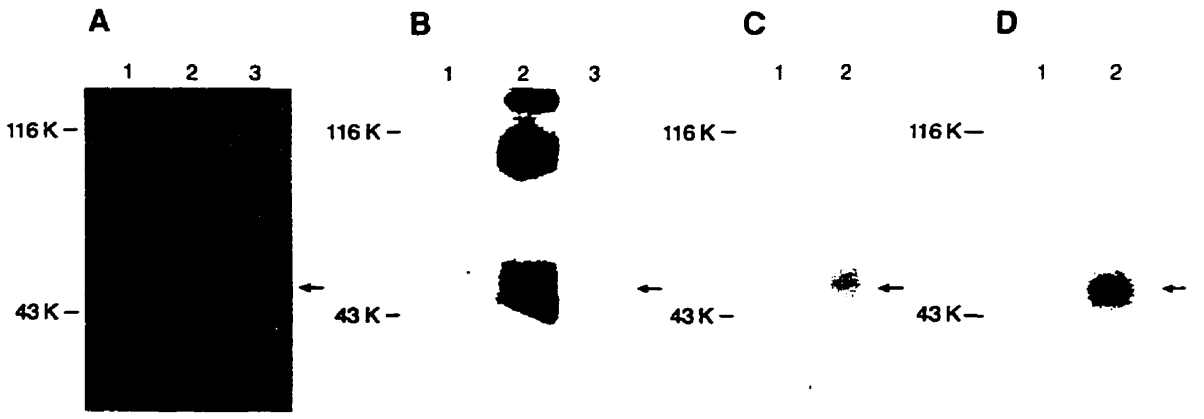
A
1 2 3
116K–
43K–
B
1 2 3
116K–
43K–
C
1 2
116K–
43K–
D
1 2
116K–
43K–

6.2.4 Agonist-induced Desensitization Of c-myc-D1 Receptor Stimulated Adenylyl Cyclase Activity

Cells expressing c-myc-D1 receptors were preincubated for 15 and 30 min with 1 μM dopamine before measurement of adenylyl cyclase enzyme activity in membranes derived from these cells. As seen in Table 3, pretreatment for 15 min with 1 μM dopamine resulted in a 16% reduction in adenylyl cyclase stimulation, and incubation for 30 min resulted in a 22% decrease in the receptor mediated enzyme activity. No change in basal, sodium fluoride, or forskolin stimulated adenylyl cyclase were seen following the 15 minute preincubation. However, following the 30 minute dopamine treatment, a modest decrease in these parameters was observed. When the desensitization was conducted using a higher concentration of dopamine (10 μM), maximal dopamine stimulation of adenylyl cyclase activity was significantly reduced by 40% accompanying a 2 fold right-ward shift of the dose-response curve (Table 3). Preincubation with dopamine for 30 min resulted in no further significant reduction in c-myc-D1 receptor responsiveness to dopamine (Table 3). Under these conditions, decreases in basal, sodium fluoride, and forskolin stimulated activities were observed following both 15 and 30 minute preincubations. Mean parameter values for receptor stimulated adenylyl cyclase activities and accompanying statistical analysis are summarized in Table 3. All results presented are from Sf9 cells expressing $\sim$7 pmol receptor/mg of protein at 48-h post-infection ($\sim$85% viability). Dopamine sensitive adenylyl cyclase activity was not detected in Sf9 cells infected with wild-type recombinant baculovirus (data not shown). These findings showed that desensitization of the D1 receptor stimulated adenylyl cyclase system was maximal following 15 min dopamine exposure.

6.2.5 Agonist-induced c-myc-D1 Receptor Uncoupling From G Protein and Reduction in

Cell Surface Receptor Binding

We examined the effects of dopamine exposure on the ability of expressed c-myc-D1 receptors to bind ligands. Mean parameter values for dopamine/[^{3}H]SCH-23390 competition binding assays in membranes prepared from vehicle-treated and dopamine-treated cells are shown in Table 4. In membranes prepared from vehicle-treated cells, the competition curve was shallow indicating two affinity states suggesting receptor coupling to endogenous G proteins. Agonist-detected high affinity binding was guanine nucleotide-sensitive as reported previously (Fig. 8). In membranes prepared from cells preincubated with dopamine for 15 or 30 min, the dopamine displacement curve was steeper and best fitted to a single affinity state model (Table 4) indicating agonist-induced receptor-G protein uncoupling. Mean agonist binding constants (K_i) and proportions of agonist-detected high and low affinity receptor states from competition binding studies are summarized in Table 4.

Table 3. Summary of the effects of dopamine exposure on c-myc-D1 receptor and non-receptor stimulation of adenylyl cyclase activity. Cells were treated for 15 or 30 min with 1 or 10 μM dopamine and the adenylyl cyclase activity measured in membranes derived from Sf9 cells as described in methods. The activities were measured in the presence of H_20 (basal), 10 μM dopamine, 100 μM forskolin and 10 mM sodium fluoride and are expressed as pmol of cAMP produced/min/mg of protein and are the average of two independent experiments $\pm$ SD.

	Adenylyl Cyclase Activity Profile (pmol cAMP/min/mg protein)		
	basal	15 min	30 min
	1 μM dopamine pretreatment		
basal	65.4$\pm$10.7	70.1$\pm$ 7.4	50.8$\pm$ 9.6
dopamine	260.6$\pm$ 7.0	218.0$\pm$23.5	201.8$\pm$ 9.0
forskolin	270.8$\pm$38.9	316.7$\pm$26.4	245.8$\pm$19.4
sodium fluoride	148.0$\pm$ 2.6	156.4$\pm$ 3.8	126.3$\pm$ 4.3
	10 μM dopamine pretreatment		
basal	102.9$\pm$24.8	65.8$\pm$15.2	64.0$\pm$18.0
dopamine	346.6$\pm$53.2	204.8$\pm$44.8	204.3$\pm$36.3
forskolin	379.1$\pm$49.0	309.2$\pm$35.0	305.1$\pm$16.5
sodium fluoride	193.0$\pm$29.9	127.0$\pm$29.8	126.7$\pm$44.5

Table 4. Summary of the effects of dopamine exposure on c-myc-D1 receptor radioligand binding. Details of the experiments and data analysis are described in text. The data shown represent the mean ± SEM. Dopamine competition binding (best fit as determined by F test at $P < 0.05$) is measured as the concentration of dopamine-detected high-affinity (K_h) and low-affinity (K_l) binding sites with the percentage of total binding sites shown in parentheses. ND, agonist high-affinity binding not detected; n, number of independent experiments; *, $P < 0.05$ when compared to vehicle values. Unless otherwise noted, no significant differences were observed between dopamine-treated compared to vehicle-treated values.

	Dopamine competition binding			[^{3}H]SCH-23390 saturation binding		
Treatment	K_h, pM (%)	K_l, pM (%)	n	K_D, pM	B_{max}, pmol/mg	n
Vehicle	10 ± 4 (25)	1100 ± 15 (75)	5	737 ± 27	7.3 ± 0.4	5
Dopamine						
15 min	ND	1120 ± 18 (100)	5	608 ± 41	6.5 ± 0.2	5
30 min	ND	1800 ±113 (100)	5	601 ± 35	6.3 ± 0.2*	5

6.2.6 Agonist-induced Phosphorylation of the c-myc-D1 Receptor

As shown in Fig. 10, dopamine exposure of c-myc-D1/cells for 15 min increased the intensity of c-myc-D1 receptor-^{32}P labelling from basal (compare lane 1 to 2). This agonist-mediated increase was blocked by the antagonist SCH-23390 (compare lane 2 to 3). Densitometric analysis of 3 such experiments revealed a 1.7 ± 0.3 fold increase ($p < 0.05$) in the intensity following agonist exposure. Further analysis included determining the specific activity of receptor labelling, by excising the radiolabelled bands from the gel for scintillation counting and determining the amount of receptor immunoprecipitated, as described in Methods. Under basal conditions, the receptor was found to be labelled to a specific activity of 1.4 ± 0.4 nCi/pmol (n=2). Following dopamine exposure for 15 min, specific activity was increased to 4.1 ± 2.5 nCi/pmol (n=2). The slightly higher increase observed using this quantitation technique probably reflected the higher sensitivity of this assay. This increase in the incorporation of ^{32}P into the receptor was blocked by the antagonist SCH-23390 and receptors under these conditions were labelled to a specific activity of 0.6 ± 0.3 nCi/pmol (n=2). In these experiments, $84 \pm 10\%$ of the dopamine receptor binding activity was immunoprecipitated reflecting a very efficient immunoprecipitation of the receptor by the 9E10 antibody.

6.2.7 Agonist-induced Palmitoylation of the c-myc-D1 Receptor

Fig. 11 shows a fluorograph of immunoprecipitated c-myc-D1 receptor following metabolic labelling of cells with [^{3}H]palmitic acid. Upon exposure to dopamine for 15 min, the intensity of c-myc-D1 receptor-palmitate labelling was increased (compare lane 1 to 2). Densitometric analysis of 3 such experiments revealed a 2.1 ± 0.7 fold increase ($p < 0.05$) in the intensity of labelling. The specific activity of receptor labelling was determined by excising the

radiolabelled band from the gel for scintillation counting as described in Methods. Under basal conditions, the receptor was labelled to a specific activity of 11.0 $\pm$ 4.0 nCi/pmol (n=2). Upon exposure to dopamine for 15 min, [^{3}H]palmitic acid incorporation was increased and receptors were labelled to a specific activity of 75.3 $\pm$ 6.3 nCi/pmol (n=2). The agonist-promoted palmitoylation of c-myc-D1 receptor was blocked by SCH-23390 and under these conditions, a specific activity of 18.3 nCi/pmol was determined for the receptor. Once more, although both quantitation methods reveal an increase in the incorporation of [^{3}H]palmitic acid, the scintillation counting of the protein band appears more sensitive in quantifying the increase. The difference may also be that the intensity of label as detected on an autoradiogram is not linear with respect to the activity of the labelled receptor measured as nCi/pmol.

To assess the nature of the attachment of [^{3}H]palmitic acid to the receptor, immunoprecipitated samples were treated with 1.0 M hydroxylamine and subsequent fluorography revealed the absence of radiolabelled bands indicating that [^{3}H]palmitate was covalently attached to the receptor by a thioester bond (lane 3). In these experiments the efficacy of receptor immunoprecipitation was 75$\pm$3%.

Fig. 10. Agonist-promoted phosphorylation of the c-myc-D1 receptor. The figure shows an autoradiogram (5 day exposure) of 9E10 immunoprecipitated c-myc-D1 receptors solubilized from membranes prepared from Sf9 cells expressing c-myc-D1 receptors, prelabelled with carrier free ^{32}P. Lane 1 represents basal labelling of c-myc-D1 receptors from cells untreated with dopamine; lane 2 represents increased incorporation of ^{32}P into c-myc-D1 receptors in cells treated for 15 min with 10 μM dopamine; lane 3 represents blockade of agonist mediated ^{32}P incorporation into c-myc-D1 receptors in cells pretreated for 15 min with 100 μM SCH-23390. This fig. is representative of three independent experiments and in this experiment $\sim$1.0 pmol of receptor was loaded per lane as determined by [^{125}I]SCH-23982 binding, described in Methods. *Reproduced, with permission, from Ng et al., Desensitization, phosphorylation and palmitoylation of the human dopamine D1 receptor, Eur. J. Pharmacol. Mol. Pharmacol. Sect. 267, 7-16, 1994.*

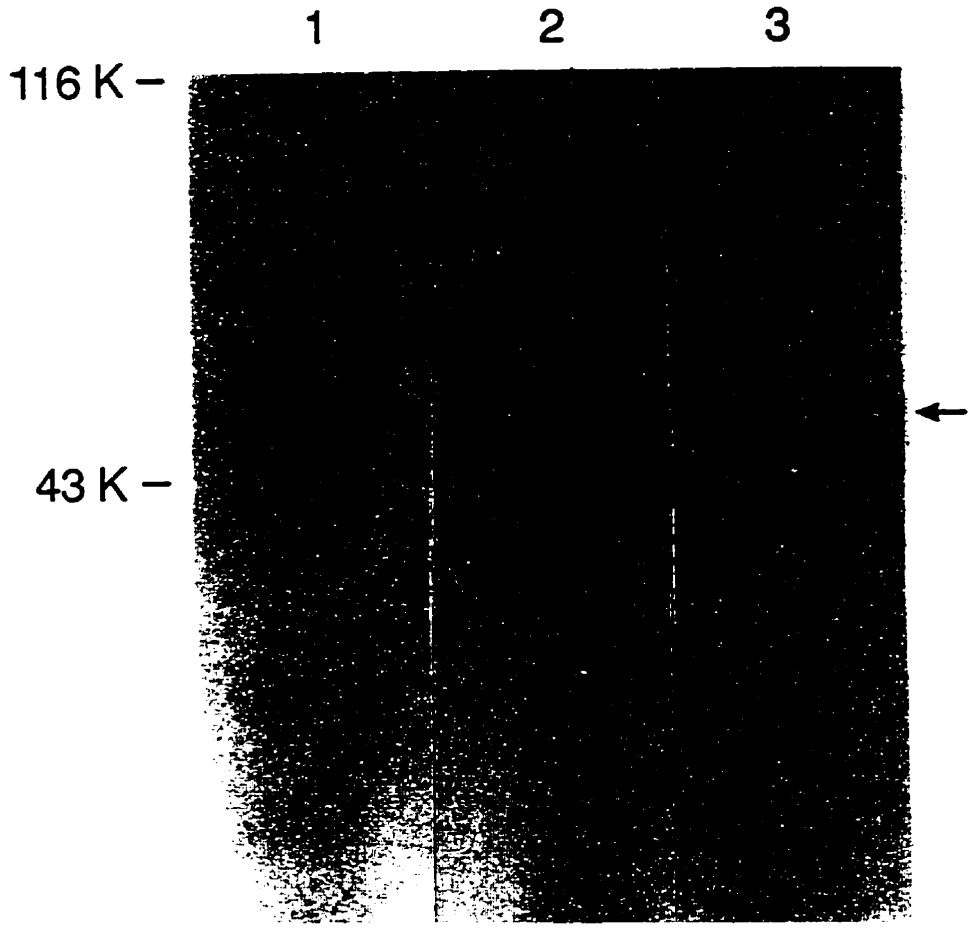
1
2
3
116 K –
43 K –

Fig. 11. Agonist-regulated palmitoylation of the c-myc-D1 receptor. Fluorograph (3 weeks exposure) of immunoprecipitated [^{3}H]palmitate labelled-c-myc-D1 receptor in the absence (lane 1) and presence of 10 μM dopamine for 15 min (lane 2). Immunoprecipitated c-myc-D1 receptor treated with 1.0 M hydroxylamine as described in methods showed no labelling (lane 3). Data shown is representative of three independent experiments. ~2 pmol of receptor was loaded in each lane as determined by [^{125}I]SCH-23982 binding as described in Methods. *Reproduced, with permission, from Ng et al., Desensitization, phosphorylation and palmitoylation of the human dopamine D1 receptor, Eur. J. Pharmacol. Mol. Pharmacol. Sect. 267, 7-16, 1994.*

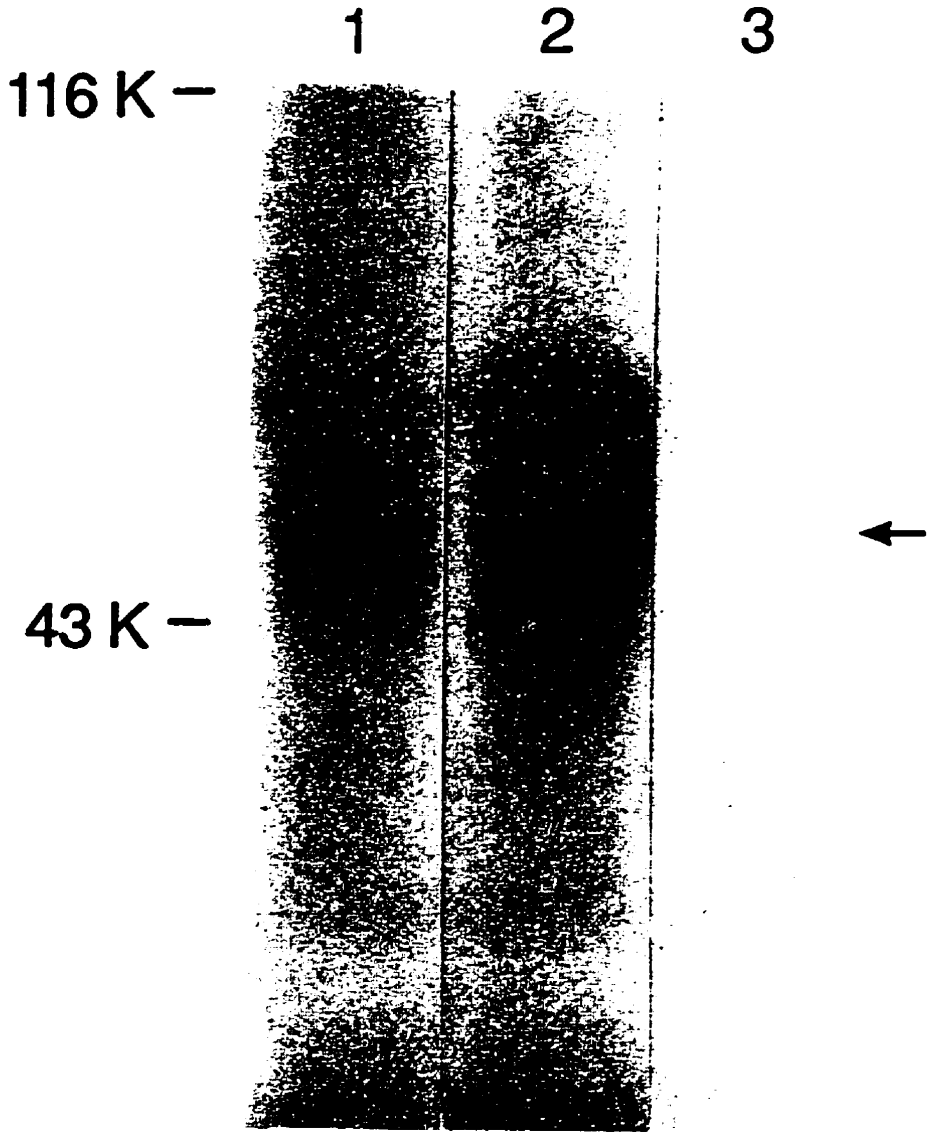
1
2
3
116 K –
43 K –

6.2.8 Agonist-induced c-myc-D1 Receptor Redistribution As Assessed by Radioligand Binding in Plasma and Light Vesicular Membrane Fractions

Agonist-induced c-myc-D1 receptor internalization was assessed by subcellular fractionation and radioligand binding. A decrease in surface plasma membrane receptors accompanied by a proportional increase in receptors in an intracellular light membrane fraction, with no change in the total number of cellular receptors indicated agonist-promoted receptor internalization. Total number of receptors in cells was defined as the sum of specific [^{3}H]SCH-23390 bound to the plasma membrane fraction added to the specific [^{3}H]SCH-23390 bound to a light vesicular membrane fraction.

In membranes prepared from vehicle-treated cells expressing c-myc-D1 receptors, the K_D value for [^{3}H]SCH-23390 binding to plasma and light membrane fractions were similar (658 $\pm$ 12 pM (n=3) and 720 $\pm$ 15 pM (n=3) respectively). No specific [^{3}H]SCH-23390 binding was detected in membranes prepared from cells infected with the wild-type baculovirus (data not shown). Dopamine/[^{3}H]SCH-23390 competition binding to c-myc-D1 receptors in the plasma membrane showed dopamine-detected high and low affinity states with proportions and affinity for dopamine (data not shown) similar to values reported for competition experiments performed on P2 membranes. These data confirmed the expected pharmacological properties of surface receptors showing coupling to G proteins. Radioligand binding determined that 52 $\pm$ 4 % (n=5) of the total cellular c-myc-D1 receptors were localized on the cell surface with the remaining pool comprising of internally located receptors in a light membrane fraction (Fig. 12). Dopamine/[^{3}H]SCH-23390 competition binding to c-myc-D1 receptors in the light vesicular

membrane fraction was best fitted to a single low-affinity state (K_i for dopamine of 866 $\pm$ 50 nM (n=4)) suggesting that this population of intracellularly located receptors was not coupled to G protein. Sustained incubations of cells expressing c-myc-D1 receptors with 10 μM dopamine brought about a time-dependent and gradual decrease in surface plasma membrane receptor density (Fig. 12). A statistically significant agonist-promoted receptor internalization of 28 $\pm$ 2% (n=5) was observed after 60 min ($P < 0.05$), and maximal 33 $\pm$ 4% (n=3) agonist-induced internalization was detected following 4-h ($P < 0.05$) incubation. Under these conditions, we could not detect any difference in the total cell receptor density between vehicle-treated and dopamine-treated cells, suggesting that this slow onset agonist-induced c-myc-D1 receptor internalization was not accompanied by down-regulation. Fig. 12 (inset) shows that preincubation of cells with 1 μM (+)-butaclamol 1 h prior to 10 μM dopamine exposure for 60 min blocked agonist-induced c-myc-D1 receptor internalization. We concluded from these data that D1 receptor internalization mechanisms are present in this cell line, and that agonist-induced D1 receptor internalization occurred temporally later than agonist-induced desensitization.

6.2.9 Agonist-induced c-myc-D1 Receptor Internalization As Assessed By Photoaffinity Labelling Photoaffinity labelling experiments using the D1 receptor specific photoaffinity label ([^{125}I]IMAB) revealed a major ~48 kDa ligand binding species in membranes prepared from vehicle-treated and dopamine-treated c-myc-D1 receptor expressing cells in agreement with the predicted molecular mass deduced from the amino acid sequence of a D1 receptor monomer (Fig. 13). Agonist treatment led to a reduction of the labelled ~48 kDa receptor species in plasma membranes (Fig. 13, compare lane 1 to lane 2) accompanied by an increase in the labelled ~48 kDa receptor species in the intracellular light vesicular membrane fraction

(Fig. 13, compare lane 3 to lane 4). These data are in good agreement with the radioligand binding data supporting the internalization of cell surface plasma membrane D1 receptors into an internal light vesicular membrane fraction following sustained agonist exposure.

Fig. 12. The effects of 10 μM dopamine treatment on the number of c-myc-D1 receptors in the plasma membrane fraction. The percentage of total cellular receptors was determined by subcellular fractionation and radioligand binding as described in methods. * signifies a significant difference ($P < 0.05$) from time zero as determined by student's *t* test. (Inset) The control vehicle-treated condition is shown in the open bar (n=3). The effect of 10 μM dopamine treatment for 60 min is shown by the solid-filled bar (n=3). The effect of preincubation with 1 μM (+)-butaclamol prior to dopamine exposure is indicated by the speckled-filled bar (n=2). Data are the mean $\pm$ SEM (n=3) or average $\pm$ SD (n=2), and is the total number of receptors in the plasma membrane fraction (% of total cellular receptors). * signifies a significant difference between dopamine-treated and vehicle-treated conditions at $P < 0.05$ as determined by student's *t* test. *Reproduced, with permission, from Ng et al., Agonist-induced desensitization of dopamine D1 receptor-stimulated adenylyl cyclase activity is temporally and biochemically separated from D1 receptor internalization, Proc. Natl. Acad. Sci. USA 92, 10157-10161, 1995.*

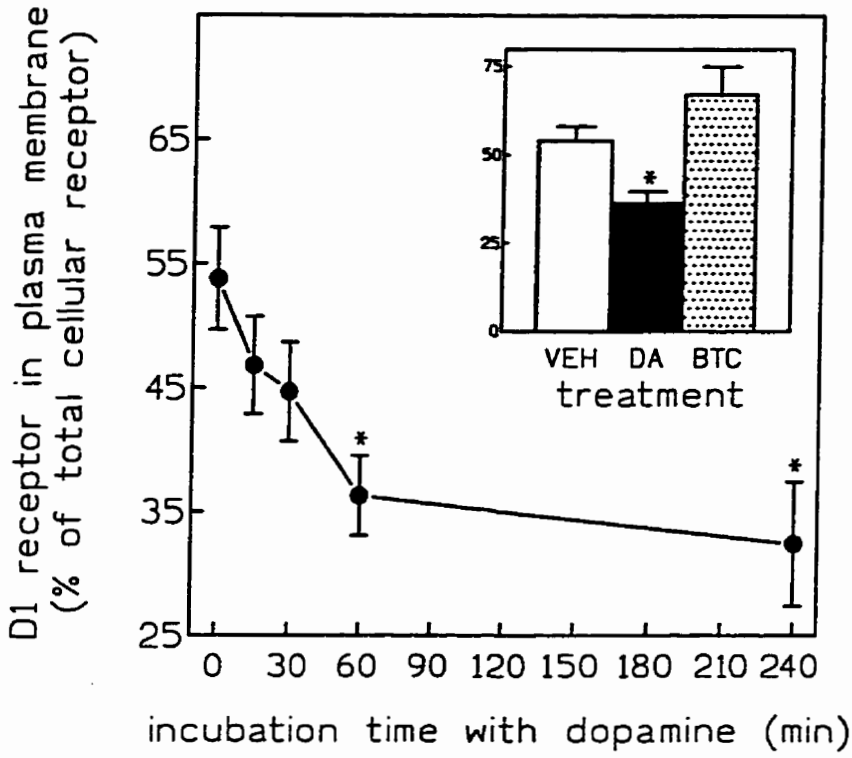
D1 receptor in plasma membrane
(% of total cellular receptor)
65
55
45
35
25
0 30 60 90 120 150 180 210 240
incubation time with dopamine (min)
*
*
75
50
25
0
*
VEH DA BTC
treatment

Fig. 13. Autoradiogram shows [^{125}I]MAB photoaffinity labelled membrane preparations electrophoresed on SDS-PAGE. Lane 1, photolabelled plasma membranes from vehicle-treated cells. Lane 2, photolabelled plasma membranes from cells preincubated with 10 μM dopamine for 4 hours. Lane 3, photolabelled light membranes from vehicle-treated cells. Lane 4, photolabelled light membranes from cells preincubated with 10 μM dopamine for 4 hours. 100 μg membrane protein was used for each labelling condition. The autoradiograms shown are from a 1 day exposure. Three independent experiments were done as described in methods to determine the specificity of the photolabel and the molecular mass of the photolabelled receptor species. *Reproduced, with permission, from Ng et al., Agonist-induced desensitization of dopamine D1 receptor-stimulated adenylyl cyclase activity is temporally and biochemically separated from D1 receptor internalization, Proc. Natl. Acad. Sci. USA 92, 10157-10161, 1995.*

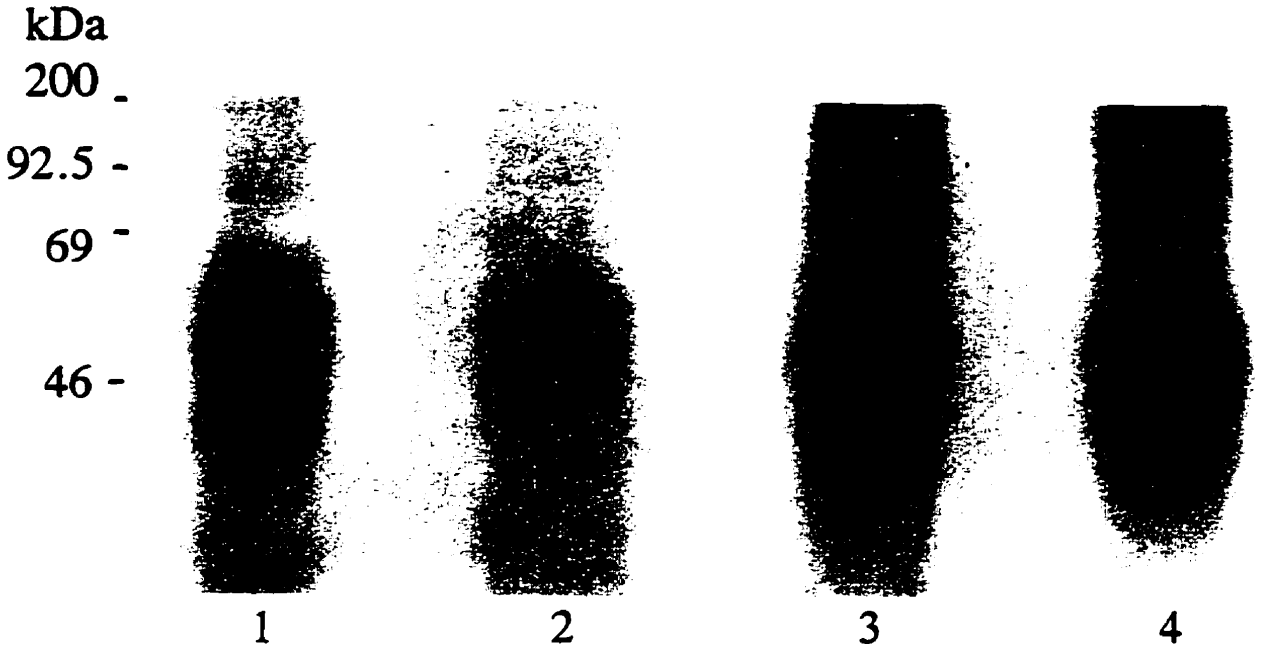
kDa
200
92.5
69
46
1
2
3
4

6.2.10 Agonist-induced Redistribution of Surface c-myc-D1 Receptors in Whole Cells As Assessed by Immunocytochemical Labelling and Conventional Fluorescence Microscopy

The surface localization of c-myc-D1 receptors expressed in Sf9 cells was examined by conventional immunofluoresence to determine if the pattern of surface receptors was affected by exposure to dopamine (Fig. 14). The 9E10 monoclonal antibody identified specific immunoreactive fluorescence in fixed Sf9 cells expressing c-myc-D1 receptors. In cells treated with dopamine for 15 min, the pattern of fluorescence changed from diffuse labelling to discrete aggregates (compare panel A to B). When the cells were pretreated with the antagonist SCH-23390 and then challenged with the agonist for 15 min, the agonist mediated effect was blocked (compare panel B to C). Following prolonged exposure for 18 h with dopamine, a significant reduction in the labelling was observed (compare panel A to D). No specific labelling was observed in control cells expressing the untagged dopamine D1 receptor or infected with the wild type baculovirus or cells treated with goat anti-mouse IgG FITC conjugate alone (data not shown). Together, the data suggested that agonist activation mediated the redistribution of surface D1 receptors.

6.2.11 Agonist-induced c-myc-D1 Receptor Redistribution in Whole Cells As Assessed by Immunocytochemical Labelling and Confocal Fluorescence Microscopy

Fixed and immunofluorescently labelled c-myc-D1/cells were imaged by confocal microscopy and the tabulation of results verified by several repetitions of the experiment (n=6). Distributed averaging protocol was used routinely for all data collection, even though in our experience, DABCO, an antibleaching agent in the mounting medium, has proven to prevent significant photobleaching during data collection of an average of 12-14 optical sections at 1.5 μm

increments and five averaged passes per cell, the parameters used in these experiments. Fig. 15 shows the cellular localization of immunofluorescently labelled c-myc-D1 receptors in vehicle-treated cells compared to cells exposed to 10 μM dopamine for 60 min through the z-axis. In nonpermeabilized vehicle-treated cells, labelled receptors appeared abundant on the cell surface appearing as a continuous bright ring of fluorescence suggesting an even and diffuse distribution (panel A). Within the ring, presumably occupied by the nucleus and cytoplasm, a total absence of intracellular fluorescence signal was noted, as expected, indicating lack of penetration of antibodies into non-permeabilized cells. On a slide preparation of cells (n = 25) from a typical experiment representative of n=6 experiments, 85-90 % of recombinant baculovirus infected cells exhibited this staining pattern, with only 10-15 % of cells exhibiting unclassified staining (including dead and ruptured cells). In contrast, non-permeabilized cells subjected to sustained dopamine exposure showed interruptions and a less intense band of fluorescence around the periphery of the cell ranging from 1 to 20 μm in length suggesting a redistribution of cell surface receptors (panel B). On a slide preparation of cells (n = 22) from a typical experiment of n=6 experiments, 75-85 % of dopamine-treated recombinant baculovirus infected cells exhibited this staining pattern with 5-7 % of cells exhibiting a ring of surface labelling and 10-18 % unclassified. Thus, the imaging of nonpermeabilized cells by confocal microscopy indicated that the agonist promoted a disappearance of cell surface D1 receptors.

In permeabilized vehicle-treated cells, labelled receptors appeared evenly distributed on the cell surface as in nonpermeabilized cells, and to a lesser extent in the cytoplasm appearing as pockets of label (Fig. 16, panel A) interspersed with areas without any staining suggesting localization in vesicles. Each cell contained a large circular area in the center of the cytoplasm,

seen in sections through the middle of the cell, without detectable fluorochrome emission presumably occupied by the nucleus. Overall, vehicle-treated cells demonstrated an internal fluorescently labelled receptor distribution near the periphery of the cell, close to the inner wall. In contrast, permeabilized cells treated with dopamine showed considerable reduction in cell surface fluorescence (panel B). The ring, when present, was less intense. Intracellularly, there appeared an increase in the aggregates of label localized deeper within the cytoplasm, closer to the unlabelled nucleus (compare panel A to B). No specific labelling was observed in permeabilized cells expressing the untagged D1 receptor (Fig. 17, panel A), cells infected with the wild-type baculovirus (panel B), wild-type Sf9 cells (panel C), or cells treated with goat anti-mouse IgG FITC conjugate alone (data not shown).

Fig. 14. Conventional fluorescence microscopy of agonist-mediated redistribution of cell surface c-myc-D1 receptors. In cells expressing c-myc-D1 receptors at 48 h post-infection, receptors were detected with the 9E10 antibody recognizing the c-myc epitope and a FITC-conjugated anti-mouse antibody as described in methods. Cells were visualized by fluorescence microscopy. (A) basal condition; (B) incubation of cells for 15 min with 10 μM dopamine; (C): incubation for 15 min with 100 μM SCH-23390 followed then by 15 min with 10 μM dopamine, and (D): incubation for 18 h with 10 μM dopamine. All experiments were performed in parallel using the same culture and photographs were taken under identical exposure conditions. *Reproduced, with permission, from Ng et al., Desensitization, phosphorylation and palmitoylation of the human dopamine D1 receptor, Eur. J. Pharmacol. Mol. Pharmacol. Sect. 267, 7-16, 1994.*

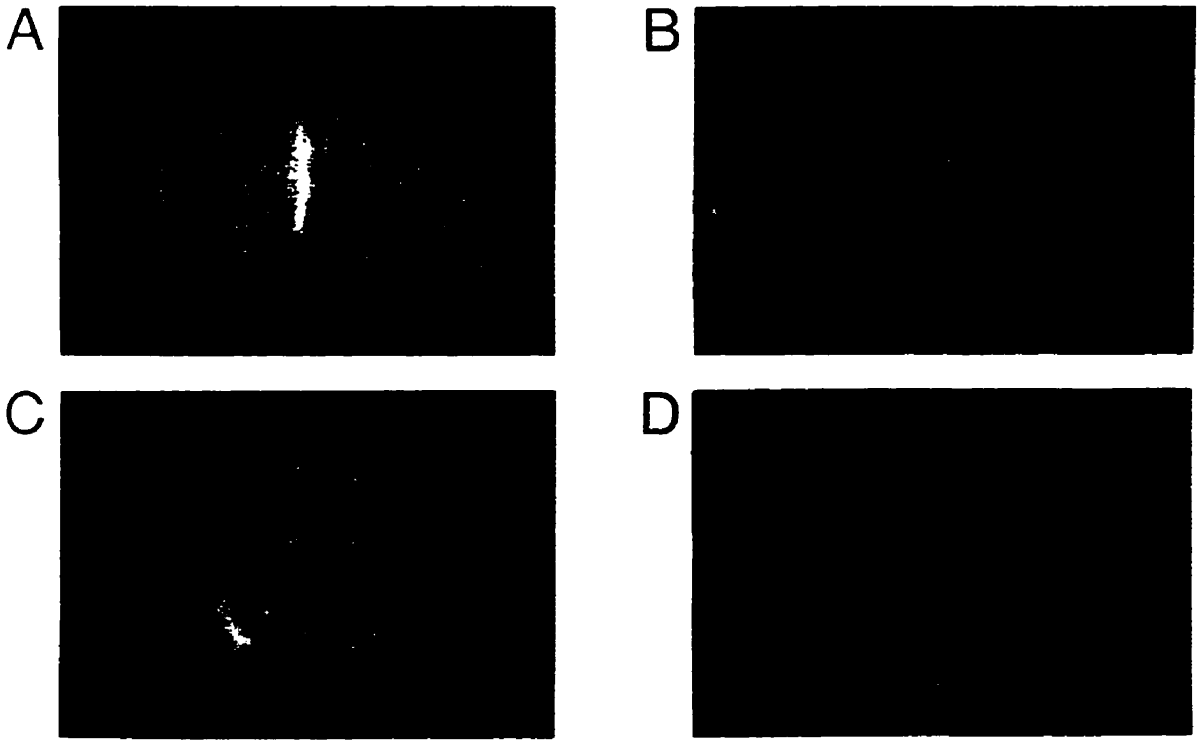
A
B
C
D

Fig. 15. Confocal microscopy of immunofluorescently labelled nonpermeabilized agonist-treated c-myc-D1/cells. c-myc-D1 receptors were labelled with the 9E10 antibody specific for c-myc, and a secondary FITC antibody. In nonpermeabilized c-myc-D1/cells, the receptors are localized on each cell's surface. Two sets are displayed. Each set shows six optical sections through the z-axis, progressing sequentially from left to right in two rows, from a series containing 12 images recorded at 1.5-μm intervals. Both cells were imaged with identical microscope settings. (A) Nonpermeabilized c-myc-D1/cell under basal conditions, showing a continuous ring of c-myc D1 receptors in each section with minor intensity variations at the top of the cell. (B) Nonpermeabilized c-myc-D1/cell after treatment with dopamine, displaying gaps in the circular distribution. Arrows denote differences between A and B. Bars = 10 μm. *Reproduced, with permission, from Trogadis et al., Dopamine D1 receptor distribution in Sf9 cells imaged by confocal microscopy: A quantitative evaluation, The Journal of Histochemistry and Cytochemistry 43, 497-506, 1995.*

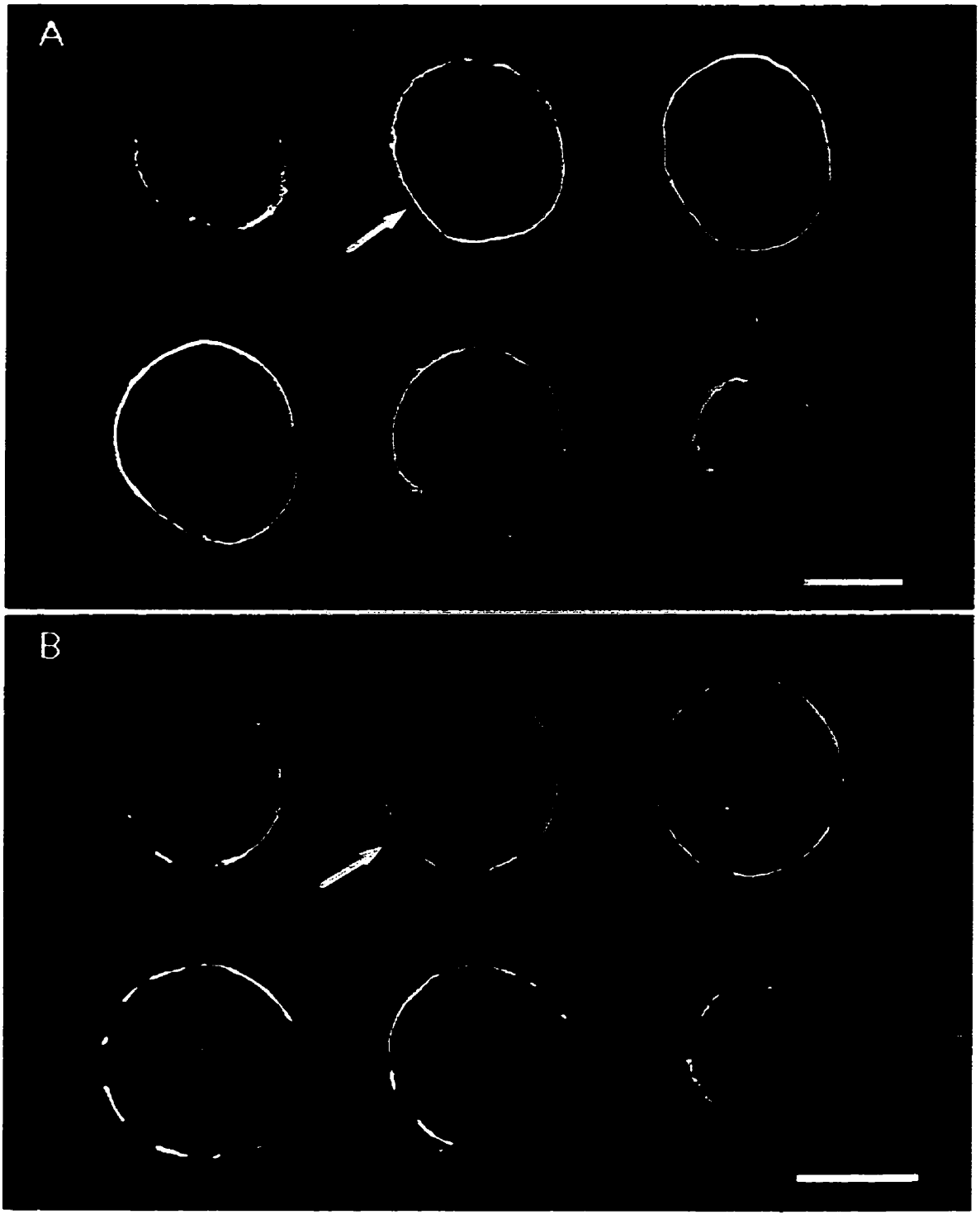
A
B

Fig. 16. Confocal images of immunofluorescently labelled permeabilized agonist-treated c-myc-D1/cells. c-myc-D1 receptors were labelled with the 9E10 antibody specific for c-myc, and a secondary FITC antibody. In permeabilized c-myc-D1/cells, receptors are seen on the cell's surface as well as in clusters intracellularly. The nucleus, a dark area in the center of each cell, contains no label. Two sets are displayed. Each set shows six optical sections through the z-axis, progressing sequentially from left to right in two rows, from a series containing 12 images recorded at 1.5-μm intervals. Both cells were imaged with identical microscope settings. (A) Under basal conditions, with clusters localized close to the cell's surface. (B) After treatment with dopamine, showing less intense peripheral distribution and clusters localized deeper intracellularly. *Reproduced, with permission, from Trogadis et al., Dopamine D1 receptor distribution in Sf9 cells imaged by confocal microscopy: A quantitative evaluation, The Journal of Histochemistry and Cytochemistry 43, 497-506, 1995.*

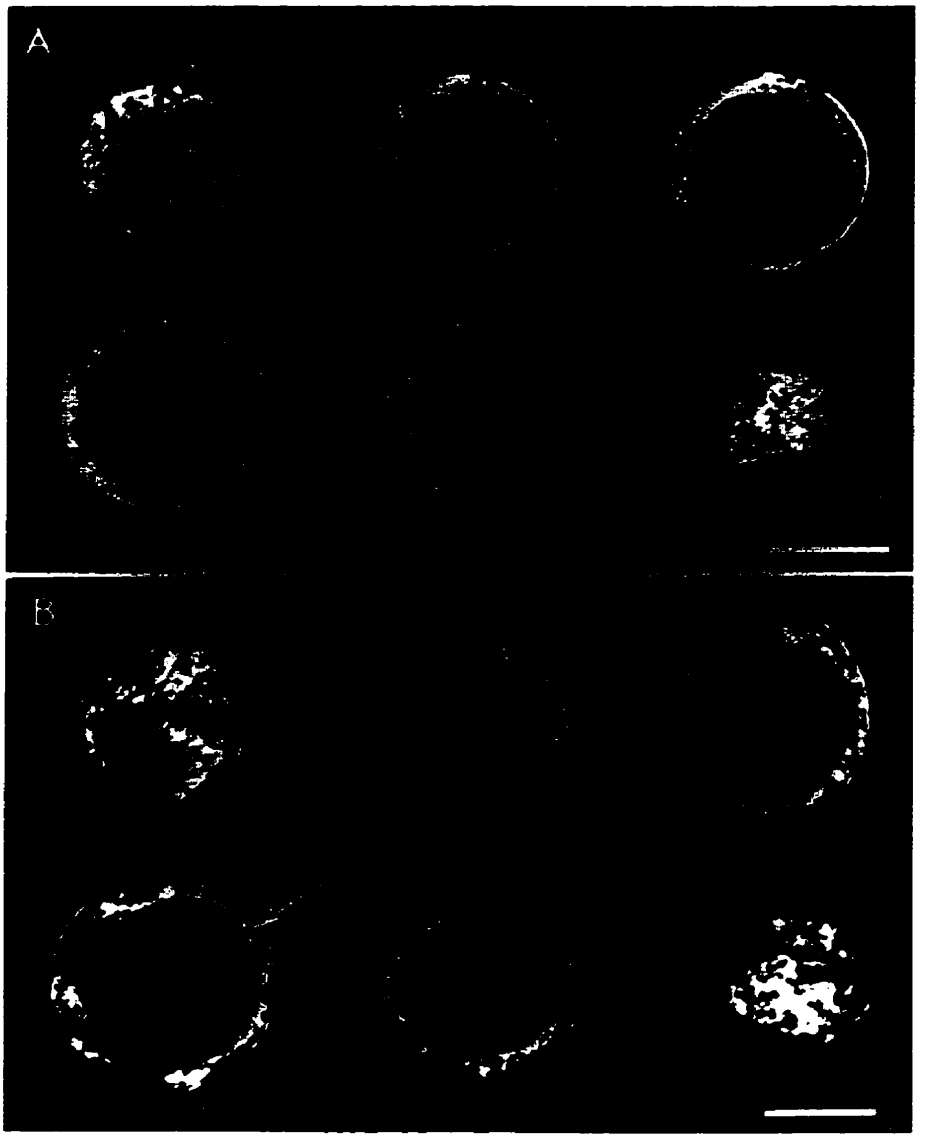
A
B

Fig. 17. Confocal images of immunofluorescently labelled control Sf9 cells. (A) Staining of Sf9 cells expressing non-tagged D1 receptors. (B) Staining of wild-type Sf9 cells. (C) Staining of Sf9 cells infected with wild-type baculovirus. All cells show negligible background staining under identical illumination conditions used in all experiments. Bars = 10 μm. *Reproduced, with permission, from Trogadis et al., Dopamine D1 receptor distribution in Sf9 cells imaged by confocal microscopy: A quantitative evaluation, The Journal of Histochemistry and Cytochemistry 43, 497-506, 1995.*

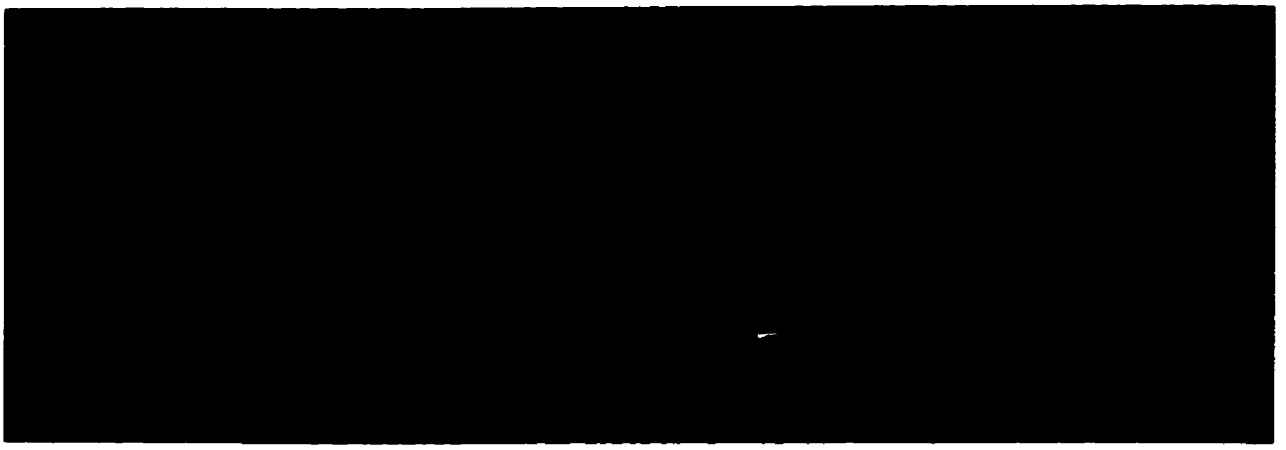

6.2.12 Three-dimensional Assessment of c-myc-D1 Receptor Distribution in Whole Cells

Three-dimensional reconstructions also produced an invaluable visual description of the experimental results. Multiple repeated reconstructions were carried out, and a non-permeabilized vehicle-treated c-myc-D1/cell is shown in Fig. 18A. Segmentation of the brightest pixel values corresponded precisely to the bright ring along the periphery of each section, representing the location of label. Green was selected to represent fluorescently labelled receptors, and these covered the entire surface of the cell. This is expected since a bright continuous fluorescent ring is seen in every confocal image. Slight irregularities and indentations of the outline reflected the contour of the cell surface, and two small holes at the top of this cell allowed a brief view of the cytoplasm, seen in white. The non-permeabilized, dopamine-treated cell shown in Fig. 15B has been reconstructed to reveal a patchy pattern of label (Fig. 18B). Single cross-sections do not adequately describe the overall spatial pattern of the bare patches with respect to size, location and frequency. The reconstructed cell showed fewer and larger areas of receptor loss rather than small diffuse series of holes as the single sections may indicate. The green color represents receptors, their distribution exposing the white soma.

Fig. 18C is a reconstructed image of the vehicle-treated permeabilized cell whose confocal slices are shown in Fig. 16C. The top of the cell has been cut away to reveal intracellular components such as the receptors (green), the nucleus (orange), and the soma (white). Segmentation of the brightest pixels in the two-dimensional images showed c-myc D1 receptors around the outside of the cell and, in addition, intracellularly close to the cell membrane. Few receptor clusters were located in the fullest area of the soma. In contrast, in

Fig. 18D, a reconstruction of the dopamine-treated cell shown in Fig. 16B, had few c-myc D1 receptors (green) on the periphery of the cell, most having translocated to a perinuclear location (orange nucleus). The posterior section of the cell surface is retained. Since the images can be interactively positioned in any arbitrary plane, other viewing angles could have been selected and any partial surface displayed. As only pixels of the highest intensity levels were segmented to obtain this image, the peripheral fluorescent ring seen in the two-dimensional slices is only partially visible in the three-dimensional reconstruction because pixel values at the outer surface of the cell were less intense, i.e., they had a lower density of labelled c-myc D1 receptors than the internal volume. These results were consistent with findings of radioligand-binding studies suggesting an agonist-promoted internalization of surface D1 receptors.

Fig. 18. Three-dimensional reconstruction of agonist-treated c-myc-D1/cells. The brightest pixel intensities were selected and reconstructed to show receptors. Low-intensity pixels representing nonspecific staining were reconstructed to show the white cytoplasm. (A, B) The non-permeabilized cells seen in Fig. 15. (A) under basal conditions and (B) after treatment with dopamine, showing a different pattern of fluorescently labelled receptor distribution. (C, D) The permeabilized cells shown in Fig. 16. In addition to the white soma and green receptors, the area in the center of each cell, devoid of any fluorescence labelling, was manually traced and reconstructed to represent the nucleus (orange). The surface of the cell body has been cut away to reveal intracellular receptors and a large nucleus. (C) Cell under basal conditions. (D) After treatment with dopamine. *Reproduced, with permission, from Trogadis et al., Dopamine D1 receptor distribution in Sf9 cells imaged by confocal microscopy: A quantitative evaluation, The Journal of Histochemistry and Cytochemistry 43, 497-506, 1995.*

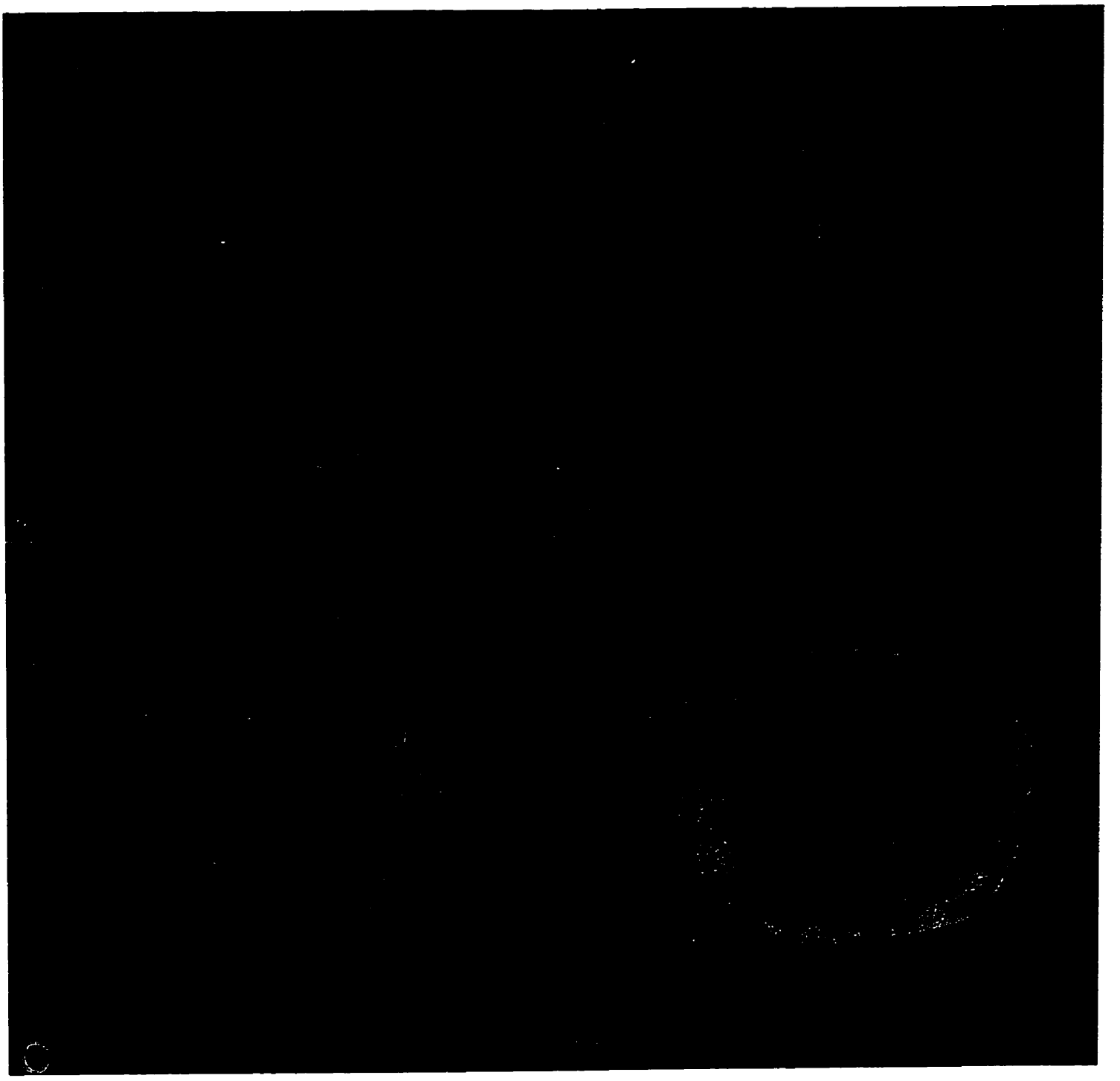

6.2.13 Agonist-induced c-myc-D1 Receptor Internalization As Assessed by Immunoblot Analysis

Immunoblot analysis of cell surface membranes from vehicle-treated cells expressing c-myc-D1 receptors revealed the presence of a ~48 kDa species possibly representing a receptor monomer and a second species at approximately twice the molecular mass ~110 kDa, the nature of which may be a receptor dimer (Fig. 19, lane 1). Sustained preincubation with 10 μM dopamine brought about a loss of the ~48 kDa species with somewhat lesser change in the ~110 kDa receptor species (Fig. 19, lane 2). These immunological studies confirmed that agonist induced D1 receptor protein internalization occurred, as demonstrated also by [^{3}H]SCH-23390 binding, photoaffinity labelling, and whole cell immunofluorescence labelling.

6.2.14 Inhibition of Agonist-induced c-myc-D1 Receptor Internalization by Concanavalin A Does Not Prevent Desensitization

Concanavalin A and hypertonic concentrations of sucrose have been shown to inhibit β_2-adrenergic receptor internalization without affecting the pharmacological properties of the expressed receptors (Waldo et al., 1983, Yu et al., 1993). Preincubation of c-myc-D1 receptor expressing cells with concanavalin A or sucrose blocked agonist-mediated receptor internalization (Fig. 20). Interestingly, in concanavalin A-treated c-myc-D1/cells, we observed a significant 29% increase in cell surface receptor density over control values. Sucrose-treatment had a similar but smaller increase (22%) in surface receptor density. Although direct evidence is lacking, we interpreted these data to show that cellular populations of receptors undergo cycling between membrane compartments even in the absence of agonist, so that inhibition of the internalization pathway may be expected to result in an accumulation of surface receptors.

In order to investigate D1 receptor internalization further, we examined the effects of dopamine exposure on concanavalin A-treated c-myc-D1/cells. Agonist treatment led to a marked 47% decrease in the maximal dopamine stimulated adenylyl cyclase activity (Vmax for control, 158.0 $\pm$ 14.1 (n=4); concanavalin A- and dopamine-treated, 85.2 $\pm$ 6.0 (n=4), $P < 0.01$), and significant loss of potency of dopamine (EC_{50} for control, 30 $\pm$ 5 (n=4); concanavalin A- and dopamine- treated, 290 $\pm$ 30 (n=4), $P < 0.01$). These observations provided convincing evidence that D1 receptor internalization and functional uncoupling were biochemically dissociable events that may represent two distinct mechanisms responsible for adaptation to sustained stimuli.

Fig. 19. Immunoblot of P2 plasma membranes prepared from agonist-treated c-myc D1/cells. Membranes (100 μg protein) were solubilized in SDS buffer, electrophoresed, and electroblotted onto nitrocellulose as described in methods. Lane 1, membranes from vehicle-treated cells. Lane 2, membranes from cells preincubated with 10 μM dopamine for 60 min. *Reproduced, with permission, from Ng et al., Agonist-induced desensitization of dopamine D1 receptor-stimulated adenylyl cyclase activity is temporally and biochemically separated from D1 receptor internalization, Proc. Natl. Acad. Sci. USA 92, 10157-10161, 1995.*

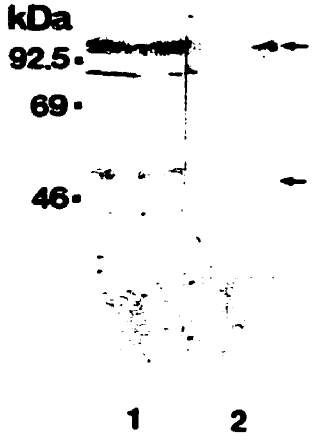
kDa
92.5
69
46
1
2

Fig. 20. Biochemical separation of agonist-induced c-myc-D1 receptor internalization and desensitization. (A) D1 receptor density in the plasma membrane fraction (% of total cellular receptors) was determined by differential centrifugation and radioligand binding as detailed in methods. The effect of vehicle (Veh), 10 μM dopamine treatment for 60 min (DA), and pretreatment with concanavalin A (con A) and sucrose (Suc) on dopamine-induced D1 receptor internalization are indicated. Data shown is the mean $\pm$ SEM (n=3). *, $P < 0.05$ when compared to values obtained for vehicle conditions. **, $P < 0.01$ when compared to values obtained for vehicle conditions. (B) Dose-response for D1 receptor-mediated dopamine stimulated adenylyl cyclase activity in P2 membranes prepared from vehicle-treated cells (●) compared to cells preincubated with concanavalin A prior to being treated with 10 μM dopamine for 60 min (*) as described in methods. All membranes were prepared from cells at 48-h post-infection. Data shown is representative of 4 independent experiments. *Reproduced, with permission, from Ng et al., Agonist-induced desensitization of dopamine D1 receptor-stimulated adenylyl cyclase activity is temporally and biochemically separated from D1 receptor internalization, Proc. Natl. Acad. Sci. USA 92, 10157-10161, 1995.*

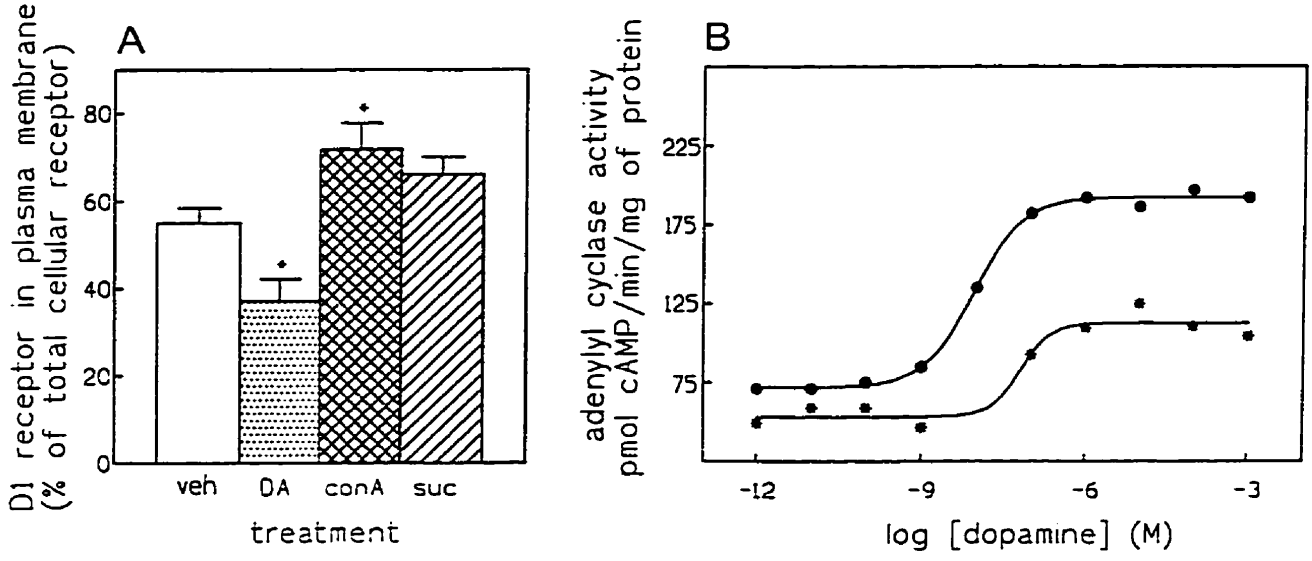
A
D1 receptor in plasma membrane
(% of total cellular receptor)
80
60
40
20
0
veh
DA
conA
suc
treatment
B
adenylyl cyclase activity
pmol cAMP/min/mg of protein
225
175
125
75
-12
-9
-6
-3
log [dopamine] (M)

6.3 Pharmacological and Biochemical Characterization of the D2L Receptor

6.3.1 Ligand Binding Properties of Expressed D2L Receptors

Figure 21A shows the saturation isotherms of [^{3}H]YM-09151-2 (also termed nemonapride) and [^{3}H]spiperone binding to the same membrane preparation from Sf9 cells expressing D2L receptors at 72-h after infection. [^{3}H]YM-09151-2 and [^{3}H]spiperone each bound saturably with mean K_D values of 238 $\pm$ 9 pM (n=3) and 334 $\pm$ 12 pM (n=3), respectively. The apparent receptor density, B_{max} (pmol/mg of protein), determined by [^{3}H]YM-09151-2 was 2.6 $\pm$ 0.4 (n=3). This was two-fold higher than the receptor density estimated by [^{3}H]spiperone at 1.1 $\pm$ 0.2 (n=3) in the same membrane preparation. These findings are in good agreement with receptor density data previously obtained from D2L receptor expressing cultured cells (Seeman et al., 1992), rat and porcine anterior pituitary tissues (Niznik et al., 1985, Terai et al., 1989), human postmortem tissue (Seeman et al., 1992) and PET studies (Wong et al., 1993). Sf9 cells infected with wild-type baculovirus did not show any specific [^{3}H]YM-09151-2 and [^{3}H]spiperone binding (data not shown) indicating that [^{3}H]YM-09151-2 and [^{3}H]spiperone bound only to expressed D2L receptors.

Antagonist competition of [^{3}H]spiperone binding to membranes prepared from D2L/cells was best fitted to a single antagonist-recognized affinity state of the receptor. The rank order of antagonist potencies was haloperidol > (-)sulpiride > clozapine > ketanserin > SCH-23390, as shown in Fig. 21B. These compounds were chosen based on previous reports for their abilities to discriminate between D1-like and D2-like receptors. These radioligand binding data indicated that the expressed D2L receptor in Sf9 cells exhibited a D2 receptor pharmacological rank order as described for the human D2L receptor expressed in mammalian cells (Bunzow et

al., 1988, Sokoloff et al., 1990).

6.3.2 D2L Receptor Coupling with Endogenous G Proteins

Dopamine competition of [^{3}H]spiperone binding in the absence of the nonhydrolysable GTP analog, Gpp(NH)p, was best fitted to a two-site model, indicating two affinity states of the expressed D2L receptor as shown in Fig. 21C. The dopamine-detected high-affinity receptor state and proportion of sites were similar to D2L receptors expressed in mammalian cell lines (Castro and Strange, 1993) (Table 5). The dopamine-detected high-affinity receptor state was sensitive to guanine nucleotides as shown by the rightward shift of the displacement curve and the complete conversion to a low-affinity state of the receptor (Fig. 21C and Table 5). These results suggested that the D2L receptor interacted with endogenous GTP sensitive G-proteins in Sf9 cells and the nature of this interaction was next examined.

Dopamine competition of [^{3}H]spiperone binding in membranes from cells expressing the D2L receptor pretreated with 1 or 2 μg/ml pertussis toxin was still best-fitted to a two-site model. One interpretation of these data might be that D2L receptors are coupled to endogenous G proteins which are not likely substrates for pertussis toxin. The most likely explanation is that expressed D2L receptors couple to both toxin-sensitive and insensitive G proteins in Sf9 cells as also demonstrated in neuronal tissues (Neve et al., 1992, Montmayeur et al., 1993).

Fig. 21. Radioligand binding studies on membranes from D2L/cells. Specific radioligand binding was defined as binding inhibited by 1 μM (+)-butaclamol. (A) Saturation isotherms of [^{3}H]spiperone and [^{3}H]YM-09151-2 specific binding in the same membrane preparation. The results shown are from one of three independent experiments, and in this experiment, B_{max} (pmol/mg of protein) and K_D (pM) are as follows: [^{3}H]spiperone (o), B_{max} = 1.2, K_D = 327; for [^{3}H]YM-09151-2 (▵), B_{max} = 2.2, K_D = 238. (B) Competition curves are shown for inhibition of specifically bound [^{3}H]spiperone by dopamine receptor antagonists, as follows: haloperidol (•); sulpiride (*); clozapine (■); ketanserin (♦); and SCH-23390 (▲). (C) Inhibition of [^{3}H]spiperone binding by dopamine in the absence (o) and in the presence (•) of guanine nucleotide Gpp(NH)p. The curves are the mean of three independent experiments statistically determined by LIGAND and values are given in Table 5. *Reproduced, with permission, from Ng et al., Phosphorylation and palmitoylation of the human D2L receptor in Sf9 cells, Journal of Neurochemistry 63, 1589-1595, 1994.*

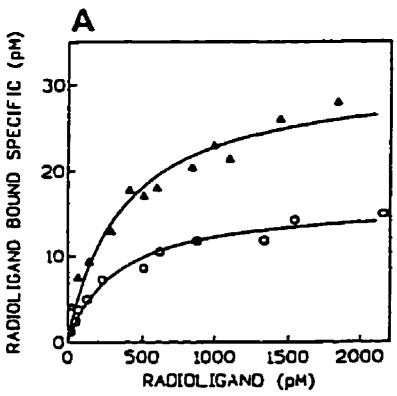
A
RADIOLIGAND BOUND SPECIFIC (pM)
30
20
10
0
0
500
1000
1500
2000
RADIOLIGAND (pM)

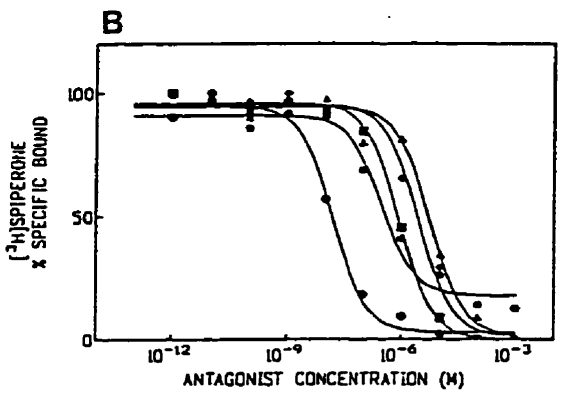
B
[3H]SPIPERONE
% SPECIFIC BOUND
100
50
0
10-12
10-9
10-6
10-3
ANTAGONIST CONCENTRATION (M)

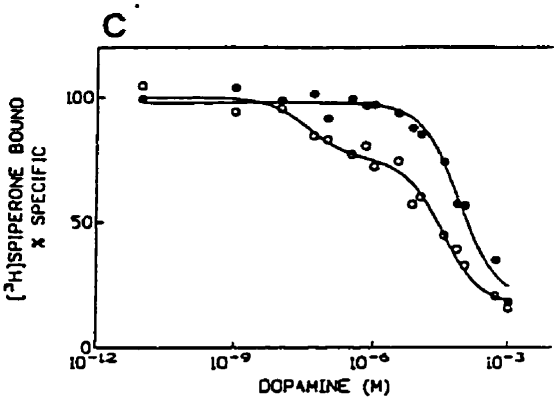
C
[3H]SPIPERONE BOUND
% SPECIFIC
100
50
0
10-12
10-9
10-6
10-3
DOPAMINE (M)

Table 5. Dopamine dissociation constants for the human D2L receptor expressed in eukaryotic cell lines. Binding to crude membranes prepared from Sf9 cells expressing the human D2L receptor at 72 h after infection. Dopamine K_i values for high ($_h$)- and low ($_l$)-affinity states, and the proportion of low-affinity sites ($\%_l$) for the two-site fit in the absence and in the presence of guanine nucleotide (GN) are given and were statistically determined by LIGAND analysis. Nonspecific binding was defined by 1 μM (+)-butaclamol. Dopamine K_i values for the D2L receptor expressed in mammalian cell lines are given for comparison. [a]Castro and Strange (1993).

		Sf9	n	Ltk 59[a]	CHO[a]
$Dopamine_h$	K_i (nM)	25.1 ± 4.6	3	8.0 ± 3.0	29.5 ± 5.9
$Dopamine_l$	Ki (nM)	15400 ± 58	3	960 ± 180	3480 ± 780
$\%_l$		72 ± 5	3	75	52
Dopamine+GN	K_i (nM)	14000 ± 180	3	990 ± 230	1470 ± 120

6.3.3 Identification of Multiple D2L Receptor Species

Immunoblot analysis using the D2 receptor-specific AL-26 antibody detected the presence of major immunoreactive species preexisting at ~44 and ~90 kDa in crude membranes from D2L/cells (Fig. 22A). The ~44 kDa molecular mass band identified likely represents an unglycosylated D2L receptor monomer based on its predicted molecular size of a 444 amino acid protein. The ~90 kDa molecular mass band, of approximately twice the size of the D2L receptor monomer, may represent a receptor dimer or a receptor-G protein complex as neither possibility could be rigorously excluded by this assay. These proteins however were not substrates for pertussis toxin-catalysed [^{32}P]ADP-ribosylation (data not shown), and the molecular mass of these species was not affected following treatment with GTPγS (Fig. 22). We interpreted these findings to be suggestive that the ~90 kDa species did not represent receptor-G protein complexes. Further, the glycan nature of the ~90 kDa ligand-binding species was not significant as PNGase F treatment had negligible effect on altering the migration of this species on SDS-PAGE (Fig. 23). The most likely interpretation of these data was that D2L receptors exist as monomers and dimers.

Fig. 22. Effects of guanine nucleotide treatment on the SDS-PAGE mobility of D2L receptors. P2 membranes prepared from D2L/cells at 72 h post-infection were incubated in the absence (-) or in the presence of 100 μM GTPγS (GN) (+) for 1 h at 21 °C. Membranes were solubilized in SDS buffer, electrophoresed, and electroblotted onto nitrocellulose, and immunoreactivity was revealed with a goat anti-rabbit IgG conjugated to alkaline phosphatase as described in Methods. The molecular mass (kDa) of protein standards is shown.

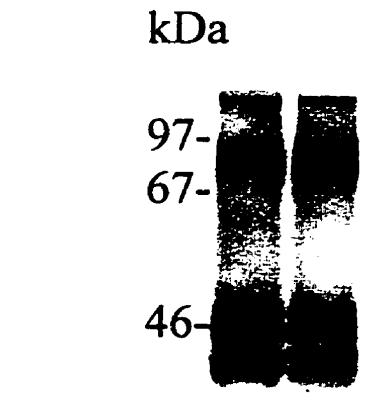
kDa
97-
67-
46-
GTPγS - +

Fig. 23. Effects of deglycosylation treatments on the SDS-PAGE mobility of D2L receptors. P2 membranes were prepared from D2L/cells at 72 h post-infection and photoaffinity labelled with [^{125}I]YM-01915-2, and incubated in the absence (-) or presence (+) of the glycosidase as described in Methods. Membranes were solubilized in SDS buffer and electrophoresed, gels dried and exposed to Kodak X-AR film for 12 h before developing. The molecular mass (kDa) of protein standards is shown.

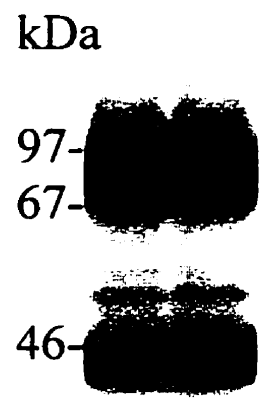
kDa
97-
67-
46-
PNGase F - +

6.3.4 Biophysical Properties of Dopamine Receptor Dimers

Immunoblot analysis showed that immunoprecipitated ~44 kDa D2L monomer and ~90 kDa dimer were stable in the presence of sodium dodecyl sulphate (SDS) and reducing agent (β-mercaptoethanol) (Fig. 24A). The dissociation of the D2L dimer to monomer was accomplished in a dose-dependent manner upon addition of the hydrophobic D2-TM VI peptide (aa 375-394) (Fig. 24A) or D2-TM VII peptide (aa 407-426) (Fig. 24B). Both D2-TM VI and VII peptides, containing no strongly polar residues, had similar ability to dissociate D2L dimers immunoprecipitated from a human caudate preparation as well (Fig. 24C). It should be noted that at the time of this writing, a D2L dimer disrupting effect was also observed for a peptide derived from the TM IV domain of the D2 receptor (data not shown). A small increase in the molecular mass of receptor monomer in samples coincubated with peptide was noted, which may be attributed to the formation of a peptide-D2L receptor heterodimer. Peptide actions were receptor and site-specific since no disruption of D2L dimers was observed under identical experimental conditions using the hydrophilic D2-C III_A peptide (aa 244-263) and D2-C III_B peptide (aa 284-303) derived from the third cytoplasmic loop of the D2 receptor, or a hydrophobic peptide (aa 276-296) corresponding to the TM-VI region of the β_2-adrenergic receptor (β_2-AR), or two peptides derived from the carboxyl tail of the D1 receptor (aa 369-383 and aa 416-431) (Fig. 24D). In addition, no dissociation of immunoprecipitated human dopamine D1 and serotonin 5-HT_{1B} receptor dimers was observed with the D2-TM VII peptide (Fig. 24F). The ability of TM VI and VII peptides to disrupt D2L dimers could be attributed to peptide-induced interference with the TM domains which participate at the dimer interface. Alternatively, it is possible that these peptides act by disrupting the 3-dimensional conformation of the receptor monomer,

resulting in the disruption of D2L dimers or inhibition of dimer formation. Taken together, these data are consistent with a model that D2L dimers exist in association-dissociation equilibrium with monomers involving receptor subtype-specific noncovalent interactions between TM regions. Consistent with this concept, D2L dimers dissociate as a function of increasing temperature (Fig. 24F) or in the presence of acid (approximate pH 3) (Fig. 24G). We conclude that D2L dimerization and possibly the dimerization of other GPCRs is mediated at the protein level involving specific intermolecular, noncovalent, electrostatic interactions of residues within TM α-helices.

Fig. 24. Biophysical characterization of D2L receptors. D2L monomers and dimers are indicated by arrows. (A) The dose-response (n=3) for the interaction between the D2-TM VI peptide (aa 375-394) and D2L receptors (lanes 1-4). (B) The dose-response (n=3) for the interaction between D2-TM VII (aa 407-426) peptide and D2L receptors (lane 1-7). (C) The effects of the D2-TM VI and D2-TM VII peptides on D2 receptors from human caudate nucleus (sample CBTB #1271). D2L receptors were incubated in peptide buffer (lane 1) and presence (lane 2) of D2-TM VI peptide, and in peptide buffer (lane 3) or presence of the D2-TM VII peptide. (D) Effects of hydrophilic and hydrophobic receptor peptides on an identical D2L receptor preparation. D2L receptors were incubated in peptide buffer (lane 1) or presence of D2-C III_A peptide (aa 244-263) (lane 2), D2-C III_B peptide (aa 284-303) (lane 3), β_2-AR TM VI peptide (aa 276-296) (lane 4), D1-C III_A peptide (aa 369-383) (lane 5) and D1-C III_B peptide (aa 416-431) (lane 6). This blot has been repeated twice. (E) Effects of D2-TM VII peptide on c-myc epitope-tagged human dopamine D1 receptor and c-myc epitope-tagged human serotonin 5-HT_{1B} receptor. D1 receptors were incubated in peptide buffer without (lane 1) or with (lane 2) of D2-TM VII peptide, and 5-HT_{1B} receptors were incubated in peptide buffer without (lane 3) or with (lane 4) D2-TM VII peptide. A representative of 3 blots is shown. (F) Stability of the D2L dimer at various incubation temperatures. D2L receptors were incubated at 23 °C (lane 1), 37 °C (lane 2), 65 °C (lane 3), and 90 °C (lane 4). This blot is representative of 3 experiments. G, Stability of the D2L dimer in various acids. D2L receptors were incubated in H_2O (lane 1), 0.1 N tartaric acid (lane 2), 0.1% glacial acetic acid (lane 3), or 0.1 N HCl (lane 4). This experiment is representative of 3 replicates.

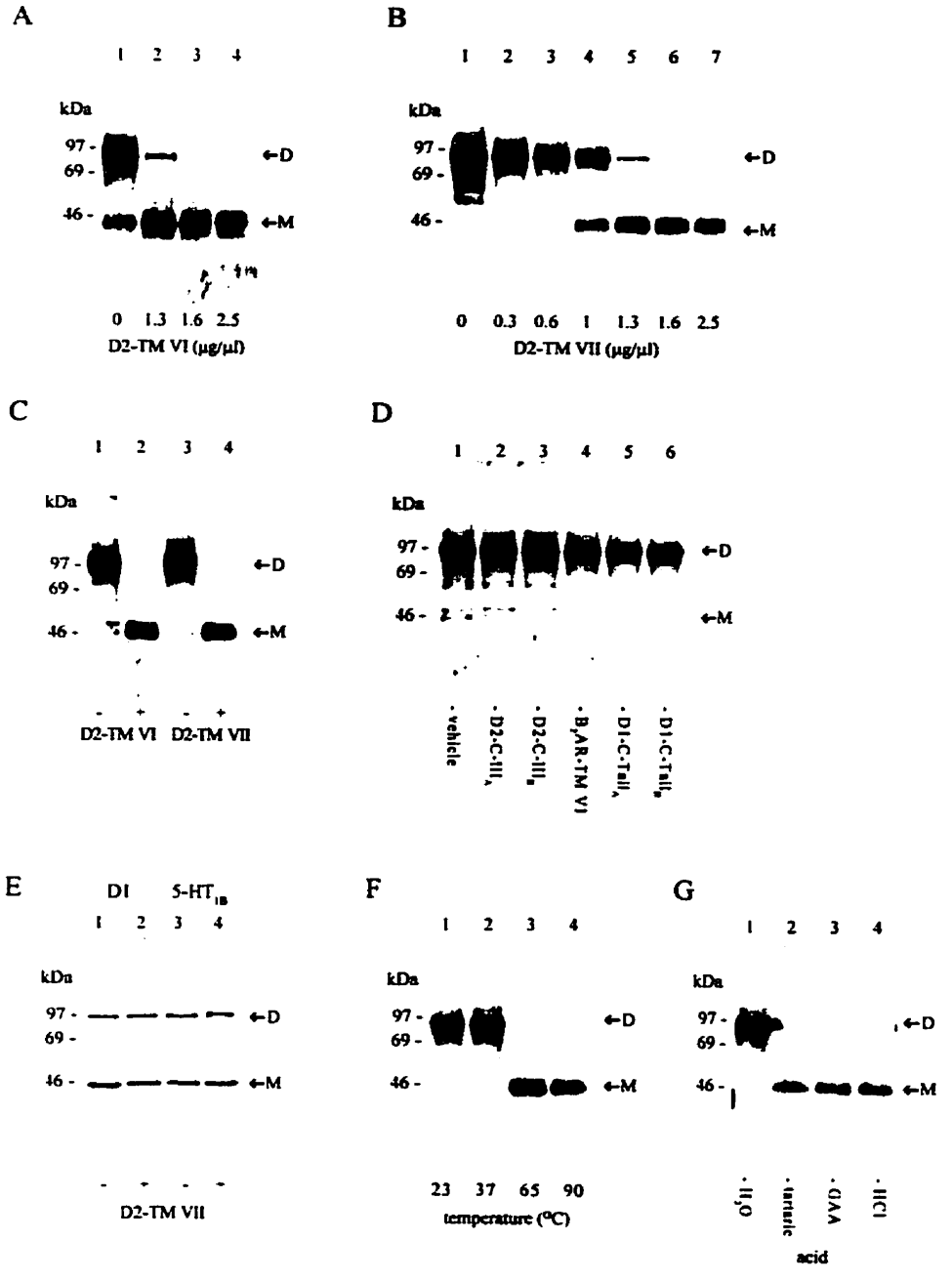
A
1 2 3 4
kDa
97 -
69 -
46 -
←D
←M
0 1.3 1.6 2.5
D2-TM VI (μg/μl)
B
1 2 3 4 5 6 7
kDa
97 -
69 -
46 -
←D
←M
0 0.3 0.6 1 1.3 1.6 2.5
D2-TM VII (μg/μl)
C
1 2 3 4
kDa
97 -
69 -
46 -
←D
←M
- + - +
D2-TM VI D2-TM VII
D
1 2 3 4 5 6
kDa
97 -
69 -
46 -
←D
←M
- vehicle
- D2-C-III$_A$
- D2-C-III$_B$
- β_2AR-TM VI
- D1-C-Tail$_A$
- D1-C-Tail$_B$
E
D1 5-HT$_{1B}$
1 2 3 4
kDa
97 -
69 -
46 -
←D
←M
- + - -
D2-TM VII
F
1 2 3 4
kDa
97 -
69 -
46 -
←D
←M
23 37 65 90
temperature (°C)
G
1 2 3 4
kDa
97 -
69 -
46 -
←D
←M
- H_2O
- tartaric
- AcOH
- HCl
acid

6.3.5 Ligand Binding Properties of D2L Receptor Monomer and Dimer

We have already shown that in the same membrane preparation from D2L/cells, the benzamide D2 antagonist [^{3}H]YM-09151-2 detected ~1.5-2 fold the receptor density estimated by the butyrophenone D2 antagonist [^{3}H]spiperone believed to represent binding to different D2L receptor species (Fig. 25A). The receptor species-specificity of these ligands was clarified by photoaffinity labelling experiments performed using [^{125}I]N-p-azidophenethylspiperone ([^{125}I]NAPS) and [^{125}I]4-azido-5-YM-09151-2 ([^{125}I]YM-09151-2). As observed in Fig. 25B, [^{125}I]NAPS labelled the D2L monomer whereas [^{125}I]YM-09151-2 labelled D2L monomer and D2L dimer in identical tissues. These data indicated that distinct classes of D2 receptor antagonists indeed detect receptor monomer and dimer differentially, accounting at least in part, for the higher D2 receptor densities estimated by benzamides compared to butyrophenones.

Fig. 25. Radioligand detection of D2L receptor monomers and dimers. (A) A representative experiment (n=6) showing the saturation isotherms for [^{3}H]spiperone and [^{3}H]YM-09151-2 specific binding to an identical P2 membrane preparation from D2L/Sf9 cells. In this experiment, Bmax (pmol/mg of protein) and K_D (pM) are as follows: [^{3}H]spiperone (○), B_{max} = 1.8, K_D = 215; for [^{3}H]YM-09151-2 (•), B_{max} = 2.8, K_D = 150. These B_{max} and K_D values differed < 10% from the mean of 6 independent experiments. (B) A representative autoradiogram (n=4) showing the photoincorporation of [^{125}I]NAPS (NAPS) in the absence (lane 1) and presence (lane 2) of 1 μM (+) butaclamol (BTC) and [^{125}I]YM-09151-2 (YM) in the absence (lane 3) and presence (lane 4) of 1 μM (+) butaclamol (BTC). D2L monomers and dimers are indicated by arrows.

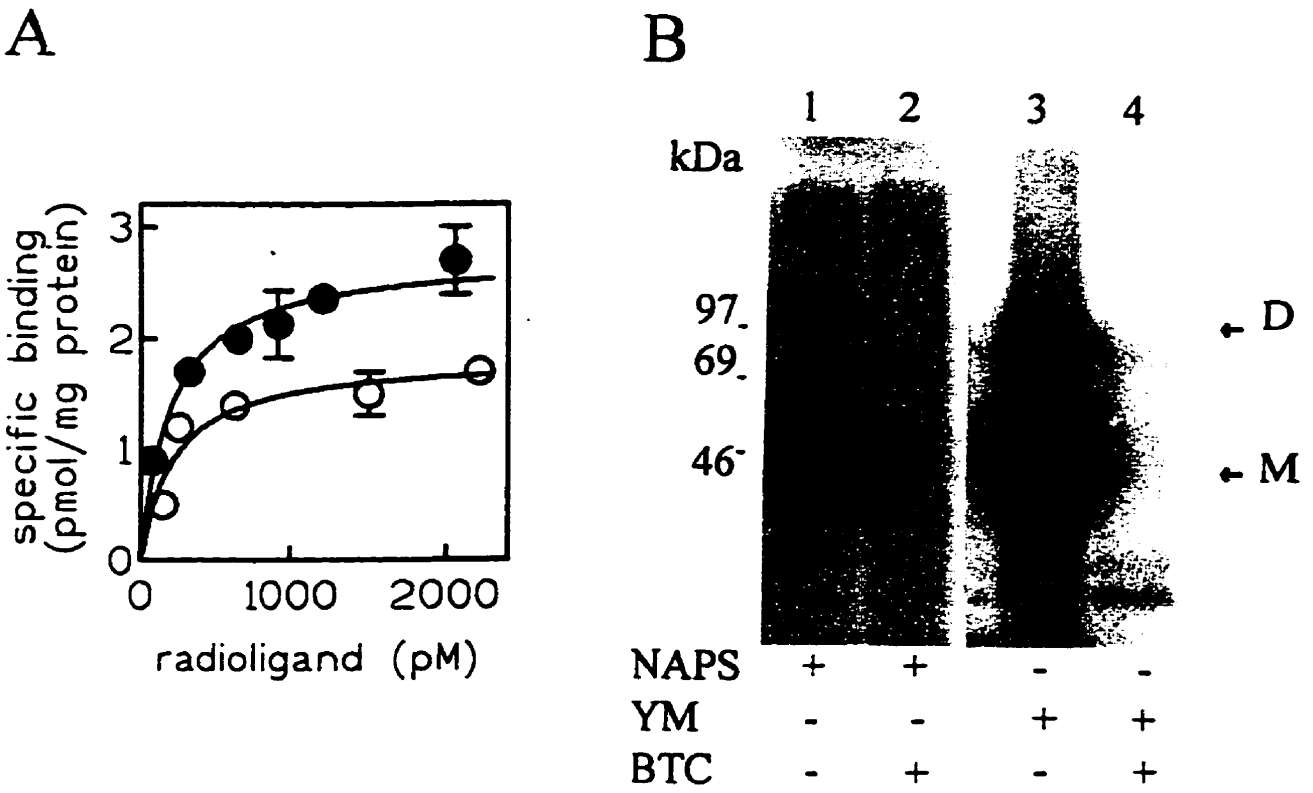
A
specific binding (pmol/mg protein)
3
2
1
0
0
1000
2000
radioligand (pM)
B
1
2
3
4
kDa
97
69
46
D
M
NAPS + + - -
YM - - + +
BTC - + - +

6.3.6 Phosphorylation and Palmitoylation of the D2L Receptor

The biochemical characteristics of the D2L receptor were examined using the D2 receptor-specific AL-26 antisera. Cells expressing the D2L receptors were metabolically labelled with $^{32}P_i$ in serum-free media. The antibody immunoprecipitated phosphorylated proteins at ~44 and ~90 kDa (Fig. 26B, lane 2), corresponding to the receptor monomer and dimer identified by immunoblot analysis (Fig. 26A, lane 1). No specific immunoreactive and phosphorylated material was detected in Sf9 cells infected with the wild-type baculovirus cultured under similar conditions (Fig. 26B, lane 3). These data constitute the first direct evidence to show that the immunoprecipitated D2L monomer and dimer are phosphorylated even in the absence of agonist.

Cells expressing the D2L were cultured in serum-free media in the presence of [^{3}H]palmitic acid to metabolically label receptors. Membranes were solubilized and subsequent immunoprecipitation experiments with the antibody revealed the presence of two labelled bands (Fig. 26C, lane 4) migrating at ~44 and ~90 kDa, corresponding to the sizes of the D2L monomer and dimer on the immunoblot (Fig. 26A, lane 1). These immunoreactive palmitoylated species were not present in immunoprecipitated samples from cells infected with the wild-type baculovirus cultured under similar conditions (Fig. 26C, lane 5). These results show for the first time direct evidence that D2L monomer and dimer are palmitoylated in the basal state in the absence of agonist.

Fig. 26. Biochemical characterization of D2L receptors. The experiment shown are representative of two or three independent experiments. (A) Immunoblot analysis. Lane 1, identification of immunoreactive D2L receptors in Sf9 membranes (200 μg of protein). Membranes were solubilized in SDS buffer, electrophoresed, and electroblotted onto nitrocellulose, and immunoreactivity was revealed with a goat anti-rabbit IgG conjugated to alkaline phosphatase as described in Methods. (B) Whole cell metabolic labelling with carrier-free ^{32}P. Lane 2, phosphorylated D2L receptors immunoprecipitated with the AL-26 antibody from solubilized membranes prepared from Sf9 cells expressing D2L; lane 3, immunoprecipitated sample using the AL-26 antibody from cells infected with wild-type baculovirus. The autoradiogram shown is from a 2-day exposure. (C) Whole cell metabolic labelling [^{3}H]palmitic acid. Lane 4, palmitoylated D2L receptors immunoprecipitated with the AL-26 antibody from solubilized membranes prepared from Sf9 cells expressing D2L receptors; lane 5, an immunoprecipitated sample using the AL-26 antibody from cells infected with the wild-type baculovirus. The autoradiogram shown is from a 1-month exposure. *Reproduced, with permission, from Ng et al., Phosphorylation and palmitoylation of the human D2L receptor in Sf9 cells, Journal of Neurochemistry 63, 1589-1595, 1994.*

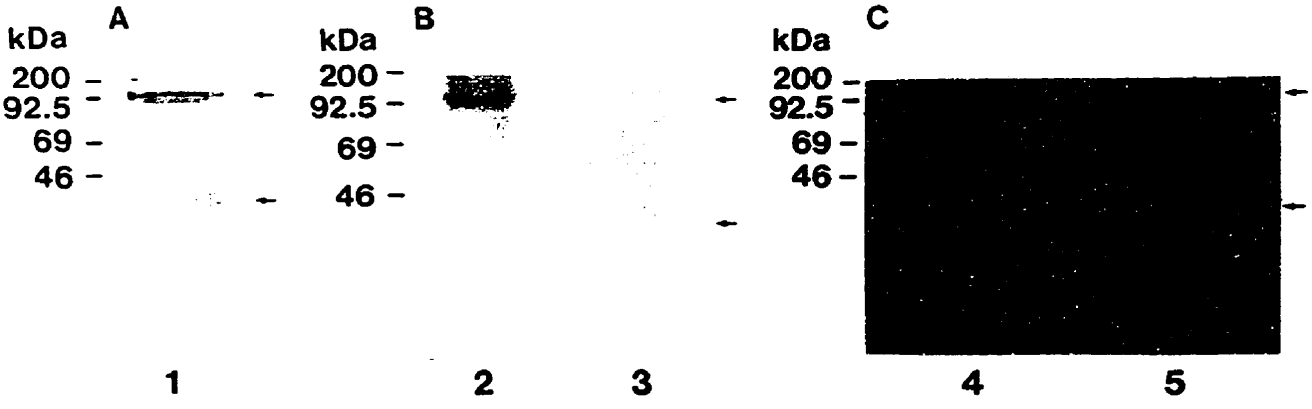
A
kDa
200
92.5
69
46
B
kDa
200
92.5
69
46
C
kDa
200
92.5
69
46
1
2
3
4
5

6.3.7 Pharmacological Characterization of D2L Receptors Under Basal Conditions and Following Varying Periods of Dopamine Exposure

Expressed D2L receptors, mediated dopamine inhibition of forskolin-stimulated adenylyl cyclase activity by 25% with an IC_{50} of 265 ± 33 nM (n=3) in P2 membranes prepared from vehicle-treated cells as shown in Fig. 27A. Following exposure of the cells to dopamine for as long as 60 min, the ability of receptors to mediate maximal dopamine inhibition of adenylyl cyclase activity was unchanged (IC_{50} of 284 ± 27 nM (n=3)) suggesting that the D2L receptor coupled adenylyl cyclase system did not undergo agonist-induced desensitization under these conditions. All experiments were performed on cells expressing ~2 pmol receptor/mg of membrane protein (48-h post infection) as assessed by [^{3}H]spiperone binding, and were ~85% viable as assessed by trypan blue staining. No dopamine sensitive adenylyl cyclase was detected in Sf9 cells infected with the wild-type baculovirus (data not shown).

Dopamine competition of specific [^{3}H]spiperone binding on P2 membranes from vehicle-treated D2L receptor expressing cells was best fitted to a two affinity receptor state model (Fig. 27B) suggesting coupling to endogenous G proteins as previously characterized. In these experiments, K_i values and proportions for dopamine-detected high-affinity and low-affinity were 21 ± 2 pM (23%) and 13 ± 0.5 nM (77%) respectively (n=3). Following preincubation with 10 μM dopamine for 60 min, high-affinity and low-affinity D2L receptor states were still detected by agonist (Fig. 27B) confirming the D2L receptor mediated inhibition of adenylyl cyclase activity observed under these conditions (Fig. 27A). Binding constants for the agonist-detected high-affinity and low-affinity D2L receptor states and the relative proportions of sites were 520 ± 50 pM (30%) and 18 ± 0.4 nM (70%) respectively (n=3).

Fig. 27. Pharmacological properties of D2L receptors under basal conditions and following preincubation with dopamine. (A) Membranes were prepared from cells expressing D2L receptors at basal state (o), and following 60 min dopamine exposure (▲) for adenylyl cyclase activity determination as described in methods. Data was fitted statistically by nonlinear regression and are representative of 3-4 independent experiments. (B) For dopamine competition experiments, membranes prepared from D2L/cells were incubated with varying concentrations (10^{-11} - 10^{-3} M) of dopamine in the presence of radiolabelled antagonist as described in methods. Dopamine competition data was fitted statistically to the best of either one or two sites using computer analysis. Nonspecific binding for all radioligand binding experiments was defined by 1 μM (+)-butaclamol. Results shown are from one of three independent experiments.

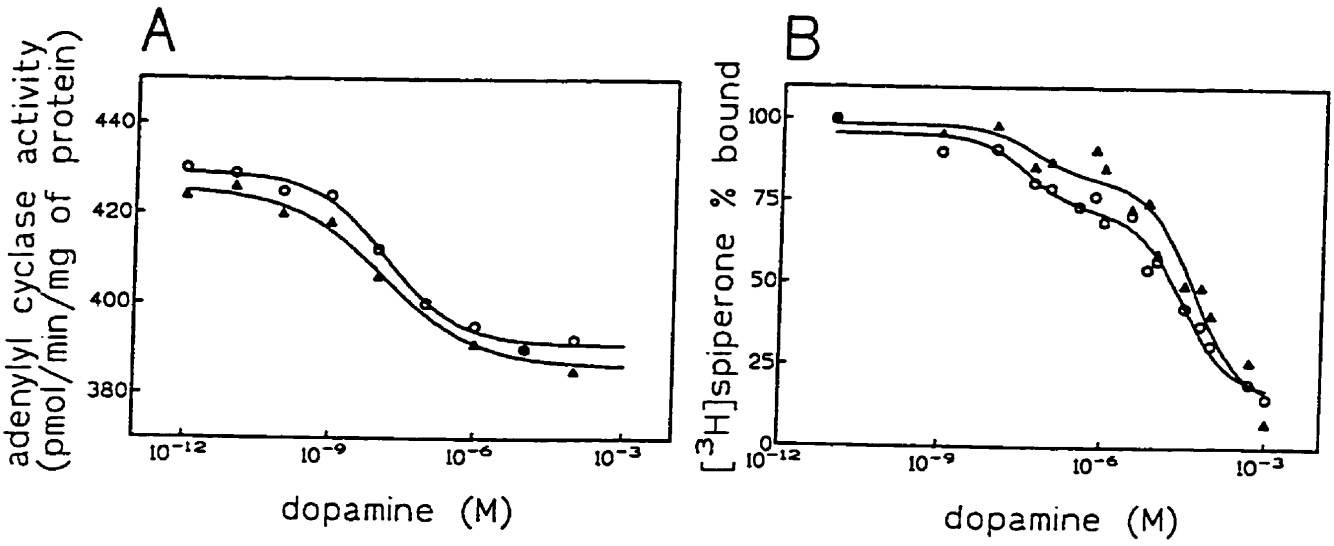
A
adenylyl cyclase activity
(pmol/min/mg of protein)
440
420
400
380
10^{-12}
10^{-9}
10^{-6}
10^{-3}
dopamine (M)
B
[^{3}H]spiperone % bound
100
75
50
25
0
10^{-12}
10^{-9}
10^{-6}
10^{-3}
dopamine (M)

6.3.8 Agonist-induced Cellular Redistribution of D2L Receptors As Assessed by Subcellular Fractionation and Radioligand Binding

We have shown by multiple independent assays that sustained agonist exposure mediated the internalization of surface D1 receptors. Similarly, subcellular fractionation experiments were conducted to determine directly by radioligand binding the number of D2L receptors in the plasma, cell surface membrane and in the light intracellular vesicular membrane fraction under basal conditions and following dopamine exposure. Receptor sequestration was again defined as a decrease in the number of receptors in the plasma cell surface and a proportional increase in the number of receptors in the light vesicular membrane following dopamine treatment.

In marked contrast to the D1 receptor, D2L receptor density increased in the plasma membrane with sustained dopamine exposure which corresponded in time and proportion with a decrease in receptors in the light membrane fraction (Fig. 28). This D2L receptor response to agonist stimulation began to plateau ($18 \pm 4\%$, $P < 0.05$) after 1 hour and was maximal ($28 \pm 6\%$, $P < 0.05$) after 6 hours. Removal of dopamine resulted in a near recovery of receptors in the plasma membrane and light vesicular membrane fractions to near control values in the Sf9 cells after 10 hours (data not shown). These data suggested that D2L receptor redistribution is a means by which the cell regulates surface receptor density upon exposure to stimuli.

Fig. 28. Agonist-induced cellular redistribution of D2L receptors as assessed by subcellular fractionation and radioligand binding. Plasma membranes (•) and light membranes (o) were prepared from recombinant baculovirus infected Sf9 cells incubated in the presence of 10 μM dopamine for various lengths of time. D2L receptor densities of tissues was assessed by binding under saturating concentrations of [^{3}H]spiperone as described in methods. Data represent the receptor densities compared to control untreated tissues expressed as mean ± SEM (n=3).

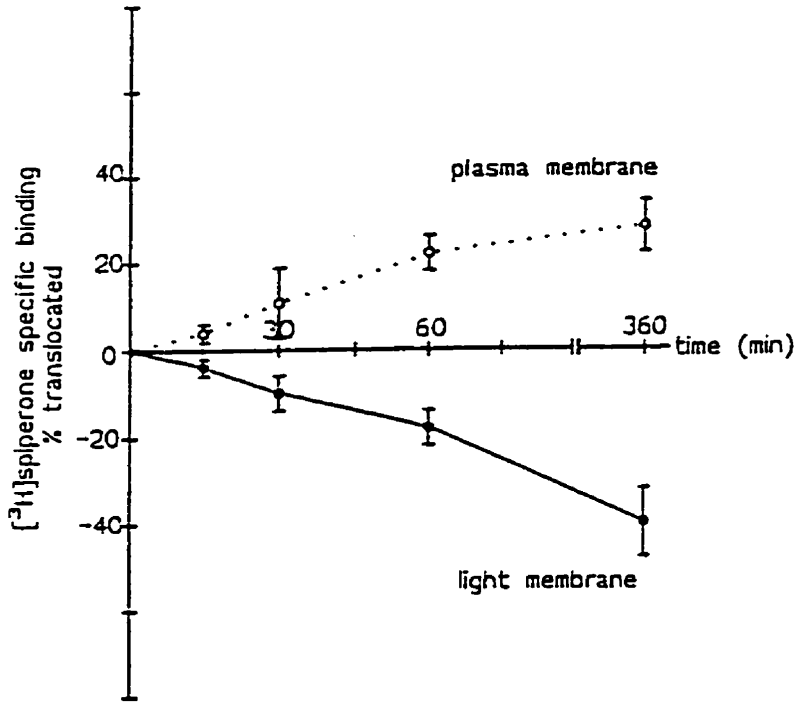
plasma membrane
light membrane
40
20
0
-20
-40
60
360
time (min)
[3H]spiperone specific binding
% translocated

Fig. 29. Identification of photolabelled c-myc-D1 and D2L receptor species in plasma membranes and in intracellular light membrane fractions. Photoaffinity labelled plasma and light membranes were electrophoresed on SDS-PAGE and visualized by autoradiography as described in methods. (A) c-myc-D1/cell membrane fractions photolabelled with [^{125}I]MAB. (B) D2L/cell membrane fractions photolabelled with [^{125}I]NAPS. Lane 1, photolabelled plasma membranes from cells at basal state. Lane 2, photolabelled plasma membranes from cells preincubated with 10 μM dopamine for 4 hours. Lane 3, photolabelled light membranes from cells at basal state. Lane 4, photolabelled light membranes from cells preincubated with 10 μM dopamine for 4 hours. 200 μg membrane protein was used for each labelling condition. The autoradiograms shown are from a 1 day exposure. Two or three independent experiments were done to determine the specificity of the photolabel and the molecular mass of the photolabelled receptor species.

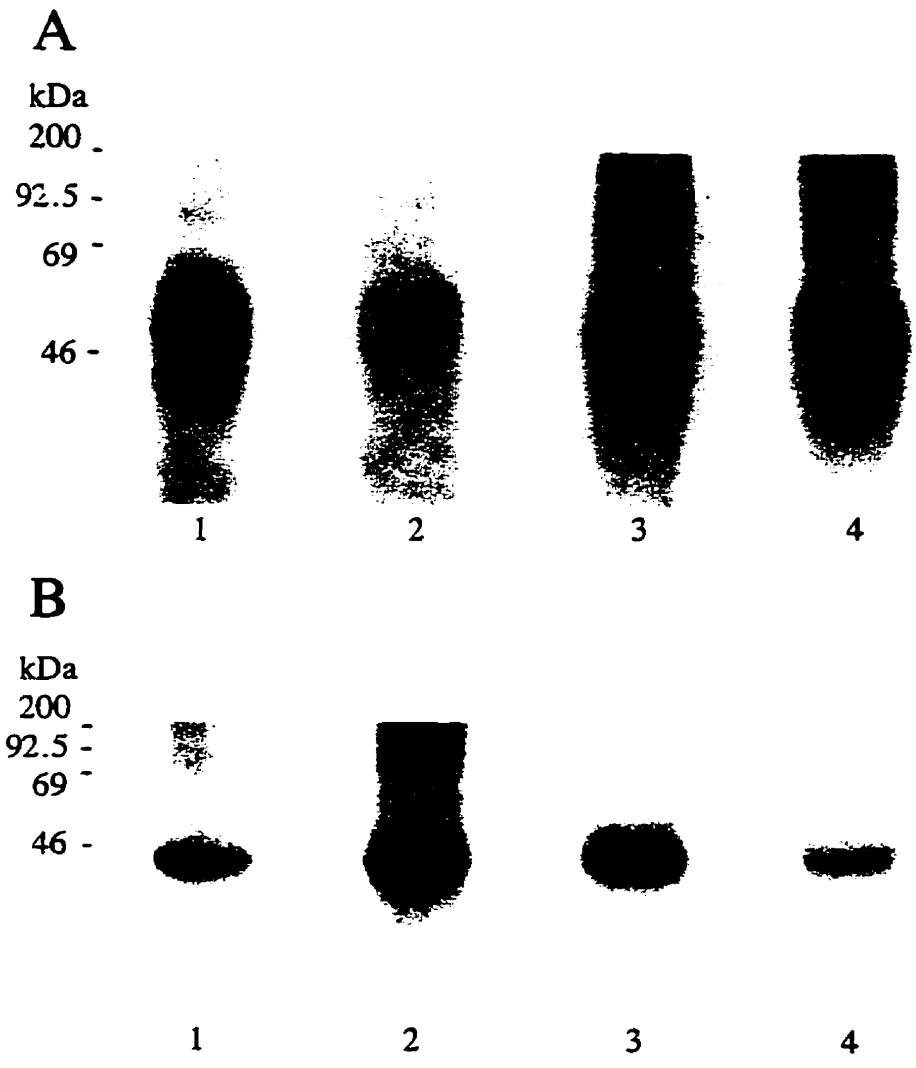
A
kDa
200
92.5
69
46
1
2
3
4
B
kDa
200
92.5
69
46
1
2
3
4

6.3.9 Agonist-induced Redistribution of Cellular D1 and D2L Receptors As Assessed by Photoaffinity Labelling

The pharmacological specificity of the photoaffinity label ([^{125}I]IMAB) for the D1 receptor, and the photoaffinity label ([^{125}I]NAPS) for the D2 receptor have been previously described (Niznik et al., 1988, Amlaiky and Caron, 1985) and were used to characterize the receptor species subjected to cellular trafficking. Photoaffinity labelling experiments of c-myc D1/cell plasma and light membranes revealed a major ~48 kDa active ligand binding species (Fig. 29A). Agonist mediated a decrease in this species in the plasma membrane and an increase in the light membrane fraction in keeping with the notion of D1 receptor internalization described previously. Photoaffinity labelling experiments of D2L/cell plasma and light membranes revealed a major ~44 kDa active ligand binding species (Fig. 29B) absent in membranes prepared from wild-type baculovirus infected cells and when labelling experiments were performed in presence of 1 μM (+)butaclamol (data not shown). Agonist mediated an increase in the ~44 kDa D2L species on the plasma membrane and a decrease in the light membrane fraction suggesting a physical translocation of the receptor from the intracellular pools to the plasma membrane. These results suggest that D1 and D2L receptors undergo distinct patterns of redistribution, involving monomeric species, upon exposure to agonist.

6.3.10 Localization of D2L Receptors in Whole Cells by Immunocytochemical Fluorescent Staining

The D2 receptor specific AL-26 polyclonal rabbit antibody enabled us to examine via another independent measure the cellular distribution of the receptor by immunocytochemical staining. Receptor labelling was visualized by confocal immunofluorescent microscopy which optically sections a cell such that each section or slice could be viewed individually. Cells were

permeablized so that both cell surface and internally located receptors could be detected. All comparative analysis was performed under identical illuminating and viewing conditions.

Immunocytochemical labelling of D2L/cells at basal state showed D2L receptors exhibiting a patchy distribution on the cell surface with most of the receptors in intracellular compartments appearing as pockets of label. Dopamine exposure mediated a reorganization of the cellular distribution of D2L receptors resulting in an increase in surface receptors appearing as a prominent ring of fluorescence on the cell surface (Fig. 30A, compare panel A to B). For comparison, agonist exposure induced the internalization of the c-myc-D1 receptor in the Sf9 cells (Fig. 30A, compare panel D to E), data we have described in detail elsewhere (Fig. 15, 16). Control cells, expressing no receptors, are barely visible reflecting no specific immunocytochemical labelling (Fig. 30A, panel C and F). These findings constitute the first direct demonstration that D1 and D2L receptors undergo subtype-specific patterns of redistribution following agonist exposure in an identical cell line suggesting, a distinction that likely owed to an inherent property of the receptor proteins.

6.3.11 Agonist-induced Increase in Cell Surface D2L Receptor Monomer and Dimer

Immunoblot analysis revealed that the increase in surface D2L receptor density in dopamine-treated D2L/Sf9 cells was composed of an increase in both D2L monomer and dimer (Fig. 30B). In agreement with these data, [^{3}H]spiperone and [^{3}H]YM-09151-2 radioligand binding showed a statistically significant mean 26 $\pm$ 2% (n=4) and 32 $\pm$ 4% (n=4) increase ($P < 0.01$) in receptor density in dopamine-treated cells, representing D2L monomers and dimers in the plasma membrane (Fig. 30C). Agonist-induced increases in D2L receptor density has also been shown in mammalian cell lines (Filtz et al., 1993, Zhang et al., 1994, Ivins et al., 1991),

and animals treated with indirect dopamine agonists (Rouillard et al., 1987, Bischoff et al., 1991, Vassout et al., 1993, Star et al., 1995). These data lend support to the notion that the equilibrium between receptor monomer and dimer may have a role in the regulation of D2L receptor activity.

6.3.12 Antagonist-induced increase in cell surface D2L receptor density

Interestingly, D2L receptor up-regulation was not specific to agonist. Treatment of D2L/cells with the benzamide antagonist (-)sulpiride caused smaller increase (average increase, 10%) in cell surface receptor density (Table 6). This was accompanied by a ~30% increased affinity of the D2L receptor for the ligand (Table 6). It is unclear at present if these observations correspond with this compound's partial ability to mediate a consistent inhibition (average decrease, ~5%) of adenylyl cyclase activity in these tissues (IC_{50} of 200 + 10 nM (n=2)). Interestingly, treatment of D2L/cells with butyrophenones such as haloperidol had no effect on cell surface D2L receptor density (data not shown).

6.3.13 Clathrin-like Immunoreactive Material and Dopamine Receptor Subtype Sorting

In many cases, receptor trafficking may be mediated by clathrin-coated vesicles. Preincubation of cells with concanavalin A or sucrose, agents which are known to inhibit clathrin processes, blocked agonist-mediated c-myc-D1 receptor internalization (Fig. 18). However D2L receptor translocation to the cell surface was not hindered under similar conditions (data not shown). Immunoblot analysis of Sf9 cell lysate with a rabbit polyclonal antibody raised against bovine brain clathrin revealed the presence of an abundance of clathrin-like immunoreactive material at the expected molecular mass for the heavy chain of neuronal clathrin (Fig. 31) (Kirchhausen and Harrison, 1981). These data suggested that clathrin may participate in D1 but not D2L receptor cellular trafficking.

Table 6. Antagonist binding constants for D2L receptors under basal conditions and following preincubation with (-)sulpiride. D2L/cells were incubated either in the absence (vehicle) or in the presence of 10 μM antagonist for 1 h. Membranes were then prepared for radioligand binding as described. Data was fitted statistically to the best of one or two sites, and K_D and B_{max} values determined by GraphPad INPLOT analysis. Data shown represent the average ± SD (n=2).

	Treatments	
	Vehicle	(-)sulpiride
[^{3}H]spiperone		
K_D	415 ± 39	274 ± 46
B_{max}	3.2 ± 0.02	3.5 ± 0.01

Fig. 30. Agonist-induced D2L receptor redistribution as assessed by confocal microscopy, immunoblot analysis and radioligand binding. (A) Immunocytochemical labelling of whole permeabilized cells (representative cells are shown) visualized under confocal laser microscopy. Panel A: D2L/Sf9 cells with vehicle; panel B: D2L/Sf9 cells following preincubation for 4 h with 10 μM dopamine; and panel C: a wild-type Sf9 cell. Panel D: c-myc-D1/Sf9 cell with vehicle; panel E: c-myc-D1/Sf9 cell following preincubation for 1 h with 10 μM dopamine; and panel F: a wild-type Sf9 cell. Cells were permeabilized to allow detection of both surface and intracellular receptors which appear in white in the cell sections. The nucleus of the cell appears in the center as black. All samples were taken under identical illuminating conditions. (B) Immunoblot of P2 membranes from D2L/Sf9 cells treated for 4 h with vehicle (lane 1) or 10 μM dopamine (lane 2). Results are representative of 4 experiments. (C)Saturation isotherms of [^{3}H]YM-09151-2 and [^{3}H]spiperone specific binding to P2 membranes from D2L/Sf9 cells treated for 4 h with vehicle or with 10 μM dopamine are shown. In this [^{3}H]YM-01951-2 experiment (top), B_{max} (pmol/mg of protein) and K_D (pM) values for vehicle (•) and dopamine-treated (▲) conditions are: B_{max} = 2.8, K_D = 121; B_{max} = 3.8, K_D = 115. In this [^{3}H]spiperone experiment (bottom), B_{max} and K_D values for vehicle (○) and dopamine-treated (△) conditions respectively are: B_{max} = 2.0, K_D = 206; B_{max} = 2.7, K_D = 197. These B_{max} and K_D values differed < 10% from the mean of 4 independent experiments.

A

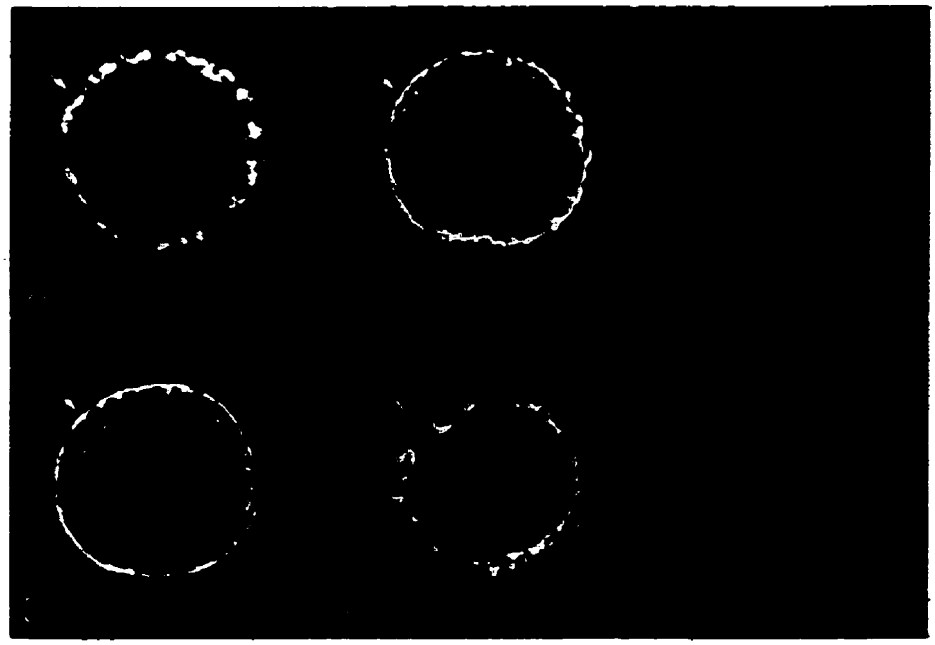

B

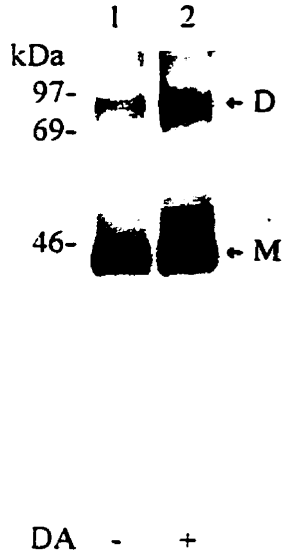
1
2
kDa
97-
69-
← D
46-
← M
DA - +

C

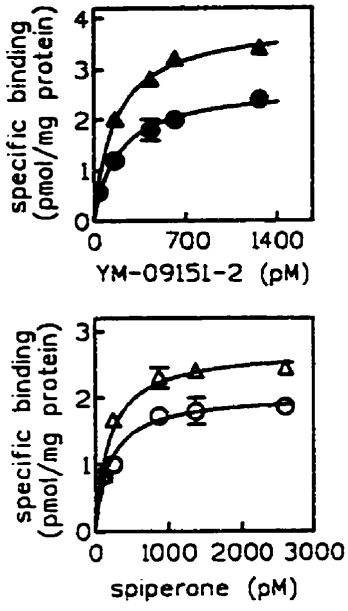
specific binding (pmol/mg protein)
4
3
2
1
0
0
700
1400
YM-09151-2 (pM)
specific binding (pmol/mg protein)
3
2
1
0
0
1000
2000
3000
spiperone (pM)

Fig. 31. Clathrin-immunoreactive material in Sf9 cell lysate. Sf9 cell lysate (100 μg protein) was separated by SDS-PAGE and electrophoretically transferred onto nitrocellulose and immunoblotted with a goat antibody directed against bovine brain clathrin as described in methods. Clathrin-like immunoreactive material was detected at ~ 160-180 kDa representative of a typical experiment repeated two times.

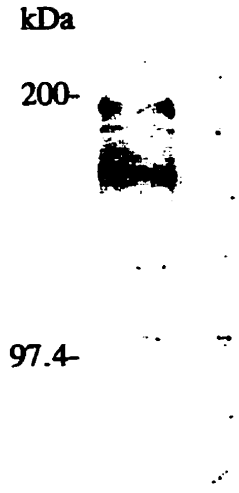
kDa
200-
97.4-
1
2

6.4 Pharmacological Characterization of Coexpressed D1 and D2L Receptors

6.4.1 Binding Properties of D1 and D2L Receptors Are Not Altered in the Presence of the Receptor Subtype

The effects of presence of the D2L receptor on D1 receptor binding, and the effects of the D1 receptor on D2L receptor binding were examined in Sf9 cells coexpressing c-myc-D1 receptors and D2L receptors to specific activities of ~6 and ~4 pmol/mg of protein respectively. Saturation binding analysis with [^{3}H]SCH-23390 and [^{3}H]spiperone on membranes prepared from D1-D2L/cells revealed K_D values of 934±57 pM and 389±41 pM respectively similar to receptors expressed in isolation (Table 7). SKF-38393/ [^{3}H]SCH-23390 competition analysis binding was best-fitted to a two affinity state model in membranes from D1-D2L/cells, with K_h and K_l values and the proportions for each site similar to D1 receptors expressed in isolation (Table 7). Quinpirole/[^{3}H]spiperone competition binding revealed agonist detected high- and low-affinity sites in membranes from D1-D2L/cells with similar affinities compared to D2L/cells (Table 7). Collectively, these data showed no modulation of ligand binding properties of D1 or D2L receptors in the presence of the other receptor subtype when coexpressed in an identical cell line.

Table 7. Binding parameters for c-myc-D1 and D2L receptors expressed in isolation and coexpressed in Sf9 cells. [^{3}H]SCH-23390 and [^{3}H]spiperone K_D (pM) values were determined by saturation binding, whereas SKF-38393 and quinpirole K_i (pM) values for high and low affinity receptor states were determined by competition for [^{3}H]SCH-23390 and [^{3}H]spiperone binding at D1 or D2L receptors respectively. The values represent the mean ± SEM for n=3 or average ± SD for n=2. ND refers to not determined.

Ligand	*Binding constants*	*D1/Sf9*	*D2L/Sf9*	*D1-D2L/Sf9*
SCH-23390	K_D (nM)	820 ± 12	ND	1048 ± 123
SCH-23390	B_{max} (pmol/mg protein)	6.7 ± 0.3	0.1 ± 0.01	6.6 ± 0.3
SKF-38392	K_i high (nM)	98 ± 36	ND	263 ± 17
SKF-38392	K_i low (nM)	375 ± 115	ND	350 ± 36
spiperone	K_D (nM)	ND	529 ± 15	324 ± 11
spiperone	B_{max} (pmol/mg protein)	0.2 ± 0.01	1.8 ± .2	1.6 ± 0.2
quinpirole	K_i high (nM)	ND	419 ± 23	797 ± 56
quinpirole	K_i low (nM)	ND	5650 ± 772	8896 ± 785

6.4.2 Absence of D1-D2L Receptor Heterodimerization in Living Cells Coexpresssing the Receptor Subtypes

The high-level of receptor expression that can be generated in Sf9 cells was taken advantage of to facilitate the detection of possible D1-D2L receptor heterodimers. For these studies, c-myc-D1 receptors and D2L receptors were expressed to levels of ~6 and ~4 pmol/mg of protein respectively. Immunoblot analysis of membranes prepared from D1-D2L/cells using a monoclonal antibody directed against c-myc of c-myc-D1 receptor showed the presence of two major species migrating at ~48 kDa and ~110 kDa identical to the staining pattern observed for membranes prepared from D1/cells (Fig. 32A). Immunoblot analysis using a D2 receptor selective antisera directed at the third intracellular loop of the D2 receptor revealed two major species at ~44 kDa and ~90 kDa identical to the immunoreactive pattern observed for membranes prepared from D2L/cells (Fig. 32B). The immunoreactive staining patterns of D1 and D2L receptors were identical under reducing and denaturing and non-reducing and denaturing conditions. Taken together, these data indicate that D1 and D2L receptors heterodimers do not appear to preexist in membranes of living cells.

6.4.3 Absence of D1-D2L Receptor Heterodimerization in Detergent Solution

To confirm whether D1 and D2L receptors had a quaternary structure, as may be predicted to occur by the three-dimensional molecular fitting at the protein-protein interface of a GPCR dimer, immunopurified receptors were coincubated in detergent solution. Immunoblot analysis of a sample of immunoprecipitated D2L receptors compared to a sample of immunoprecipitated D2L receptors coincubated with immunoprecipitated D1 receptors in detergent buffer revealed D2L monomer and dimer at the expected molecular mass for the D2L receptor (Fig. 33). No other band at ~ 100 kDa

was observed indicating that D1 and D2L receptors do not undergo association to form D1-D2L heterodimers in detergent solutions under these conditions. Collectively, these results confirm that stable receptor dimers are formed by highly receptor subtype-specific structural interactions, and that heterodimerization of D1 and D2L receptors is an unlikely basis of the reported synergism between these two receptor systems.

Fig. 32. Immunoblot analysis of c-myc-D1 and D2L receptors expressed in isolation and coexpressed in Sf9 cells. (A) D1 receptor monomers and dimers were revealed in P2 membranes prepared from D1-D2L/Sf9 cells coexpressing c-myc-D1 and D2L receptors and D1/Sf9 cells expressing D1 receptors (D1) using the monoclonal 9E10 antibody directed against the c-myc epitope attached to the amino terminus of the D1 receptor. No immunoreactive species were detected with the 9E10 antibody in P2 membranes from D2L/Sf9 cells or wild-type (WT) Sf9 cells. (B) D2L monomers and dimers were revealed in D1-D2L/Sf9 cells coexpressing c-myc-D1 and D2L receptors and D2L/Sf9 cells expressing D2L receptors using the polyclonal antibody raised against 120 aa residues of the third intracellular loop of the D2 receptor (nt 661-1020). Little background labelling was detected with the AL-26 antibody in D1/Sf9 cells or wild-type Sf9 cells. Receptor monomers and dimers, indicated by arrows, were found to be stable in the presence of SDS and reducing agents such as β-mercaptoethanol and DTT during SDS-PAGE. The blot shown is representative of n=2.

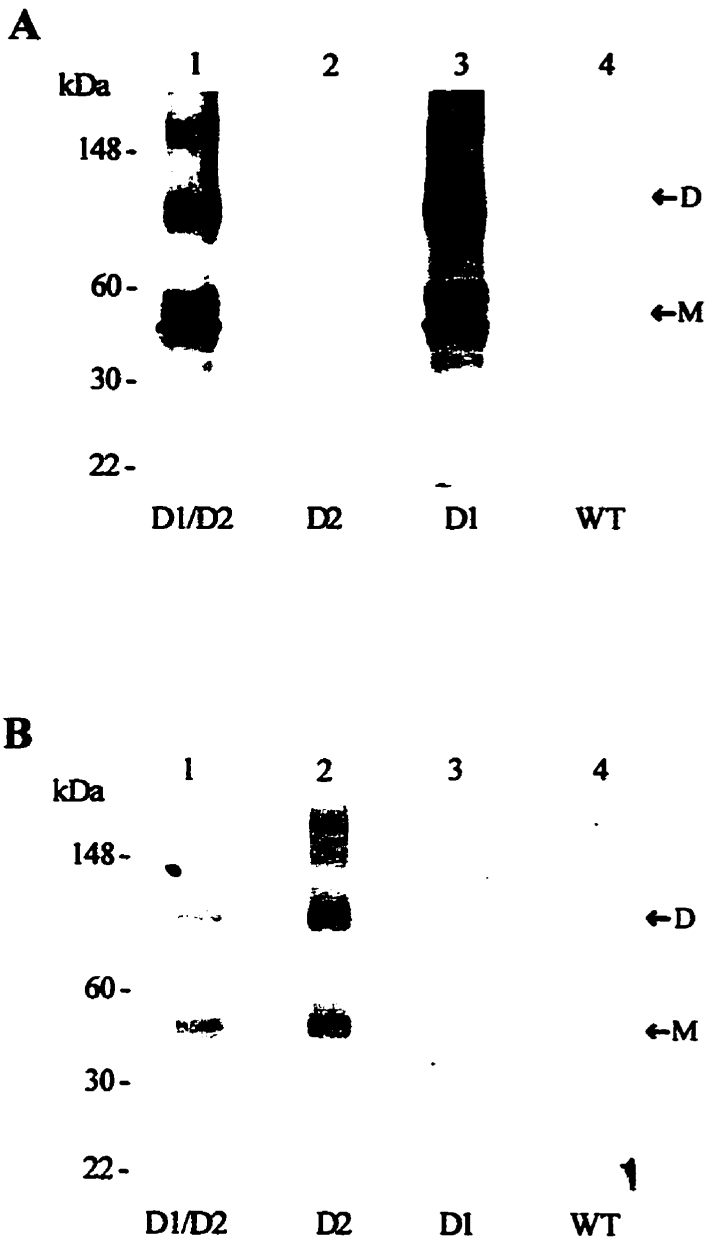
A
1
2
3
4
kDa
148-
60-
30-
22-
←D
←M
D1/D2
D2
D1
WT
B
1
2
3
4
kDa
148-
60-
30-
22-
←D
←M
D1/D2
D2
D1
WT

Fig. 33. Immunoblot of immunoprecipitated D2L receptors coincubated in the absence or presence of immunoprecipitated c-myc-D1 receptors in detergent. Immunoblot analysis was performed with the AL-26 D2 antibody against 3 pmol of immunoprecipitated D2L receptors (lane 1), and 1.5 pmol of immunoprecipitated D2L receptor incubated for 1 h at room temperature with 1.5 pmol of immunoprecipitatated c-myc D1 receptor prior to SDS-PAGE (lane 2).

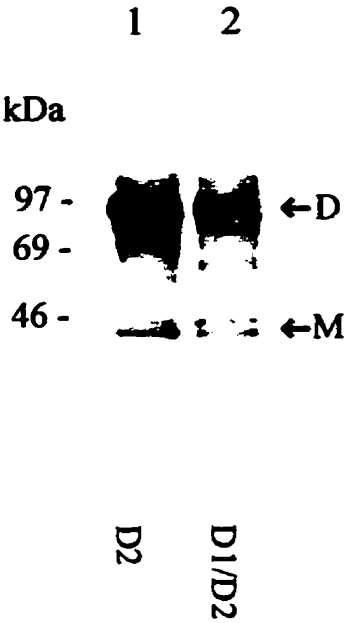
1
2
kDa
97 -
69 -
46 -
←D
←M
D2
D1/D2

6.4.4 D1-D2L Receptor Interaction Downstream the Level of the Receptor

The effect of the presence of the D2L receptor on D1 receptor stimulated adenylyl cyclase, and the effects of the D1 receptor on D2L receptor inhibition of adenylyl cyclase were examined in Sf9 cells coexpressing c-myc-D1 receptors and D2L receptors. Maximal D1 receptor-mediated SKF-38393 stimulated adenylyl cyclase activity was consistently higher in membranes prepared from cells coexpressing D1 and D2L receptors compared to membranes prepared from cells expressing D1 receptors alone (Fig. 34). Interestingly, the SFK-38393 EC_{50} values did not differ (Fig. 34). Consistent with this D2L-potentiation of D1 receptor stimulated adenylyl cyclase activity, maximal D2L receptor-mediated quinpirole inhibition of adenylyl cyclase activity was greater in membranes prepared from cells coexpressing the receptor subtypes compared to cells expressing the D2L receptor in isolation (Fig. 34). No difference in quinpirole IC_{50} value was observed in these preparations (Fig. 34). However, no synergism was observed in membranes from D1-D2L/cells when dopamine was used as the agonist. In fact, maximal D1 receptor-mediated dopamine stimulated adenylyl cyclase activity was reduced in membranes prepared from D1-D2L/cells compared to D1/cells (Fig. 34) suggesting possibly the net contribution of D1 receptor stimulation and concurrent D2L receptor inhibition of adenylyl cyclase under these conditions. The results of these studies suggest that D1 and D2L receptor coupled adenylyl cyclase systems can functionally interact with each other at the G protein and/or effector level.

Fig. 34. D1 and D2L receptor coupled adenylyl cyclase activities in D1-D2L/cells. (A) The dose-response for SKF-38393 mediated D1 receptor stimulated adenylyl cyclase activity is shown in membranes prepared from D1/cells or D1-D2L/cells. SKF-38393 EC_{50} values for membranes from D1/cells compared to D1-D2L/cells were 177 $\pm$ 41 nM (n=2) and 110 $\pm$ 11 nM (n=2) respectively. (B) The dose-response for quinpirole mediated D2L receptor inhibition of adenylyl cyclase activity is shown in membranes prepared from D2L receptor expressing Sf9 cells or Sf9 cells coexpressing D1 and D2L receptors. Quinpirole IC_{50} values for membranes from D2L/Sf9 cells compared to D1-D2L/Sf9 cells were 2 $\pm$ 0.3 nM (n=2) and 1.1 $\pm$ 0.1 nM (n=2) respectively. (C)The dose-response for dopamine mediated D1 receptor stimulated adenylyl cyclase activity is shown in membranes prepared from D1 receptor expressing Sf9 cells or Sf9 cells coexpressing D1 and D2L receptors. Dopamine EC_{50} values for membranes from D1/cells compared to D1-D2L/cells were 189 $\pm$ 24 nM (n=2) and 202 $\pm$ 31 nM (n=2) respectively.

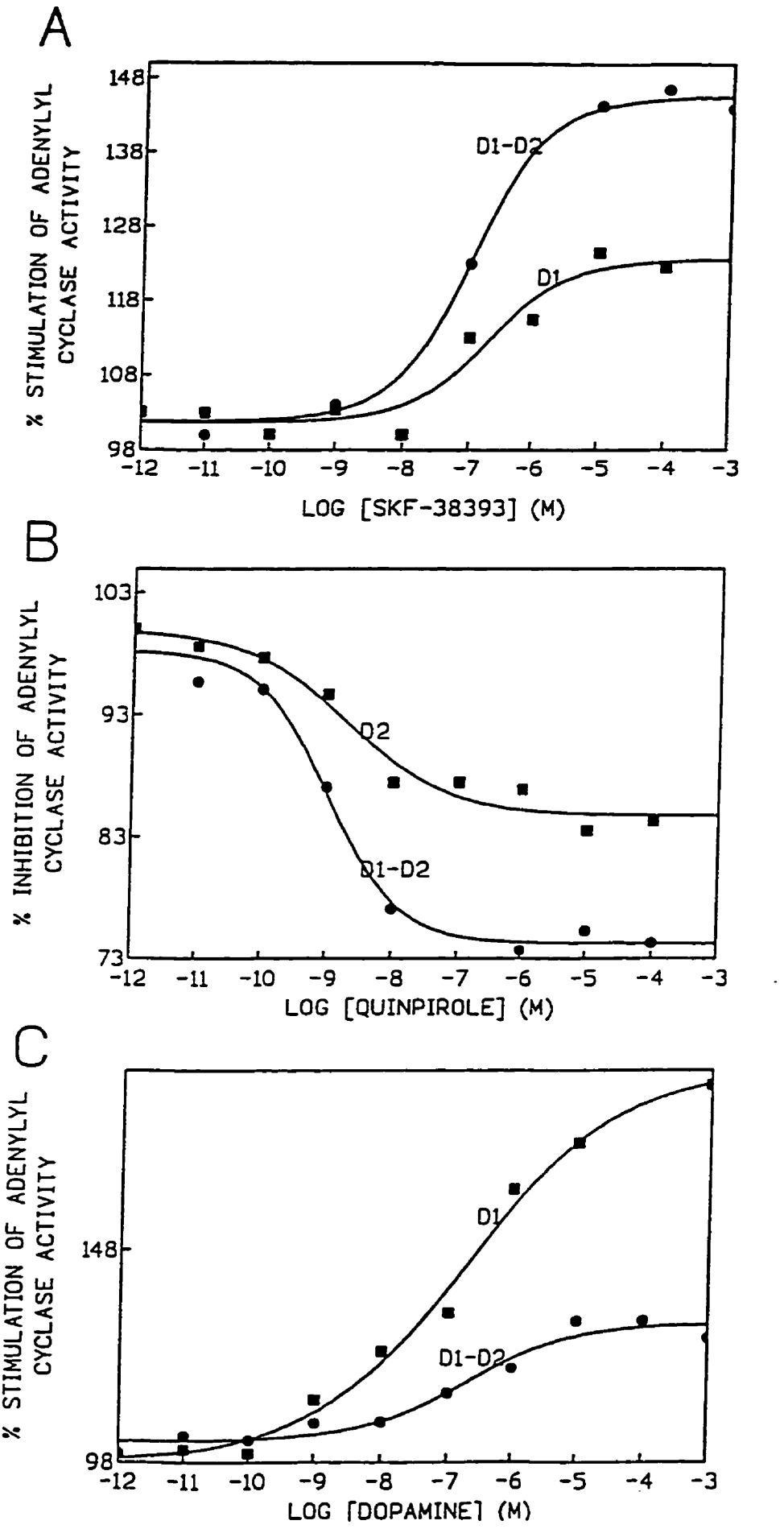
A
% STIMULATION OF ADENYLYL CYCLASE ACTIVITY
148
138
128
118
108
98
D1-D2
D1
-12 -11 -10 -9 -8 -7 -6 -5 -4 -3
LOG [SKF-38393] (M)
B
% INHIBITION OF ADENYLYL CYCLASE ACTIVITY
103
93
83
73
D2
D1-D2
-12 -11 -10 -9 -8 -7 -6 -5 -4 -3
LOG [QUINPIROLE] (M)
C
% STIMULATION OF ADENYLYL CYCLASE ACTIVITY
148
98
D1
D1-D2
-12 -11 -10 -9 -8 -7 -6 -5 -4 -3
LOG [DOPAMINE] (M)

7. DISCUSSION

Dopamine D1 and D2 receptors bind dopamine to mediate a plethora of biological activities such as modulating emotional states, motor control and reproduction. The molecular basis of this functional diversity is poorly understood, but can be explained in part by the multiplicity of dopamine receptors. The D1 receptor and the D2L receptor exhibit the seven transmembrane spanning domains linked by intracellular and extracellular loops characteristic of all GPCRs. Amino acid sequence analysis of the D1 and D2L receptors reveals the presence of serine and threonine residues in the third putative intracellular cytoplasmic loop, consensus sequences recognized by phosphorylating enzymes. Additionally, cysteine residues are present in the cytoplasmic tail of both D1 and D2L receptors recognized by a palmitoylating enzyme. These structural determinants suggest that these receptors could be subject to regulation by these key posttranslational modifications that govern the activity of other proteins. However in contrast to the D1 receptor, the D2L receptor has a significantly larger third intracellular loop and shorter carboxyl tail, suggesting potentially different patterns of regulation for these receptors. Until now, neither biochemical characterization nor ligand-induced regulation of these receptors has yet been described in detail owing to the coexpression or coexistence of related receptor subtypes in tissues, and the low amounts of native protein available for detailed analysis. Further the challenge is made greater by the inability to purify D1 and D2L receptors, and the lack of foster cell lines able to express these receptors with appropriate biological activity.

A number of GPCRs such as β_2-adrenergic (Mouillac et al., 1992), muscarinic (Parker et al., 1991, Richardson and Hosey, 1992, Vasudevan et al., 1992), α_2-C4 adrenergic (Oker-Blom et al., 1993) and serotonin 5-HT_{1A} (Mulheron et al., 1994) receptors have been successfully

studied in the baculovirus/Sf9 insect cell system. Distinguishing features of the Sf9 cell line include high signal to low noise background, and the ability to generate biologically active and immunoreactive recombinant proteins. The biology of D1 and D2L receptors at the molecular level has remained largely unclear, a fact that has changed now that cloned D1 and D2L receptors have been successfully expressed and studied in the foster Sf9 insect cell line.

7.1 Biochemical and Pharmacological Properties of the D1 Receptor

7.1.1 Pharmacology of D1 Receptors

The initial step was to determine whether D1 receptors expressed in Sf9 cells were similar to the neuronal D1 receptor. The strategy employed to study D1 receptor biology was to express a c-myc epitope tagged D1 receptor which would enable receptor characterization using a monoclonal antibody directed against c-myc of c-myc-D1 receptor. D1 receptors were expressed efficiently in Sf9 cells under the transcriptional control of the AcNPV polyhedrin promoter. Expressed receptors showed selective, reversible, and saturable binding of [^{3}H]SCH-23390 with K_D values similar to binding constants reported for D1 receptor in human caudate (Seeman, 1987). Displacement of [^{3}H]SCH-23390 by agonists and antagonists was in the appropriate rank order of potency characteristic of the human brain D1 receptor profile (Seeman and Niznik, 1988) indicating that D1 receptors expressed in Sf9 cells bound ligands indistinguishable from native receptors. Most importantly, expressed D1 receptors appeared biologically active. Indeed, the guanine nucleotide-sensitive agonist-detected high affinity state, and the ability of dopamine to stimulate adenylyl cyclase suggested that expressed D1 receptors were coupled to endogenous G_s-like proteins in the Sf9 cells. These encouraging results prompted detailed structure-function studies of the D1 receptor which had not been possible in

previous model systems.

7.1.2 Biophysicochemical Properties of D1 receptors

To characterize the nature of expressed D1 receptors, photolabelling and immunoblot analysis identified D1 receptor species of ~48 kDa in good agreement with the predicted molecular mass of the D1 receptor (Sunahara et al., 1990). In cells metabolically labelled with $^{32}P_i$ or [^{3}H]palmitic acid, the immunoprecipitated ~48 kDa species was found to be phosphorylated and palmitoylated demonstrating for the first time posttranslational modifications of D1 receptors. Additionally the ~110 and ~200 kDa immunoreactive species, at approximately twice- and four-times the molecular mass of the receptor monomer, were believed to represent D1 dimers and tetramers. However their lack of photolabel [^{125}I]IMAB binding, as well as absence of posttranslational modifications, suggested that these species may not have a direct role in D1 signalling. The most likely conclusion is that the D1 receptor monomer likely represents the major biologically active species. We next sought to identify the biochemical mechanisms that might regulate the functional coupling of recombinant D1 receptors to adenylyl cyclase.

7.1.3 Agonist-induced Desensitization of D1 receptors

Preincubation of D1/cells with 1 μM dopamine for 15 min led to a 16% reduction of dopamine-stimulated adenylyl cyclase with no change in basal, forskolin- or sodium fluoride-stimulated adenylyl cyclase activity, consistent with a receptor-specific homologous desensitization. Stimulation for a longer period of time (30 min) or with a higher concentration of dopamine (10 μM) resulted in a broader pattern of desensitization which led to a decreased responsiveness to forskolin and sodium fluoride. This might reflect the combination of both homologous and heterologous

desensitization under these conditions. The mechanisms underlying the desensitization of the D1 receptor coupled adenylyl cyclase system appeared to involve the agonist-induced uncoupling of receptors from G proteins and effector molecule. The biochemical basis of this most likely involved the posttranslational modifications of the D1 receptor since desensitization was accompanied by an increase in receptor phosphorylation level. It has been shown that phosphorylation of the structurally related β_2-adrenergic receptor results directly in the functional uncoupling of this receptor (Bouvier et al., 1988). Consensus sequences for cyclic AMP-dependent protein kinase phosphorylation are present in the primary structure of the D1 receptor (Sunahara et al., 1990). Additionally, serine and threonine residues present in the carboxyl tail of the D1 receptor could serve as potential sites for GRK phosphorylation (reviewed by Lefkowitz, 1993). Thus, an increased state of D1 receptor phosphorylation appears to be a biochemical determinant mediating the functional uncoupling of this receptor. However, we now show that the desensitization of the D1 receptor stimulated adenyly cyclase system was also associated with increased D1 receptor palmitoylation.

Thioesterification of the D1 receptor with palmitic acid may involve the cysteine residue (Cys^{348}) present in the carboxyl tail (Sunahara et al., 1990), since it has been previously shown that the Cys^{341} located in an equivalent region of the β_2-adrenergic receptor is the site for palmitoylation (O'Dowd et al., 1989). For the β_2-adrenergic receptor, mutation of this cysteine led to a receptor form with a decreased ability to stimulate adenylyl cyclase. We now show that agonist treatment mediated a significant increase in [^{3}H]palmitate acid incorporation in the D1 receptor. According to the proposed model, palmitoylation of Cys^{348} in the carboxyl tail of the D1 receptor

would impose an additional fourth intracellular loop anchoring part of the carboxyl tail to the plasma membrane governing the susceptibility of the receptor for phosphorylation. We conclude that agonist modulated palmitoylation of the D1 receptor may represent a novel regulatory mechanism. It will be important to determine the relatedness of D1 receptor palmitoylation and G-protein coupling with a substitution of $Cys^{348} \rightarrow$ Ala in the D1 receptor. In light of these data, it would also be of interest to elucidate the dependence or interdependence of phosphorylation and palmitoylation and the effect(s) on D1 receptor regulation.

7.1.4 Agonist-induced Redistribution of D1 Receptors

Immunofluorescent labelling showed that acute agonist treatment of the D1/cells induced a rapid redistribution of the surface receptors into discrete aggregates accompanying a small $\sim 13\%$ reduction in cell surface receptor density, but no D1 receptor internalization as determined by differential centrifugation and radioligand binding. It could be hypothesized that acute agonist exposure triggered a conformational change and/or aggregation of surface D1 receptors rendering receptors refractory or inaccessible to ligand binding. This response has never been demonstrated previously for any dopamine receptor, but is consistent with the lack of change in the cellular distribution of receptors, as suggested previously for a model of β_2-adrenergic receptor sequestration (Wang et al., 1989). However, sustained agonist exposure for an hour or more resulted in a significant D1 receptor internalization with the response beginning to plateau following 1 hour and reaching maximal after 4 hours. Photoaffinity labelling experiments provided visual confirmation indicating an agonist-promoted physical translocation of a ~ 48 kDa receptor species from the surface plasma membrane to a light membrane fraction. This conclusion was supported further by immunocytochemical localization studies employing

powerful confocal microscope techniques which revealed agonist-induced redistribution of surface receptors from a diffuse pattern of distribution to aggregates, with internalization of receptors in to punctate pockets in the cytoplasm. Additionally, these data are highly suggestive that this process could be sequential in manner such that receptor aggregation and possibly dimerization may serve to package receptors for internalization. Indeed immunoblot analysis confirmed an agonist-mediated reduction in the ~48 kDa receptor monomer in plasma membranes, with little change in the level of immunoreactivity of the ~110 kDa dimer species. These data indicated that using either biochemical or immunological techniques, agonist exposure mediated a time-dependent D1 receptor internalization long after agonist-induced desensitization had occurred. We have provided first evidence that agonist-induced D1 receptor internalization may be a mechanism distinct from receptor desensitization that serves to regulate the activity of D1 receptors following agonist exposure. The physiological role of D1 receptor internalization remains an active area of research. One explanation might be that D1 receptor redistribution may represent a mechanism by which the cell acts to reestablish steady-state conditions. In this model, it is suggested that uncoupled and phosphorylated receptors are rapidly sequestered away from the cell surface, and are dephosphorylated and returned to the surface in an active form (reviewed by Perkins et al., 1990). The recovery of receptors in the plasma membrane and light membrane fraction to near control values following the removal of agonist is consistent with this model. Further evidence of multiple levels of D1 receptor regulation comes from the fact that pretreatment of D1/cells prior to dopamine exposure with concanavalin A or a hypertonic concentration of sucrose completely blocked agonist-induced D1 receptor internalization but not

desensitization. Moreover, following 18 h of agonist treatment, almost no specific labelling could be detected on the surface of D1/cells indicating longer-term down-regulation or loss of the total number of receptors. We conclude that the human D1 receptor is posttranslationally modified by phosphate and palmitate residues, and undergoes rapid agonist-promoted desensitization which is accompanied by enhanced phosphorylation and palmitoylation of the receptor. We also provide the first evidence for at least three temporally distinct pathways, involving the rapid functional uncoupling of the D1 receptor, intermediate-term D1 receptor internalization, and longer-term D1 receptor down-regulation, that regulate D1 receptor-linked transmembrane signalling and its inactivation.

7.2 Biochemical and Pharmacological Properties of D2L Receptors

7.2.1 Pharmacological Characterization of D2L receptor Monomers and Dimers

D2L receptors expressed in Sf9 cells exhibited a pharmacological rank order characteristic of D2 receptors in neuronal tissues (Seeman et al., 1992) and cloned D2L receptors expressed in mammalian cell lines (Castro and Strange, 1993). Agonist/[^{3}H]spiperone competition binding was guanine nucleotide-sensitive suggesting that expressed receptors were coupled to endogenous G_i/G_o-like proteins in Sf9 cells. Immunoblot analysis of membranes prepared from D2L/Sf9 cells revealed major immunoreactive species at ~44 kDa, and at approximately twice the molecular mass at ~90 kDa, similar to immunoreactive receptor species identified in membranes from D2L receptor expressing mammalian cells (Levey et al., 1993). Radioligand binding analysis also suggested the identification of multiple D2L receptor species. In the same membranes preparation from D2L/cells, [^{3}H]YM-09151-2 detected twice the receptor density identified by [^{3}H]spiperone in agreement with reported findings (Niznik et al., 1985, Terai et al., 1989, Seeman et al., 1992, Wong et al., 1993).

Receptor dimerization may be a likely interpretation of these immunoblot and radioligand binding data.

7.2.2 Biophysicochemical Properties of D2L Dimers

We have shown that D2L receptor monomers and dimers are stable in the presence of detergents such as SDS and triton, and reducing agents such as 2-mercaptoethanol and DTT indicating that dimerization did not result from disulphide bonding. Structure-based receptor studies provided a clue to the nature underlying GPCR dimerization. The seven transmembrane helices of GPCRs are thought to be sequentially arranged in anticlockwise fashion, thus forming a very tightly packed TM receptor core (reviewed by Baldwin, 1993). Residues located on the inner surfaces of different TM helices are thought to be involved in the binding of ligands that act on GPCRs (reviewed by Strader et al., 1989). Mutagenesis studies have suggested that the proper folding of GPCR monomers involves intramolecular interactions between TM I and TM VII (Suryanarayana et al., 1992, Liu et al., 1995). Others have shown that coexpression of N-terminal domains (containing TM I-V) and C-terminal receptor domains (containing VI and VII) resulted in the appearance of functional ligand binding and effector coupling Maggio et al., 1993). The results of these studies suggested that TM regions contain not only the structural determinants for ligand binding, but contain also specific binding sites that mediate the profper 3-dimensional self-assembly of receptor proteins. These studies led us to test the hypothesis that interactions involving TM VI and VII helices may be responsible for receptor dimerization.

Consistent with our hypothesis, the dissociation of the D2L dimer to monomer was accomplished in a dose-dependent manner upon addition of the TM VII peptide derived from the TM VII domain of the D2L receptor. Peptides derived from the TM IV and VI domains of the D2L

receptor had similar dose-dependent effects on dimer stability. In samples coincubated with peptides, we noted a consistent upward shift in the molecular weight of the monomer. This suggested that peptides bind to a TM region of the D2L receptor which normally associates with a companion D2L monomer to form a stable D2L dimer. In effect, D2L receptor dimerization is prevented by competitive inhibition of the association of receptor monomers by peptide. Binding of the peptide to the D2L monomer likely disrupts the tertiary structure of the D2L receptor monomers and inactivates D2 receptors. Alternatively, peptides may act by interfering at the outerface of the TM domains which participate at the dimer interface. In doing so, this may lead to the creation of a receptor monomer and a receptor-peptide heterodimer, or two receptor-peptide heterodimers assuming that the stochiometry is 1 peptide: 1 receptor. This model of action is unlikely since this would suggest that dimerization is mediated by any combination of TM-TM interactions, and one might expect from such interactions infinite aggregations of receptor monomers with no uniformity in size of the receptor complex. Peptide actions were receptor and site-specific since no disruption of D2L dimers was observed under identical experimental conditions using peptides derived from the third intracellular loop of the D2L receptor, or peptides derived from the TM VI domain of the β_2-adrenergic receptor or peptides derived from the carboxyl tail of the D1 receptor. In addition, no dissociation of human D1 and 5-HT_{1B} receptor dimers was observed with the D2-TM VII peptide. Collectively, these data support the hypothesis that D2L dimers, which are stable in the presence of detergent and reducing agents, exist in association-dissociation equilibrium with monomers linked by receptor subtype-specific noncovalent interactions between TM regions. Consistent with this model, D2L dimers diluted in sodium dodecyl sulfate buffer can be dissociated as a function of increasing temperature. The dimer was completely

dissociated at 65 °C after a 30 min incubation. Our pH stability experiments are also in agreement with the interpretation that two D2L monomers are in equilibrium to form a dimer. Dissociation of the D2L dimer was achieved by addition of 0.1 N tartaric acid, 0.1% glacial acetic acid, or 0.1 N HCl (final pH of approximately 3) after a 30 min incubation. We conclude that D2L dimerization and possibly the dimerization of other GPCRs is mediated at the protein level involving specific intermolecular, noncovalent and electrostatic interactions of certain residues within TM IV, VI and VII domains. Interestingly, sequence alignments show that virtually all GPCRs share several invariant proline and tryptophan amino acids located in TM IV, VI and VII (reviewed by Probst etal., 1992). This gives rise to the intriguing speculation that if dimerization is universal to GPCRs, the high degree of conservation of these residues may indicate that these amino acids play a critical role in the dimerization of these receptors. It will be important now to determine the precise region and amino acid(s) required to form stable receptor dimers.

The presence of multiple D2L receptor species was confirmed by radioligand binding. In the same membrane preparation from D2L/Sf9 cells, the benzamide D2 antagonist [^{3}H]YM-09151-2 detected ~1.5-2 fold the receptor density estimated by the butyrophenone D2 antagonist [^{3}H]spiperone. These findings are in good agreement with receptor density data previously obtained from D2L receptors in cultured cells (Seeman et al., 1992), in rat and porcine anterior pituitary tissues (Niznik et al., 1985, Terai et al., 1989), human postmortem tissue (Seeman et al., 1992) and PET studies (Wong et al., 1993). The receptor species-specificity of these ligands was clarified by photoaffinity labelling experiments using [^{125}I]NAPS and [^{125}I]YM-09151-2. As observed in Fig. 26B, [^{125}I]NAPS labelled the D2L monomer whereas [^{25} I]YM-09151-2 labelled D2L monomer and D2L dimer in identical tissues. These data indicated that distinct classes of

D2 receptor antagonists detect receptor monomer and dimer differentially, accounting at least in part, for the higher D2 receptor densities estimated by benzamides compared to butyrophenones. Of potentially great clinical significance, these studies suggest that dopamine receptor dimers and monomers may be different targets of neuroleptic drug actions. Taken together, these data constitute the first direct evidence that D2L receptors and other GPCRs exist as dimers and monomers.

Analysis of the amino acid structure of the D2L receptor indicates the presence of several threonine and serine residues (Bunzow et al., 1988) that are putative sites for phosphorylation by regulatory protein kinases, supporting the notion that receptor phosphorylation may be an important determinant of D2 receptor function. Cells expressing D2L receptors were cultured in serum-free media and incubated with $^{32}P_i$ to metabolically label receptors. Immunoprecipitation experiments demonstrated for the first time that the ~44 kDa and ~90 kDa D2L receptor species were each phosphorylated even in the absence of agonist, with the dimer being labelled with higher specific activity. Agonist-independent phosphorylation of receptors suggest that this owes to an inherent property, intrinsic or constitutive activity, of the receptor proteins. Agonist-independent phosphorylation has been best studied for the glucocorticoid receptor and is believed to be important in regulating receptor recycling and reuse (Orti et al., 1989). This raises the interesting speculation that the receptor dimer is in a more active or higher energy state than monomer. The basis of this may owe to receptor-receptor cooperativity as described in the mathematical model for histamine receptor binding (Sinkins and Wells, 1993, Sinkins et al., 1993). However the precise molecular determinants of GPCR dimer formation remains unknown at this time.

Palmitoylation has been shown for the serotonin 5-HT_{1B} and α_{2A}-adrenergic receptors (Ng

et al, 1993, Kennedy and Limbird, 1993), two other structurally related receptors with short carboxyl tails. The occurrence of cysteine residues in the carboxyl tail of the D2 receptor (Bunzow et al., 1988) suggested that it may be a candidate for palmitoylation. Indeed, immunoprecipitation experiments showed that the ~44 kDa and ~93 kDa D2L receptor species were both palmitoylated. These data constitute the first direct evidence showing agonist-independent palmitoylation of the D2L receptor. It appears that in the absence of agonist, as in the case of receptor phosphorylation, receptor palmitoylation may be mediated by an intrinsic or constitutive property of the receptor protein. However, the precise role of D2L receptor palmitoylation remains a subject of further research. Palmitoylation could be a modulator of ligand binding or receptor activity as shown for the D1 receptor. Alternatively, palmitoylation could constitute a site for receptor-membrane docking and presentation of monomers for dimerization. Further definition of the role of D2L palmitoylation on a molecular level seems important.

7.2.3 Differential Regulation Of The D2L Receptor Coupled Adenylyl Cyclase System Following Agonist Exposure

We now present evidence demonstrating that the D2L receptor coupled adenylyl cyclase system, compared to the D1 system, is differentially regulated by agonist in the same foster cell line. Following sustained exposure to 10 μM dopamine for as long as 60 min, D2L receptor mediated inhibition of forskolin-stimulated adenylyl cyclase activity was not significantly affected suggesting that the D2L receptor does not readily undergo agonist-induced desensitization. Indeed, such treatments did not result in a loss of agonist-detected high affinity binding. The continued occurrence of D2L receptor functional coupling following sustained agonist exposure might be attributed to a tight association of the D2L receptor-G protein-adenylyl cyclase complex not

common to the D1 receptor coupled adenylyl cyclase system. Although the classical response of receptor systems to stimulation by agonist is desensitization, paradoxical regulation of the D2L receptor system by agonist is not unprecedented. Resistance of D2L receptor coupled adenylyl cyclase to agonist-induced desensitization has been demonstrated in several different mammalian cell lines (Ivins et al., 1991, Filtz et al., 1993, Zhang et al., 1994, Star et al., 1995). Conceivably, agonist-bound D2L receptors exist in a more stable state (Costa and Feldman, 1987, Wiese et al., 1992). Alternatively, resistance to desensitization may be conferred by continuously replacing or making available signalling receptor species for as long as agonist is present. This notion is consistent with the agonist-induced up-regulation of surface D2L receptors. Alternatively, differential sensitivity to agonist may owe to an inherent property of the D2L receptor protein and/or the biophysicochemical state of the receptor. We have shown that the D2L receptor is phosphorylated and palmitoylated and undergoes dimerization supporting the hypothesis that such posttranslational modifications may contribute to the activity of the receptor.

7.2.4 Agonist-induced Redistribution of D2L Receptors

In contrast to the D1 receptor, agonist mediated a slow time-dependent redistribution (recruitment) of D2L receptors from intracellular pools to the cell surface as assessed by radioligand binding and confirmed by immunocytochemical labeling and confocal laser microscopy techniques. Immunoblot and [^{3}H]spiperone and [^{3}H]YM-09151-2 binding analysis revealed that the dopamine-induced increase in surface D2L receptor density was composed of an increase in both D2L monomer and dimer. D2 receptor up-regulation and behavioural supersensitivity to D2 agonist have been observed in animals treated with indirect dopamine agonists (Lee et al., 1988, Rouillard et al., 1987), and have been reported for the D2-like, D3 receptor as well (Cox et al.,

1995). Interestingly, the up-regulation of D2L receptors was induced not only by agonist, but also by the benzamide antagonist, (-)sulpiride, but not the butyrophenone, haloperidol, confirming the results of other studies (Filtz et al, 1993, Star et al., 1995). We now attribute the effects of the benzamide to partial agonist activity at the D2L receptor, which correlates well with the lower incidence of Parkinson-like side-effects reported for this compound compared to other neuroleptics (Motohashi et al., 1992). Although these results imply some selectivity for agonists in inducing D2L receptor up-regulation, the basis of ligand-induced increase in surface D2L receptor density is not entirely clear. Agonist-induced receptor up-regulation has been associated with the transcriptional control (biosynthesis rate and altered stability and levels of receptor mRNA) of the 5-HT_2 receptor on cultured cerebellar neurons, and β_2-adrenergic and β_3-adrenergic receptors in cultured cells (Thomas et al., 1992, Akiyoshi et al., 1993, Collins et al., 1992). However, this is likely not the mechanism for the D2L receptor since largely coding sequences and not untranslated regions, important for transcriptional regulation, are present in the recombinant D2L-baculovirus. It is likely that increased surface D2L receptor density results from a redistribution of existing intracellular pools of D2L receptors to the surface, and not biosynthesis of new receptors. It has been postulated that intracellular receptors could serve as reserve receptor pools that may be induced by agonist to translocate to the cell surface or to functional microdomains (Von Zastrow et al., 1993, Clapham and Neer, 1993). It also follows that with the continuous up-regulation of surface receptors, the D2L receptor system should remain refractory to agonist-induced desensitization. It will now be important to uncover the physiological relevance of this ligand-induced D2L receptor response.

7.3 Mechanistic Basis Of Dopamine Receptor-subtype Specific Redistribution

Coated vesicles have been shown to be involved in the short and long term agonist-induced trafficking of adenosine A_1 and glutamate receptors (Gonzalez-Calero et al., 1990, Martin et al., 1991). Recently D1 and D2L receptors have been colocalized with their signalling system in clathrin coated vesicles in brain (Ozaki et al., 1994) suggesting some functional relationship between coated vesicles and dopamine receptor subtype trafficking. Preincubation of D1/cells and D2L/cells with concanavalin A or with sucrose, agents shown to block clathrin-mediated processes, inhibited agonist-induced D1, but not D2L receptor redistribution. Immunoblot analysis using an antibody raised against bovine neuronal clathrin revealed the presence of an abundance of clathrin immunoreactive-like material in Sf9 cell lysate corresponding in size to the heavy chain of neuronal clathrin. These data suggest that clathrin-like processes may be involved in dopamine receptor subtype-specific trafficking. D1 receptors have been colocalized with its signalling system in coated vesicles (Ozaki et al., 1994). It has been postulated that cellular protein trafficking by coated vesicles constitutes a rapid process whereby receptors are concentrated to increase the efficiency of their delivery to their targets. In addition coated vesicles have been shown to function as a recycling device (Goldstein et al., 1985, Brodsky, 1988). These observations are all consistent with the biology of the D1 receptor, but not the biology of the D2L receptor following agonist exposure. This suggest an intriguing possibility that a further level of functional heterogeneity distinguishing these receptors may also be present at the level of the intracellular trafficking and subcellular sorting of these receptors. Several observations provide interesting speculations about possible molecular candidates for the mediators of D2L receptor trafficking. First, $G_{\alpha i3}$ proteins have been implicated in the activation of noncoated vesicle-mediated exocytosis (Aridor et al., 1993), and second, $G_{\beta\gamma}$ dimers have been shown to regulate not only receptor phosphorylation and desensitization, but in

addition intracellular vesicular trafficking (reviewed by Clapham and Neer, 1993, Milligan, 1993). Thus, there appears to be a more complex level of cellular organization distingishing receptor subtypes than previously anticipated.

7.4 Pharmacological Properties of Coexpressed D1 and D2L Receptors

A D1-D2 receptor interaction has been reported in nervous tissue (Seeman et al., 1989, LaHoste et al., 1992), cultured cells (Walters et al., 1987, Piomelli et al., 1991, Surmeier et al., 1992) and animals (Star and Star, 1989), the basis of which remains unknown. We have taken advantage of the suitability of the Sf9/baculovirus expression system for the study of GPCRs to coexpressed D1 and D2L receptors for the study of D1-D2 receptor interactions. Cells expressing the D1 and D2L receptors to specific activities of ~6 and ~4 pmol/mg of protein respectively were used in these studies. It should be noted that a similar ratio of D1 and D2 receptors are found in neurons making it reasonable to assume that processes observed in this model may occur in native tissues.

Saturation binding isotherms for [^{3}H]SCH-23390 binding and SKF-38393/ [^{3}H]SCH-23390 competition analysis binding to membranes prepared from D1-D2L/Sf9 cells were indistinguishable from D1 receptors expressed in isolation. Saturation binding isotherms for [^{3}H]spiperone and quinpirole/[^{3}H]spiperone competition binding to membranes prepared from D1-D2L/Sf9 cells were similar to D2L/Sf9 cells. Collectively, these data showed no modulation of ligand binding properties of D1 or D2L receptors when co-expressed in an identical cell line. We reported also that in cells coexpressing the D1 and D2L receptors, that biochemical and immunological studies revealed no D1 and D2L receptor heterodimerization, although these receptor subtypes formed homodimers that were stable in the presence of detergents and reducing agents. Although these data indicated no D1-D2L receptor synergism or antagonism at the level of the receptor, this was

observed at the level of adenylyl cyclase when D1 and D2L receptors were independently activated.

In membranes prepared from D1-D2L cells, selective D1 receptor activation by SKF-38393 resulted in greater adenylyl cyclase activity with no change in efficacy (EC_{50} ~200 nM) compared to membranes prepared from D1/cells. In membranes prepared from D1-D2L cells, selective D2L receptor activation by quinpirole inhibited to a greater extent adenylyl cyclase activity with no change in efficacy (IC_{50} ~5 nM) compared to membranes prepared from D2L/cells. Synergistic D1 and D2L receptor activation or inhibition of adenylyl cyclase may owe to the additional interaction of the effector molecule by $G_{\beta\gamma}$ dimers generated upon ligand binding to the receptor and dissociation of $G_{\alpha\beta\gamma}$ to G_{α} and $G_{\beta\gamma}$ (reviewed by Clapman and Neer, 1993). However, synergistic activity of the D1 and D2L receptor coupled adenylyl cyclase systems was not observed with dopamine as the agonist. In membranes prepared from cells coexpressing D1 and D2L receptors, dopamine stimulated adenylyl cyclase activity was reduced compared to membranes prepared from cells expressing the D1 receptor in isolation. Presumably under these conditions, the net dopamine activated adenylyl cyclase activity is the contribution of D1 receptor stimulation and concurrent D2L receptor inhibition since both D1 and D2L receptors are targets of dopamine actions. In summary, the high level expression of the receptors and the multiple lines of evidence allows us to conclude that D1 and D2L receptors do not undergo direct interaction, but that an interaction between D1 and D2L receptor coupled adenylyl cyclase systems occurs downstream from the level of the receptor. We propose that this cellular organization of the signal transducing components will be important for the ability of the cell to respond correctly to multiple external stimuli.

8. SUMMARY AND COMMENTARY

Taking advantage of the similarity in processing pathways used by the Sf9 cells and by mammalian cells, we have shown that the baculovirus/Sf9 expression system is a highly suitable model system to generate sufficient, functional, recombinant dopamine receptors for biochemical and pharmacological characterization at the molecular level. In fact much of our current understanding of receptor structure and function derive from the study of cloned receptors generated in heterologous expression systems (reviewed by Dohlman et al., 1991). The levels of expression in these models add only to the confidence of experimental results, and the evidence is convincing that processes observed in the Sf9 cells may occur in cells endogenously expressing D1 and D2L receptors. Indeed, D1 and D2L receptor agonist affinities and efficacies for adenylyl cyclase activation, and ability of the D1 and resistance of D2L receptors to undergo agonist-induced desensitization are in excellent agreement with findings in cell types which endogenously express the dopamine receptors (reviewed by Sibley and Monsma, 1992). A wide variety of approaches has also yielded evidence that show that the biology of D1 and D2L receptors is more complex and interesting than previously predicted. I will now speculate about the maintenance of a sophisticated level of cellular organization of these receptors, how receptor dimers may play a important role in their function, and the possible applications of these research findings.

The results of these experiments demonstrated for the first time that D1 and D2L receptors are posttranslationally modified indicating that these receptors are subject to regulation by phosphorylation and palmitoylation. However, the differences observed in the ability of dopamine to distinctly regulate D1 receptor stimulated adenylyl cyclase and D2L receptor inhibited adenylyl cyclase suggested possibly important differences in the physiological roles of dopamine mediated

through these receptor types. It is tempting to speculate that, since D1 and D2 receptors are found colocalized in the same brain regions (Levey et al., 1993, Mansour et al., 1990) and perhaps even on the same neurons (Surmeier et al., 1992), conceivably at low concentrations of dopamine the D1 receptor would be preferentially activated owing to its higher affinity for dopamine, whereas for D2 receptor activation, higher concentrations of dopamine or longer exposure may be required. Interestingly, drugs of abuse are known to increase dopamine release and the rewarding properties are believed to be mediated by the D2 receptor (Wise and Bozarth, 1989, Harris and Aston-Jones, 1994). Conceivably, the proposed temporal and concentration-dependent activation of D1 and then D2L receptors may contribute to mechanisms regulating the start and termination of the dopamine signal. The rapid pattern of D1 receptor desensitization would ensure that D1 receptor-linked cellular signalling events are rapidly inactivated again, whereas D2L receptor activation will result in a longer, more sustained pattern of activation of D2L receptor linked intracellular events. These findings suggest that in tissues containing both D1 and D2L receptors, the repertoire of dopamine-mediated postreceptor events may be modulated in a temporal manner as well, with a changing ratio or shifting balance of D1:D2L receptor effects. Although the mechanisms are unknown, it may be postulated that after dopamine stimulation, the sum of early effects relate to D1 receptor activation, whereas in a later time frame, the sum of effects will relate to D2L receptor activation. In particular, since D2 receptor mediated mechanisms are important for autoreceptor function in dopamine neurons, and in tonic inhibitory functions, such as the inhibition of prolactin or αMSH, the relative insensitivity to desensitization by agonist activation would form an important aspect of the functional role of D2 receptors. Alternatively, this distinction may reflect receptor sorting into functional microdomains making it possible for separation of receptor subtype-specific intracellular

signals within a cell. We conclude that D1 and D2L receptor subtype-specific regulation may represent functional differences distinguishing these two members of the dopamine receptor family which may account, at least in part, for the diverse biological activities of dopamine. Much of our current thinking about G protein-coupled receptors is based on the idea that monovalent receptors are the targets of agonist. In this model, classically referred to as the ternary complex model (De Lean et al., 1980), the agonist-bound receptor stimulates a G protein and in turn an effector molecule such as adenylyl cyclase with the receptor:G protein:effector stochiometry of 1:1:1. Circumstantial evidence has suggested that GPCRs are more highly organized than predicted in this model. GPCR binding and receptor radiation inactivation studies (Wregget and Wells, 1995, Venter and Fraser, 1983) have suggested that GPCRs may exist as dimers. Additionally, immunoblots of crude membrane from Sf9 cells expressing muscarinic M1 and M2 receptors (Parker et al., 1991), the human serotonin 5-HT_{1B} receptor (Ng et al., 1993), and immunoblots of crude membrane from hamster kidney cells expressing the cloned metabotropic glutamate receptor (Pickering et al., 1993) revealed the existence of species believed to be receptor monomers and species at approximately twice the molecular mass suggested to be receptor dimers. Further, a mechanistic basis for receptor-receptor interactions such as dimerization has been reported (Sinkins and Wells, 1993, Sinkins et al., 1993) suggesting that the ternary complex model may be an over-simplification of the mechanisms underlying hormonal signalling by GPCRs. We have now provided the first direct evidence that the dopamine receptors exists as dimers in equilibrium with monomers, resulting from specific noncovalent interactions between receptor transmembrane domains. This raises the intriguing possibility that some GPCRs may signal via receptor dimers.

By analogy with the receptor tyrosine kinases (reviewed by Schlessinger, 1990), certain ligands require associations with multivalent receptors for appropriate binding or stimulation to occur. According to this model, the ligand-binding receptor species would be composed of at least two or more monomers with each subunit contributing to binding. Ligand binding might require the presence of preexisting receptor complexes on the cell surface, or ligands might be able to generate such complexes by recruiting monomers. It will be important now to determine whether GPCR monomers can signal alone or function as part of a larger receptor complex. Further definition of the targets for agonist seems important. A partial answer comes already with the biochemical studies which showed that only the D1 monomer is posttranslationally modified suggesting that monomers are more active than dimers. In this instance, D1 dimerization may serve to package desensitized receptors for recycling. In contrast, similar biochemical studies showed that the D2L dimer is phosphorylated and palmitoylated to a greater extent than the monomer suggesting that the dimer is spontaneously more active and is the candidate signalling species. If this proves to be important for D2L signalling, D2L monomers may act as a reservoir or capacitor for this receptor system. Consistent with this view, D2L monomers are recruited to the cell surface becoming available to undergo dimerization to the signalling species upon agonist exposure. This reserve receptor capacity may contribute to the resistance of the D2L receptor coupled adenylyl cyclase system in undergoing agonist-induced desensitization. Collectively, these observations suggest that dimerization may have different roles in the distinct biology of closely related receptor subtypes, and renders questionable the widely held belief that only monovalent GPCRs participate in signalling (De Lean et al., 1980). It would still be premature, however, to discard this notion. Further work along these lines are needed, and should provide valuable insight into the molecular biology of the structure-

function of GPCRs. What is clear is that the emerging biology of GPCRs appears to be more complicated than previously thought, and that the demonstration of G protein-coupled receptor dimers constitute a new beginning towards the better understanding of the biology of this important class of membrane proteins.

Taking advantage of the high level of expression of the Sf9/baculovirus system, we showed by multiple independent assays that D1 and D2L receptors do not undergo receptor heterodimerization in living cells or in solution excluding this process as a basis for the reported D1-D2 linkage. One explanation may be that dopamine receptor dimerization may occur only through related members within the D1-like or D2-like families. The highest levels of structural similarity among GPCRs is observed in the transmembrane spanning domains which were identified as the mediators of dimerization involving highly receptor-subtype specific associations of TM α helices. It will be attractive to identify the receptor subtypes able to undergo heterodimerization as this type of receptor diversity amplifies the signalling and regulatory potential of the dopamine system. A intriguing possibility is that this research confers a potential role for truncated receptor species encoded by GPCR pseudogenes or primary transcript via alternative splicing. D5 pseudogenes (ψD5-1 and ψD5-2, reviewed by O'Dowd, 1992) and truncated D3 mRNA ($D3_{nf}$, Liu et al., 1994) were previously thought to have no biological functions and were of only evolutionary significance. Although the D5 pseudogene or truncated D3 mRNA are not expected to encode for signalling receptors, these truncated receptors may undergo dimerization with native receptors to form pseudoreceptor-receptor dimers. These pseudodimers may represent a novel class of transmembrane signalling molecules, or alternatively could impair hormone signalling by acting as a competitor of D5 dimers or D3 dimers. This can now be tested. The findings could be universal for other

receptors such as the large serotonin receptor family which includes the ψ5-HT_{1D} pseudogene (Nguyen et al., 1992). One might reasonably speculate that altered receptor proportions in the brain may underlie a susceptibility to psychiatric disorders or determine whether a patient will respond to drug treatments.

One other promising area of research deals specifically with the applications arising from the knowledge that GPCR dimers are formed by receptor subtype-specific noncovalent and electrostatic transmembrane domain interactions. Peptides could be used as a novel means of mapping and identifying the structural determinants of dimer formation as applied in this thesis research. Additionally, these discoveries now offer new vistas of drug discovery such as creation of novel peptide-based receptor-specific pharmaceuticals. Peptides may be able to interfere with or modulate the response of the cells through their ability to disrupt receptor monomer folding and thus dimer formation. Peptide-receptor complexes could have many consequences. Those lacking parts of extracellular and/or cytoplasmic domains may lead possibly to stimulation or inhibition of different functions, depending on the receptor. This raises the possibility now to test these hypothesis in animals models. Such studies may provide the missing mechanistic details associating dopamine receptor systems with psychiatric and neuroendocrine disorders. The applications are tremendous and could well be extended to other GPCRs and disease.

This thesis research describes the steps of discovery taken to elucidate the biochemical and pharmacological properties of D1 and D2L receptors at the molecular level which has shown them to exhibit more complex biology than previously predicted. Based on the high structural homology found among all G protein-coupled receptors, these findings could be of universal importance for the entire receptor superfamily. I think you will agree that this thesis research has now opened a

pandoras box with greater challenges and discovery ahead.

9. REFERENCES

Adham, N., Kao, H.T., Schechter, L.E., Bard, J., Olsen, M., Urquhart, D., Durkin, m., Hartig, P.R., Weinshank, R.L., and Branchek, T.A. (1993) Cloning of another human serotonin receptor (5-HT1F): a fifth 5-HT1 receptor subtype coupled to the inhibition of adenylate cyclase. *Proc. Natl. Acad. Sci. U.S.A.* **90**, 408.

Akiyoshi, J., hough, C., and Chuang, D.-M. (1993) Paradoxical increase of 5-hydroxytryptamine$_2$-receptors and 5-hydroxytryptamine$_2$ receptor mRNA in cerebellar granule cells after persistent 5-hydroxytryptamine$_2$ receptor stimulation. *Mol. Pharmacol.* **43**, 349.

Argraves, W.S., Pytela, R., Suzuki, S., Millan, J.L., Pierschbacher, M.d., and Ruoslahti, E. (1986) cDNA sequences from the alpha subunit of the fibronectin receptor predict a transmembrane domain and a short cytoplasmic peptide. *J. Biol. Chem.* **261**, 12922.

Aridor, M., Rajmilevich, G., Beaven, M.A., Sagi-Eisenberg, R. (1993) Activation of exocytosis by the heterotrimeric G protein Gi3. *Science* **262,** 1569.

Baldessarini, R.J., and Frankenburg, F.R. (1991) Clozapine: A novel antipsychotic agent, *New England J. Med.* **324**, 746.

Baldwin, J.M. (1993) The probable arrangement of the helices in G protein-coupled receptors. *EMBO J.* **12**, 1693.

Barton, A.C., Black, L.E. and Sibley, D.R. (1991) Agonist-induced desensitization of D2 dopamine receptors in human Y-79 retinoblastoma cells. *Mol. Pharmacol.* **39**, 650.

Barton, A.C. and Sibley, D.R. (1990) Agonist-induced desensitization of D1-dopamine receptors linked to adenylyl cyclase activity in cultured NS20Y neuroblastoma cells. *Mol. Pharmacol.* **38**, 531.

Bates, M.D., Olsen, C.L., Becker, B.N., Albers, F. J., Middleton, J.P., Mulheron, J.G., Jin. S.-L., Conti, M., and Raymond, J.R. (1993) Elevation of cAMP is required for down-regulation, but not agonist-induced desensitization, of endogenous dopamine D1 receptors in opossum kidney cells. Studies in cells that stably express a rat cAMP phophodiesterase (rPDE3) cDNA. *J. Biol. Chem.* **268**, 14757.

Benovic, J.L., M. Bouvier, M.G. Caron, and R.J. Lefkowitz (1988) Regulation of adenylyl cyclase-coupled β-adrenergic receptors. *Ann. Rev. Cell Biol.* **4**, 405.

Benovic, J.L., H. Kuhn, I. Weyland, J. Codina, M.G. Caron and R.J. Lefkowitz (1987) Functional desensitization of the isolated β-adrenegic receptor by β-adrenergic receptor kinase: potential role of an analog of the retinal protein arrestin (48 kDa protein). *Proc. Natl. Acad. Sci. USA.* **84**, 8879.

Benovic, J.L., Pike, L.J., Cerione, C., Staniszewski, T., Yoshimasa, J., Codina, J., Caron, M.G., and Lefkowitz, R.J. (1985) Phosphorylation of the mammalian beta-adrenergic receptor by cyclic AMP-dependent protein kinase. Regulation of the rate of receptor phosphorylation and dephosphorylation by agonist occupancy and effects on coupling of the receptor to the stimulatory guanine nucleotide regulatory protein. *J. Biol. Chem.* **260**, 7094.

Benovic, J.L., Strasser, R.H., Caron, M.G., and Lefkowitz, R.J. (1986) Beta-adrenergic receptor kinase: identification of a novel protein kinase that phosphorylates the agonist-occupied form of the receptor. *Proc. Natl. Acad. Sci. U.S.A.* **83**, 2797.

Berridge, M.J. and Irvine, R.F. (1984) Inositol triphosphate, a novel second messenger in cellular signal transduction. *Nature* **312**, 315.

Billard, W., Ruperto, V., Crosby, G., Iorio, L.C., Barnett, A. (1984) Characterization of the binding

of [^{3}H]SCH-23390, a selective D1 receptor antagonist ligand, in rat striatum. *Life Sci.* **35**, 1885.

Binart, N., Lombes, M., Rafestin-Oblin, M.E., and Baulieu, E.E. (1991) Characterization of human mineralocorticosteroid receptor expressed in the baculovirus system. *Proc. Natl. Acad. Sci. USA* **88**, 10681.

Bischoff, S., Krauss, J., Grunenwald, C., Gunst, F., Heinrich, M., Schaub, M., Stöcklin, K., Vassout, A., Waldmeier, P. And Mâitre, L. (1991) Endogenous dopamine (DA) modulates [3H]spiperone binding in vivo in rat brain. *J. Recep. Res.* **11**, 163.

Blum, K., Noble, E.P., Sheridan, P.J., Montgonery, A., Ritchie, T., Jagadeeswaran, P., Nogami, H., Briggs, A.H. and Cohn, J.B. (1990) Allelic association of human dopamine D2 receptor gene in alcoholism. *JAMA* **263**, 2055.

Boni-Schnetzler, M., and Pilch, P.F. (1987) Mechanism of epidermal growth factor receptor. *Proc. Natl. Acad. Sci. USA* **84**, 7832.

Bouhelal, R., Smounya, L., and Bockaert, J. (1988) 5-HT1B receptors are negatively coupled with adenylate cyclase in rat substantia nigra. *Eur. J. Pharmacol.* **151**, 189.

Bouthenet, M.-L., Martres, M-P., Sales, N. and Schwartz, J.-C. (1987) A detailed mapping of dopamine D-2 receptors in rat central nervous system by autoradiography with [^{125}I]iodosulpiride, *Neuropharmacol.* 26, 117.

Bouthenet, M.-L., Souil, E., Martres, M.-P., Sokoloff, P., Giros, B., and Schwartz, J.-C. (1991) Localization of dopamine D3 receptor mRNA in the rat brain using in situ hybridization histochemistry: comparison with dopamine D2 receptor mRNA. *Brain Res.* 564, 203.

Bouvier, M., Hnatowich, M., Collins, S., Kobilka, B.K., Deblasi, A., Lefkowitz, R.J., and Caron,

M.G. (1987) Expression of a human cDNA encoding the beta 2-adrenergic receptor in Chinese hamster fibroblasts (CHW): functionality and regulation of the expressed receptors. *Mol. Pharmacol.* **33**, 133.

Bouvier, M., N. Guilbault and H. Bonin (1991) Phorbol-ester-induced phosphorylation of the β2-adrenergic receptor decreases its coupling to Gs. *FEBS* **279**, 243.

Bouvier, M., W.P. Hausdorff, A. De Blasi, B.F. O'Dowd, B.K. Kobilka, M.G. Caron and R.J. Lefkowitz (1988) Removal of phosphorylation sites from the β2-adrenergic receptor delays onset of agonist-promoted desensitization. *Nature* **333**, 370.

Bozarth, M.A. (1986) Neural basis of psychostimulant and opiate reward. Evidence suggesting the involvement of a common dopaminergic pathway. *Behavioral Brain Res.* **22**, 107.

Bradford, M.M. (1976) A rapid and sensitive method for the quantification of microgram quantities of protein using the principle of protein dye binding. *Anal. Biochem.* **72**, 248.

Brodsky, F.M. (1988)Living with clathrin: its role in intracellular membrane traffic. *Science* **242**, 1396.

Brown, E.M., FedaK, S.A., Woodard, C.J., and Aurbach, G.D. (1976) Beta-adrenergic receptor interactions. Direct comparison of receptor interaction and biological activity. *J. Biol. Chem.* **251**, 1239.

Bunzow, J.R.,Van Tol, H.H.M., Grandy, D.K., Albert, P., Salon, J., Christie, M., Machida, C.A. , Neve K.A. and Civelli, O.(1988) Cloning and expression of a rat D2 dopamine receptor cDNA. *Nature* **336**, 783.

Casey, P.J. and Gilman, A.G. (1988) G protein involvement in receptor-effector coupling. *J. Biol.Chem.* **263**, 2577.

Castro, S.W. and Strange, P.G. (1993) Coupling of D2 and D2 dopamine receptors to G-proteins. *FEBS Lett.* **315**, 223.

Charo, I.F., Fitzgerald, L.A., Steiner, B., Rall, S.C., Jr., Bekeart, L.S., and Phillips, D.R. (1986) Platelet glycoproteins IIb and IIIa: evidence for a family of immunologically and structurally related glycoproteins in mammalian cells. *Proc. Natl. Acad. Sci. USA* **83**, 8351.

Chidiac, P., Hebert, T.E., Valiquette, M., Dennis, M., and Bouvier, M. (1994) Inverse agonist activity of β-adrenergic antagonists. *Mol. Pharmacol.* **45**, 490.

Chio, C.L., Hess, G.F., Graham, R.S. and Huff, R.M. (1990) A second form of D2-dopamine receptor in rat and bovine caudate nucleus. *Nature* **343**, 266.

Chio, C.L., Lajiness, M.E., and Huff, R.M. (1990) Activation of heterologously expressed D3 dopamine receptors: comparison with D2 dopamine receptors, *Mol. Pharmacol.* 45, 51.

Chiu, A.S., Li, P.P., and Warsh, J.J. (1988) G-protein involvement in central nervous system muscarinic receptor-coupled polyphosphoinositide hydrolysis. *Biochem. J.* **256**, 995.

Clapham, D.E. and Neer, E.J. (1993) New roles for G-protein βγ-dimers in transmembrane signalling. *Nature* **365**, 403.

Collins, S., Caron, M.G., Lefkowitz, R.J. (1992) From ligand binding to gene expression: new insights into the regulation of G-protein-coupled receptors. *Trends Biochem. Sci.* **17**, 37.

Costa, E.M. and Feldman, D. (1987) Measurement of 1,25-dihydroxyvitamin D3 receptor turnover by dense amino acid labelling: changes during receptor up-regulation by vitamin D metabolites. *Endocrinology* **120**, 1173.

Costa, T., Ogino, Y., Munson, P.J., Onaran, H.O. and Rodbard, D. (1992) Drug efficacy at

guanine nucleotide-binding regulatory protein-linked receptors: thermodynamic interpretation of negative antagonism and of receptor activity in the absence of ligand. *Mol. Pharmacol.* **41**, 549.

Cox, B.A., Rosser, M.P., Kozlowski, M.R., Duwe, k.M., Neve, R.L., and Neve, K.A. (1995) Regulation and functional characterization of a rat recombinant dopamine D3 receptor. *Synapse* (in press).

Cross, A.J. (1988) *in Neuronal Serotonin* (Osborne, N.N., and Hamon, M., eds) pp 231-253, John Wiley and Sons Ltd., Chichester, U.K.

Dal Toso, R., B. Sommer, M. Ewert, A. Herb, D.B. Pritchett, A. Bach, B.D. Shivers and P.H. Seeburg (1989) The dopamine D2 receptor: two molecular forms generated by alternative splicing. *EMBO* **8**, 4025.

Demchyshyn, L., Sunahara, R.K., Miller, K., Teitler, M., Hoffman, B.J., Kennedy, J.L., Seeman, P., Van Tol, H.M.M., and Niznik, H.B. (1992) A human serotonin 1D receptor variant (5HT1D beta) encoded by an intronless gene on chromosome 6. *Proc. Natl. Acad. Sci. U.S.A.* **89**, 5522.

De Lean, A., Stadel, J.M., and Lefkowitz, R.J. (1980) A ternary complex model explains the agonist-specific binding properties of the adenylate cyclase-coupled beta-adrenergic receptor. *J. Biol. Chem.* **255**, 7108.

Dohlman, H.G., Thorner, J., Caron, M.G., and Lefkowitz, R.J. (1991) Model systems for the study of seven-transmembrane-segment receptors. *Annu. Rev. Biochem.* **60**, 653.

Ebina, Y., Ellis, L., Jarnagin, K., Edery, M., Graf, L., Clauser, E., Ou, J.-H., Masiarz, F., Kan, Y.W., Goldfine, I.D., Roth, R.A., and Rutter, W.J. (1985) The human insulin

cDNA: the structural basis for transmembrane signalling. *Cell* **40**, 747.

Elazar, Z., Siegel, G., and Fuchs, S. (1989) Association of two pertussis toxin-sensitive G proteins with the D2 dopamine receptor from bovine striatum. *EMBO J.* **8**, 2353.

El Mestikawy, S., Taussig, D., Gozlan, H., Emerit, M.B., Ponchatt, M., and Hamon, M. (1989) Chromatographic analyses of the serotonin 5-HT1A receptor solubilized from the rat hippocampus. *J. Neurochem.* **53**, 1555.

Emrich, T., Forster, R. And Lipp, M. (1993) Topological characterization of the lymphoid-specific seven transmembrane receptor BLR1 by epitope-tagging and high level expression. *Biochem. Biophys. Res. Commun.* **197**, 214.

Evan, G.I., Lewis, G.K., Ramsay G.and Bishop J.M. (1985) Isolation of monoclonal antibodies specific for human c-myc proto-oncogene product. *Mol. Cell. Biol.* **5**, 3610.

Fanger, B.O., Austin, K.S., Earp, H.S., and Cidlowski, J.A. (1986) Cross-linking of epidermal growth factor receptors in intact cells: detection of initial stages of receptor clustering and determination of molecular weight of high-affinity receptors. *Biochemistry* **25**, 6414.

Fargin, A., Raymond, J.R., Lohse, M.J., Kobilka, B.K., Caron, M.G., and lefkowitz, R.J. (1988) The genomic clone G-21 which resembles a beta-adrenergic receptor sequence encodes the 5-HT1A receptor. *Nature* **335**, 358.

Filtz, T.M., Artymyshyn, R.P., Guan, W., and Molinoff, P.B. (1993) Paradoxical regulation of dopamine receptors in transfected 292 cells. *Mol. Pharmacol.* **44**, 371.

Fishburn, C.S., Bellei, D., David, C., Carmon, S., and Fuchs, S. (1993) A novel short isoform of the D3 dopamine receptor generated by alternative splicing in the third cytoplasmic loop. *J. Biol. Chem.* **268**, 5872.

Frazer, A., Maayani, S., and Wolfe, B.B. (1990) Subtypes of receptors for serotonin. *Annu. Rev. Pharmacol. Toxicol.* **30**, 307.

Fuxe, K., Fredholm, B.B., Ogren, S.O., Agnati, L.F., Hokfelt, T., Gustafsson, J.A. (1978) Pharmacological and biochemical evidence for the dopamine agonistic effect of bromocriptine, *Acta Endocrinologica, supplement* **2166**, 27.

George, S.T., M.A. Arbabian, A.E. Ruoho, J. Kiely and C.C. Malbon (1989) High efficiency expression of mammalian β-adrenergic receptors in baculovirus-infected cells. *Biochem. Biophys. Res.Comm.* **163**, 1265.

Gershanik, O., Heikkila, R.E. and Duvoisin, R.C. (1983) Behavioral correlations of dopamine receptor activation. *Neurology* **33**, 1489.

Gingrich, J.A., Amlaiky, N., Senogles, S.E., Chang, W.K., McQuade, R.D., Berger, J.G., and Caron, M.G. (1988) Affinity chromatography of the D1 dopamine receptor from rat corpus striatum. *Biochemistry***27**, 3907.

Giros, B., Sokoloff, P., Martres, M.P., Riou, J.F., Emorine, L.J., and Schwartz, J.C. (1989) Shorter variants of the D3 dopamine receptor produced through various patterns of alternative splicing. *Nature* **342**, 923.

Goldstein, J.L., Brown, M.S., Anderson, R.G.W., Russell, D.W. and Schneider, W.J. (1985) Receptor-mediated endocytosis: concepts emerging from the LDL receptor system. *Annu. Rev. Cell. Biol.* **1**, 1.

Gonzalez-Calero, G., Martin, M., Cubero, A., and Andres, A. (1990) Bovine brain coated vesicles contain adenosine A1 receptors. Presence of adenylate cyclase coupled to the receptor. *J. Neurochem.* **55**, 106.

Graber, S.G., Figler, R.A., and Garrison, J.C. (1992) Expression and purification of functional G protein alpha subunits using a baculovirus expression system. *J. Biol. Chem.* **267**, 1271.

Grandy, D.K., Marchionni, M.A., Makam, H., Stofko, R.E., Alfano, M., Frothingham, L., Fischer, J.B., Burke-Howie, K.J., Bunzow, J.B., Server, A.C., and Civelli, O. (1989) Cloning of the cDNA and gene for a human D2 dopamine receptor. *Proc. Natl. Acad. Sci. USA* **86**, 9762.

Guan, XM., T.S. Kobilka and B.K. Kobilka (1992) Enhancement of membrane insertion and function in a type IIIb membrane protein following introduction of a cleavable signal peptide. *J. Biol. Chem.* **267**, 21995.

Hall, H., Kohler, C., and Gawell, L.L. (1985) Some in vitro receptor binding properties of [^{3}H]eticlopride, a novel substituted benzamide, selective for dopamine D2 receptors in the rat brain, *Eur. J. Pharmacol.* **111**, 191.

Hamblin, M.W. and Metcalf, M.A. (1991) Primary structure and functional characterization of a human 5-HT1D-type serotonin receptor. *Mol. Pharmacol.* **40**, 143.

Harris, G.C. and Aston-Jones, G. (1994) Involvement of D2 dopamine receptors in the nucleus accumbens in the opiate withdrawal syndrome. *Nature* **371**, 155.

Hausdorff, W.P., M. Bouvier, B.F. O'Dowd, G.P. Irons, M.G. Caron and R.J.Lefkowitz, R.J. (1989) Phosphorylation sites on two domains of the β_2-adrenergic receptor are involved in distinct pathways of receptor desensitization. *J. Biol. Chem.* **264**, 12657.

Hausdorff, W.P., Caron, M.G., and Lefkowitz, R.J. (1990) Turning off the signal: desensitization of beta-adrenergic receptor function. *FASEB J.* **4**, 2881.

Hertel, C., Nunnally, M.H., Wong, S.KF., Murphy, E.A., Ross, E.M., and Perkins, J.P. (1990) A truncation mutation in the avian beta-adrenergic receptor causes agonist-induced

internalization and GTP-sensitive agonist binding characteristic of mammalian receptors. *J. Biol. Chem* **269**, 17988.

Hertel, C., Staehelin, M., Perkins, J.P. (1983) Evidence for intravesicular-adrenergic α1-receptors in membrane fractions from desensitized cells: binding of the hydrophilic ligand only in the presence of alamethicin. *J. Cyclic Nucleotide Prot. Phosphorylation Res.* **9**, 119.

Hess, E.J., Battaglia, G., Norman, A.B., Iorio, L.C., Creese, I. (1986) Guanine nucleotide regulation of agonist interactions at [^{3}H]SCH-23390 labelled D1 dopamine receptors in rat striatum, *Eur. J. Pharmacol.* **121**, 31.

Heuring, R.E. and Peroutka, S.J. (1987) Characterization of a novel 3H-5-hydroxytryptamine binding site subtype in bovine brain membranes. *J. Neurosci.* **7**, 894.

Hoyer, D. And Boddeke, H.W.G.M. (1993) Partial agonists, full agonists, antagonists: dilemmas of definition. *Trends Pharmacol. Sci.* **14**, 270.

Imperato, A. And DiChiara, G. (1986) Preferential stimulation of dopamine release in the nucleus accumbens of freely moving rats by ethanol. *J. Pharmacol. Exp. Ther.* 239, 219.

Irorio, L.C., Barnett, A., Leitz, F.H., Houser, V.P., Korduba, C.A. (1983) SCH-23390, A potential benzazepine antipsychotic with unique interaction on dopaminergic systems, *J. Pharmacol. Exp. Ther.* **226**, 462.

Ivins, K.J., Luedtke, R.R., Arthmyshyn, R.P., and Molinoff, P.B. (1991) Regulation of dopamine D2 receptors in a novel cell line (SUP1). *Mol. Pharmacol.* 39, 531.

Jin, H., Oksenberg, D., Ashkenzai, A., Peroutka, S.J., Duncan, A.M.V., Rozmahel, R., Yang, Y., Mengod, G., Palacios, J.M. and O'Dowd, B.F. (1992) Characterization of the human 5-hydroxytryptamine1B receptor. *J. Biol. Chem.* **267**, 5735.

Julius, D., MacDermott, A.B., Axel, R., and Jessell, T.M. (1988) Molecular characterization of a functional cDNA encoding the serotonin 1c receptor. *Science* **241**, 558.

Kebabian and Calne, D.B. (1979) Multiple dopamine receptors for dopamine. *Nature* **277**, 93.

Kennedy, M.E. and Limbird, L.E. (1993) Mutations of the α_{2A}-adrenergic receptor that eliminate detectable palmitoylation do not perturb receptor-G protein coupling. *J. Biol. Chem.* **268**, 8003.

Kobilka, B.K., Kobilka, T.S., Daniel, K., Regan, J.W., Caron, M.G. and Lefkowitz, R.J. (1988) Chimeric alpha 2-,beta 2-adrenergic receptors: delineation of dopamine involved in effector coupling and ligand binding specificity. *Science* **240**, 1310.

Kwatra, M.M., Schwinn, D.A., Schreurs, J., Blank, J.L., Kim, C.M., Benovic, J.L., Krause, J.E., Caron, M.G. and Lefkowitz, R.J. (1993) The substance P receptor, which couples to Gq/11, is a substrate of beta-adrenergic receptor kinase 1 and 2. *J. Biol. Chem.* **268**, 9161.

Laemmli, U.K. (1970) Cleavage of structural proteins during the assembly of the head of bacteriophage T4. *Nature* **227**, 680.

LaHoste, J. and Marshall, J.F. (1992) Dopamine supersensitivity and D1/D2 synergism are unrelated to changes in striatal receptor density, *Synapse* **12**, 14.

Lee, T.H., Ellinwood, E.H., and Nishita, J.K. (1988) Dopamine receptor sensitivity changes with chronic stimulants. *Ann. N.Y. Acad. Sci.* **537**, 324.

Lefkowitz, R.J., Hausdorff, W.P. and Caron, M.G. (1990) Role of phosphorylation in the desensitization of the adrenoceptor. *TiPs* **11**, 189.

Lefkowitz, R.J. (1993) G protein-coupled receptor kinases. *Cell* **74**, 409.

Levesque, D., Diaz, J., Pilon, C., Martres, M.-P., Giros, B., Souil, E., Schott, D., Morgat, J.-L., Schwartz, J.-C., and Sokoloff, P. (1992) Identification, characterization, and localization of the dopamine D3 receptor in rat brain using 7-[3H]hydroxy-N-N-di-n-propyl-2-aminotetralin, *Proc. Natl. Acad. Sci. U.S.A.* **89**, 8155.

Levey, A.I., Hersch, S.M., Rye, D.B., Sunahara, R.K., Niznik, H.B., Kitt, C.A., Price, D.L., Maggio, R., Brann, M.R., and Ciliax, B.J. (1993) Localization of D1 and D2 dopamine receptors in brain with subtype-specific antibodies. *Proc. Natl. Acad. Sci. U.S.A.* **90**, 8861.

Leyson, J.E., Gommeren, W., Laduron, P.M. (1978) Spiperone: A ligand of choice for neuroleptic receptors, kinetics and characteristics of in vitro binding, *Biochemical Pharmacology* **27**, 307.

Lindvall, O., and Bjorklund, A. (1983) Dopamine and norepinephrine-containing neuron systems: their anatomy in the rat brain, in *Chemical Neuroanatomy* (Emson, P.C. Ed.) Raven Press, New York, 229.

Liu, Y.F., Civelli, O., Grandy, D.K., and Albert, P.R. (1992) Differential sensitivity of the short and long human dopamine D2 receptor subtypes to protein kinase C. *J. Neurochem.* **59**, 2311.

Liu, J., Schoneberg, T., Van Rhee, M., and Wess, J. (1995) Mutational analysis of the relative oreintation of transmembrane helices I and VII in G protein-coupled receptors. *J. Biol. Chem.* **270**, 19532.

Lohse, M.J., Benovic, J.L., Caron, M.G. and Lefkowitz , R.J. (1990) Multiple pathways of rapid β2-adrenergic receptor desensitization, delineation and specific inhibitors. *J. Biol. Chem.* **265**, 3202.

Luckow, V.A. and M.D. Summers (1988) Signals important for high level expression of foreign genes in Autographa californica nuclear polyhedrosis virus expression vectors. *Virology* **167**, 5671.

Maggio, R., Vogel, Z., and Wess, J. (1993) Coexpression studies with mutant muscarinic/adrenergic receptors provide evidence for intermolecular "cross-talk" between G-protein-linked receptors. *Proc. Natl. Acad. Sci. U.S.A.* **90**, 3103.

Mahan, L.C., Burch, Monsma, F.J., Jr., and Sibley, D.R (1990) Expression of striatal D1 dopamine receptor coupled to inositolphosphate production and Ca^{+2} mobilization in Xenopus oocytes, *Proc. Natl. Acad. Sci. U.S.A.* **87**, 2196.

Malgaroli, A., Vallar, L., Elahi, F.R., Pozzan, T., Spada, A., and Meldolesi, J., J. (1987) Dopamine inhibits cytosolic Ca^{+2} increases in rat lactotroph cells. Evidence of a dual mechanism of action, *J. Biol. Chem.* **262**, 139020.

Mansour, A., Meador-Woodruff, J.H., Bunzow, J.R., Civelli, O., Akil, H., and Watson, S.J. (1990) Localization of dopamine D2 receptor mRNA and D1 and D2 receptor binding in the rat brain and pituitary: An in situ hybridization-receptor autoradiographic analysis. *J. Neuroscience* **10**, 2587.

Martin, M., Ros, M., Gonzalez-Calero, G., and Cubero, A. (1991) Presence of phospholipase C in coated vesicles from bovine brain. Dual regulatory effects of GTP-analogs. *Eur. J. Pharmacol.* **207**, 215.

McAllister, G., Charlesworth, A., Snodin, c., Beer, M.S., Noble, A.J., Middlemiss, D.N., Iversen, L.L., and Whiting, P. (1992) Molecular cloning of a serotonin receptor from human brain (5HT1E): a fifth 5HT1-like subtype. *Proc. Natl. Acad. Sci. USA* **89**, 5517.

McClelland, A., Kuhn, L., and Ruddle, F.H. (1984) The human transferrin receptor gene: genomic organization, and the complete primary structure of the receptor deduced from a cDNA sequence. *Cell* **39**, 267.

Milligan, G. (1993) Agonist regulation of cellular G protein levels and distribution: mechanisms and functional implications, *TiPS* **14**, 413.

Mills, A., Allet, B., Bernard, A., Chabert, C., Brandt, E., Cavegn, C., Chollet, A., and E. Kawashima (1993) Expression and characterization of human D4 dopamine receptors in baculovirus-infected insect cells. *FEBS* **320**, 130.

Miyamoto, C., G.E. Smith, J. Farrell-Towt, R. Chizzonite, M.D. Summers and G. Ju (1985) Production of human c-myc protein in insect cells infected with a baculovirus expression vector. *Mol.Cell. Biol.* **5**, 2860.

Monsma, F.J., McVittie, L.D., Gerfen, C.R., Mahan, L.C., and Sibley, D.R. (1989) Multiple D2 dopamine receptors produced by alternative RNA splicing. *Nature* **343**, 926.

Montmayeur, J.P., Guiramand, J., and Borrelli, E. (1993) Preferential coupling between dopamine D2 receptors and G-proteins. *Mol. Endocrinol.* **7**, 161.

Mostov, K.E., Friedlander, M., and Blobel, G. (1984) Structure and function of the receptor for polymeric immunoglobulins. *Nature* **308**, 27.

Motohashi, N., Takashima, m., Mataga, N., Nishikawa, T., Ogawa, A., Watanabe, S. And Toru, M. (1992) Effects of sulpiride and oxypertine on the dopaminergic system in the rat striatum. *Neuropsychobiology* **25**, 29.

Mouillac, B., M. Caron, H. Bonin, M. Dennis and M. Bouvier (1992) Agonist-modulated palmitoylation of β2-adrenergic receptor in Sf9 cells. *J. Biol. Chem.* **267**, 21733.

Munson, P.J. and D. Rodbard (1980) LIGAND: a versatile computerized approach for characterization of ligand-binding systems. *Anal. Biochem.* **107**, 220.

Nagai, Y., Ueno, S., Saeki, Y., Soga, F., and Yanagihara, T. (1993) Expression of the D3 dopamine receptor gene and a novel variant transcript generated by alternative splicing in human peripheral blood lymphocytes. *Biochem. Biophys. Res. Commun.* **194**, 374.

Nakamura, F., Ogata, K., Shiozaki, K., Kameyama, K., Ohara, K., Haga, T., and Nukada, T. (1991) Identification of two novel GTP-binding protein α-subunits that lack apparent ADP-ribosylation sites for pertussis toxin. *J. Biol. Chem.* **266**, 12676.

Naylor, L., Woodward, R., Daniell, S., Coley, C., and Strange, P. (1995) Determinants of ligand binding at the D2 dopamine receptor. *Biochem. Soc.Trans.* **23**, 87.

Neer, E.J. and Clapham, D.E. (1988) Roles of G protein subunits in transmembrane signalling. *Nature* **333**, 129.

Neer, S.J., Lok, J.M., and Wolf, L.G. (1984) Purification and properties of the inhibitory guanine nucleotide regulatory unit of brain adenylate cyclase. *J. Biol. Chem.* **259**, 222.

Neve, K.A., Kozlowski, M., and Rosser, M.P.(1992) Dopamine D2 receptor stimulation of Na^+/H^+ exchange assessed by quantification of extracellular acidification, *J. Biol. Chem.* **267**, 25748.

Ng, G.YK., O'Dowd, B.F., Caron, M., Dennis, M., Brann, M.R., and George, S.R. (1994) Phosphorylation and palmitoylation of the human D2L dopamine receptor in Sf9 cells. *J. Neurochem.* **63**, 1589.

Ng, G.YK., Mouillac, B., George, S.R., Caron, M., Dennis, M., Bouvier, M., and O'Dowd, B.F. (1994) Desensitization, phosphorylation, and palmitoylation of the human dopamine D1

receptor. *Eur. J. Pharmacol.* **267**, 7.

Ng, G.YK., George, S.R., Zastawny, R.L., Caron, M., Bouvier, M., Dennis, M., and O'Dowd, B.F. (1993) Human serotonin1B receptor expression in Sf9 cells: Phosphorylation, palmitoylation, and adenylyl cyclase inhibition. *Biochemistry* **32**, 11727.

Ng, G.YK., Trogadis, J., Stevens, J., Bouvier, M., O'Dowd, B.F., and George, S.R. (1995) Agonist-induced desensitization of dopamine D1 receptor-stimulated adenylyl cyclase activity is temporally and biochemically separated from D1 receptor internalization. *Proc. Natl. Acad. Sci. U.S.A.* **92**, 10157.

Nguyen, T., Sunahara, R., Marchese, A., Van Tol, H.M., Seeman, P., O'Dowd, B.F. (1991) Transcription of a human dopamine D5 pseudogene. *Biochem. Biophys. Res. Commun.* **181**, 16.

Nguyen, T., Marchese, A., Kennedy, J.L., Petronis, A., Peroutka, S., Wu, P.H., O'Dowd, B. (1993) An Alu sequence interrupts a human 5-hydroxytryptamine1D receptor pseudogene. *Gene* **124**, 295.

Niznik, H.B., Fogel, E.L., Chen, C.J., Gongo, D., Brown, E.M., and Seeman, P. (1988) Dopamine D1 receptors of the calf parathyroid gland: identification and characterization. *Molecular Pharmacology* **34**, 29.

Niznik, H.B., Jarvie, K.R., and Brown, E.M. (1989) Dopamine D1 receptors of the calf parathyroid gland: identification of a ligand binding subunit with lower apparet molecular weight but similar primary structure to neuronal D1-receptors. *Biochemistry* **28**, 6925.

Niznik, H.B., K.R. Jarvie, N.H. Bzowej, P. Seeman, R.K. Garlick, J.J. Miller, N. Baindur and J.L. Neumeyer (1988) Photoaffinity labelling of dopamine D1 receptors. *Biochemistry*

27, 7594.

Niznik, H.B., Grigoriadis, D.E., Pri-Bar, I., Buchman, O., and Seeman, P. (1985) Dopamine D2 receptors selectively labelled by a benzamide neuroleptic: [^{3}H]YM-09151-2. *Naunyn Schmied. Arch. Pharmacol.* **329**, 333.

O'Dowd, B.F. (1993) Structures of dopamine receptors. *J. Neurochemistry* **60**, 804.

O'Dowd, B.F., M. Hnatowich, M.G. Caron, R.J. Lefkowitz and M. Bouvier (1989) Palmitoylation of the human β2-adrenergic receptor. Mutation of Cys^{341} in the carboxy tail leads to an uncoupled nonpalmitoylated form of the receptor. *J. Biol. Chem.* **264**, 7564.

Oker-Bom, C., Jansson, C., Karp, M., Lindqbist, C., Savola, J.-M., Vlak, J., Akerman, K. (1993) Functional analysis of the human α2C-C4 adrenergic receptor in insect cells expressed by a luciferase-based baculovirus vector. *Biochim. Biophys. Acta.* **1176**, 269.

O'Malley, L.L., Mack, K.L., Gandelman, K., and Todd, R. (1990) Organization and expression of the rat D2A receptor gene: identification of alternative transcripts and a variant donor splice site. *Biochemistry* **29**, 1367.

Orti, E., Mendel, D.B., Smith, L.I., Bodwell, J.E., and Munck, A. (1989) A dynamic model of glucocorticoid receptor phosphorylation and cycling in intact cells. *J. Steroid Biochem.* **34**, 85.

Osborne, N.N. (1982) *in Biology of serotonergic transmission* (Osborne, N.N., Ed.) pp 7-27, John Wiley and Sons Ltd., Chichester, United Kingdom.

Ozaki, N., Moroi, K., Kadota, T., Suzuki, S., and Kadota, K. (1994) Dopamine D1 and D2 receptors and their signal system present in coated vesicles prepared from bovine striatal

tissue. *J. Neurochem.* **62**, 582.

Parker, E.M., K. Kameyama, T. Higashijima and E.M. Ross (1991) Reconstitutively active G protein-coupled receptors purified from baculovirus-infected insect cells. *J. Biol. Chem.* **266**, 519.

Perkins, J.P., W.P. Hausdorff and R.J. Lefkowitz (1990) Mechanisms of ligand-induced desensitization of the β-Adrenergic receptor, in Perkins, J.P., ed. *The β-Adrenergic Receptor.* New York, Human Press, 73.

Peroutka, S.J. (1993) 5-Hydroxytryptamine receptors. *J. Neurochem.* **60**, 408.

Pickering, D.S.,Thomsen, C., Suzdak, P.D., Fletcher, E.J., Robitaille, R., Salter, M.W., MacDonald, J.F., Huang, X.-P., and Hampson, D.R. (1993) A comparison of two alternatively spliced forms of a metabotropic glutamate receptor coupled to phophoinositide turnover, *J. Neurochem.* **61**, 85.

Piomelli, D., Pilon, C., Giros, B., Sokoloff, P., Martres, M.P., and Schwartz, J.C. (1991) Dopamine activation of the arachidonic acid cascade as a basis for D1/D2 receptor synergism. *Nature* **353**, 164.

Probst, W.C., Snyder, L.A., Schuster, D.I., Brosius, J., and Sealfon, S.C. (1992) Sequence alignment of the G protein-coupled receptor superfamily. *DNA and CELL BIOLOGY* **11**, 1.

Provost, N.M., somers, D.E., and Hurley, J.B. (1988) A Drosophila melanogaster G protein α subunit gene is expressed primarily in embryos and pupae. *J. Biol. Chem.* **263**, 12070.

Pytela, R., Pierschbacher, M.D., and Ruoslahti, E. (1985) A 125/115-kDa cell surface receptor specific for vitronectin interacts with the arginine-glycine-aspartic acid adhesion sequence

derived from fibronectin. *Proc. Natl. Acad. Sci. USA* **82**, 5766.

Rao, D.D., McKelvy, J., Kebabian, J., and MacKenzie, R.G. (1990) Two forms of the rat dopamine receptor as revealed by the polymerase chain reaction. *FEBS Lett.* **263**, 18.

Raymond, J.R. (1991) Protein kinase C induces phosphorylation and desensitization of the human 5-HT1A receptor. *J. Biol. Chem.* **266**, 14747.

Ribeiro-Neto, F., Mattera, P., Grenet, D., Sekura, R.D., Birnbaumer, L., Field, J.B. (1987) Adenosine diphosphate ribosylation of G proteins by pertussis and cholera toxin in isolated membranes. Different requirements for and effects of guanine nucleotides and Mg2+. *Molecular Endocrinology* **1**, 472.

Richardson, R.M. and M.M. Hosey (1992) Agonist-induced phosphorylation and densensitization of human m2 muscarinic cholinergic receptors in Sf9 insect cells. *J. Biol. Chem.* **267**, 22249.

Robb, R.J., Rusk, C.M., Yodoi, J., and Greene, W.C. (1987) Interleukin 2 binding molecule distinct from the Tac protein: analysis of its role in formation of high-affinity receptors. *Proc. Natl. Acad. Sci. USA* **84**, 2002.

Rouillard, C., Bedard, P.J., Falardeau, P., and Di Paolo, T. (1987) Behavioral and biochemical evidence for a different effect of repeated administration of L-dopa and bromocriptine on denervated versus non-denervated striatal dopamine receptors. *Neuropharmacology* **26**, 1601.

Salomon, Yl., C. Londos and M. Rodbell (1974) A highly sensitive adenylyl cyclase assay. *Anal. Biochem.* **58**, 541.

Schlessinger, J. (1986) Allosteric regulation of the epidermal growth factor receptor kinase. *J.*

Cell Biol. **103**, 2069.

Schmauss, C., Haroutunian, V., Davis, K.L., and Davidson, M. (1993) Selective loss of dopamine D3-type receptor mRNA expression in parietal and motor cortices of patients with chronic schizophrenia. *Proc. Natl. Acad. Sci. USA* **90**, 8942.

Seeman, P. (1987) Dopamine receptors and the dopamine hypothesis of schizophrenia. *Synapse* **1**, 133.

Seeman, P., Guan, H.C., Civelli, O., Van Tol, H.H.M., Sunahara, R.K., and Niznik, H.B. (1992) The cloned dopamine D2 receptor reveals different densities for dopamine receptor antagonist ligands. Implications for human brain positron emission tomography. *Eur. J. Pharmacol.* **227**, 139.

Seeman, P. and H.B. Niznik (1988) Dopamine D1 receptor pharmacology. *ISI Atlas of Science: Pharmacol.* **161**, 35.

Seeman, P. and Niznik, H.B. (1990) Dopamine receptors and transporters in Parkinson's disease and schizophrenia, *FASEB J.* **4**, 2737.

Seeman, P., C. Ulpian, K.A. Wreggett and J.W. Wells (1984) Dopamine receptor parameters detected by [^{3}H]spiperone depend on tissue concentration: analysis and examples. *J. Neurochemistry* **43**, 221.

Seeman, P., Bzowej, N.H., Guan, H.C., Bergeron, C., Reynolds, G.P., Bird, E.D., Riederer, P., Jellinger, K. and Tourtellotte, W.W. (1987) Human brain D1 and D2 dopamine receptors in schizophrenia. Alzheimer's, Parkinson's, and Huntington's diseases. *Neuropsychopharm.* **1**, 5.

Seeman, P., Niznik, H.B., Guan, H.C., Booth, G., and Ulpian, C. (1989) Link between D1 and D2

dopamine receptors is reduced in schizophrenia and Hungtington diseased brain. *Proc. Natl. Acad. Sci. USA* **86**, 10156.

Seeman, P. and Schaus, J.M. (1991) Dopamine receptors labelled by [^{3}H]quinpirole. *Eur. J. Pharmacol.* 203, 105.

Selbie, L.A., Hayes, G., and Shine, J. (1989) The major dopamine D2 receptor: molecular analysis of the human D2A subtype. *DNA* **8**, 683.

Sellers, E.M., Higgins, G.A., and Sobell, M.B. (1992) 5-HT and alcohol abuse. *Trends Pharmacol. Sci.* **13**, 69.

Setler, P.E., Sarau, H.M., Zirkle, C.L., and Saunders, H.L.(1978) The central effects of a novel dopamine agonist, *Eur. J. Pharmacol.* **50**, 419.

Sheppard, C.J.R. (1993) Confocal microscopy-principles, practice and options. In *Fluorescent and luminescent probes for biological activity* (Mason W.T., ed) pp 229, San Diego, Academic Press.

Shotton, D. (1989) Confocal scanning optical microscopy and its applications for biological specimens. *J. Cell Sci.* **94**, 175.

Sibley, D.R., Strasser, R.H., Caron, M.G. and Lefkowitz, R.J. (1985) Homologous desensitization of adenylate cyclase is associated with phosphorylation of the beta-adrenergic receptor. *J. Biol. Chem.* **260**, 3883.

Sibley, D.R. and Monsma, F.J. (1992) Molecular biology of dopamine receptors. *Trends Pharmacol. Sci.* **13**, 61.

Sinkins, W.G., Kandel, M., Kandel, S.I., Schunack, W., and Wells, J.W. (1993) Protein-linked receptors labelled by histamine in guinea pig cerebral cortex. I. Pharmacological

characterization. *Mol. Pharmacol.* **43**, 569.

Sinkins, W.G. and Wells, J.W. (1993) Protein-linked receptors labelled by histamine in guinea pig cerebral cortex. II. Mechanistic basis for multiple states of affinity. *Mol. Pharmacol.* **43**, 583.

Smith, G.E., Summers, M.D., and Fraser, M.J. (1983) Production of humna beta interferonA in insect cells infected with a baculovirus expression vector. *Molecular and Cellular Biology* **3**, 2156.

Smith, D.W. and Parker, E.M. (1995) G protein coupled serotonin receptors-multiple subtypes, multiple opportunities. *Current Pharmaceutical Design* **1**, 317.

Snyder, L.A., Roberts, J.L., and Sealfon, S.C. (1991) Distribution of dopamine D2 receptor mRNA splice variants in the rat by solution hybridization/protection assay. *Biochem. Biophys. Res. Commun.* **180**, 1031.

Sokoloff, P., Giros, B., Martres, MP., Bouthenet, ML. and Schwartz, JC. (1990) Molecular cloning and characterization of a novel dopamine receptor (D3) as a target for neuroleptics. *Nature* **347**,146.

Spano, P.F., Govoni, S., and Trabucchi, M. (1978) Studies on the pharmacological properties of dopamine receptors in various areas of the central nervous system. *Adv. Biochem. Psychopharmacol.* **19**, 155.

Starke, K., Gothert, M., and Kilbinger, H. (1989) Modulation of neuro-transmitter release by presynaptic autoreceptors, *Physiological Rev.* **69**, 864.

Starr, M.S., and Starr, B.S. (1989) Behavioral synergism between the dopamine agonists SKF38393 and LY 171555 in dopamine-depleted mice: Antagonism by sulpiride reveals

only stimulant postsynaptic D2 receptors, *Pharm. Biochem. Behav.* **33**, 41.

Sternweiss, P.C. and Robishaw, J.D. (1984) Isolation of two proteins with high affinity for guanine nucleotides from membranes of bovine brain. *J. Biol. Chem.* **259**, 13806.

Stevens, J.K. (1994) An introduction to confocal 3D volume investigation. In *Three-dimensional confocal microscopy* (Stevens, J.K., Mills, L.R., Trogadis, J.E., eds) pp 1. San Diego, Academic Press.

Stevens, J.K., Trogadis, J.E. (1990) Three-dimensional volume investigation of serial confocal data sets. *Proc XIIth Int. Cong. Electron Microsc.* **375**.

Stormann, T.M., Adula, D.D., Weiner, D.M., and Brann, M.R. (1990) Molecular cloning and expression of a dopamine D2 receptor from human retina. *Mol. Pharmacol.* **37**, 1.

Strader, C.D., Sigal, I.S., Blake, A.D., Cheung, A.H., Register, R.B., Randa, E., Zemcik, B.A., Candelore, M.R., and Dixon, R.A.F. (1987) The carboxyl terminus of the hamster beta-adrenergic receptor expressed in mouse L cells is not required for receptor sequestration. *Cell* **49**, 855.

Strader, C.D., Signal, I.S. and Dixon, R.A.F. (1989) Structural basis of adrenergic receptor function. *FASEB J.*, **3**, 1825.

Summers, M.D. and G.E. Smith (1987) A manual of methods for baculovirus vectors and insect cell culture procedures. *Tex. Agric. Exp. Stn. Bull.* **1555**, 1.

Sunahara, R.K., H.C. Guan, B.F. O'Dowd, P. Seeman, L.G. Laurier, G. Ng, S.R. George, J. Torchia, H.H.M. Van Tol and H.B. Niznik (1991) Cloning of the gene for a human dopamine D5 receptor with higher affinity for dopamine than D1. *Nature* **350**, 614.

Sunahara, R.K., H.B. Niznik, D.M. Weiner, T.M. Stormann, M.R. Brann, J.L. Kennedy, J.E.

Gelernter, R. Rozmahel, Y. Yang, Y. Israel, P. Seeman and B.F. O'Dowd (1990) Human dopamine D1 receptor encoded by an intronless gene on chromosome 5. *Nature* **347**, 80.

Suryanarayana, S., von Zastrow, M., and Kobilka, B.K. (1992) Identification of intramolecular interactions in adrenergic receptors. *J. Biol. Chem.* **267**, 21991.

Surmeier, D.J., Eberwine, J., Wilson, C.J., Cao, Y., Stefani, A., and Kitai, S.T. (1992) Dopamine receptor subtypes colocalize in rat striatonigral neurons. *Proc. Natl. Acad. Sci. U.S.A.* **89**, 10178.

Starr, S., Kozell, L.B., and Neve, K.A. (1995) Drug-induced up-regulation of dopamine D2 receptors on cultured cells. *J. Neurochem.* **65**, 569.

Suzuki, T., Nguyen, C.T., Nantel, F., Bonin, H., Valiquette, M., Frielle, T., Bouvier, M. (1992) Distinct regulation of β_1- and β_2-adrenergic receptors in Chinese hamster fibrolast. *Mol. Pharmacol.* **41**, 542.

Tang, L., Todd, R.D., Heller, A. And O'Malley, K.L. (1994) Pharmacological and functional characterization of D2, D3 and D4 dopamine receptors in fibroblast and dopaminergic cell lines. *J. Pharmacol. Exp. Ther.* **266**, 495.

Terai, M., Hidaka, K., and Nakamura, Y. (1989) Comparison of [^{3}H]YM-09151-2 with [^{3}H]spiperone and [^{3}H]raclopride for dopamine D2 receptor binding to rat striatum. *Eur. J. Pharmacol.* **173**, 177.

Thomas, R.F., Holt, B.D., Schwinn, D.A., and Liggett, S.B. (1992) Long-term agonist exposure induces upregulation of β_3-adrenergic receptor expression via multiple cAMP response elements. *Proc. Natl. Acad. Sci. USA* **89**, 4490.

Todd, R.D., T.S. Khurana, P. Sajovic, K.R. Stone and K.L. O'Malley (1989) Cloning of ligand-specific cell lines via gene transfer: identification of a D2 dopamine receptor subtype. *Proc. Natl. Acad. Sci. USA* **86**, 10134.

Trogadis, J.E., Stevens, J.K. (1994) Spatial organization of microtubules in PC12 cells using 3-dimensional electron microscopy and confocal microscopy. In *Three-dimensional confocal microscopy* (Trogadis, J.E. and Stevens, J.K. eds.) pp 301, San Diego, Academic Press.

Tsudo, M., Kozak, R.W., Goldman, C.K., and Waldmann, T.A. (1986) Contribution of a p75 interleukin 2 binding peptide to a high-affinity interleukin 2 receptor complex. *Proc. Natl. Acad. Sci. USA* **83**, 9694.

Tsutsumi, M., Laws, S.C., and Sealfon, S.C. (1993) Homologous up-regulation of the gonadotropin-releasing hormone receptor in αT_3-1 cells is associated with unchanged receptor messenger RNA (mRNA) levels and altered mRNA activity. *Mol. Endo.* **7**, 1625.

Uhing, R.J., Prpic, V., Jiang, H., and Exton, J.H. (1986) Hormone-stimulated polyphosphoinositide breakdown in rat liver plasma membranes. Roles of guanine nucleotide and calcium. *J. Biol. Chem.* **261**, 2140.

Valiquette, M., Bonin, H., Hnatowich, M., Caron, M.G., Lefkowitz, R.J. and Bouvier, M. (1990) Involvement of tyrosine residues located in the carboxyl tail of the human beta 2-adrenergic receptor in agonist-induced down-regulation of the receptor. *Proc. Natl. Acad. Sci.* **87**, 5089.

Vallar, L., Muca, C., Magni, M., Albert, P., Bunzow, J., Meldolesi, J., and Civelli, O. (1990) Differential coupling of dopaminergic D2 receptors expressed in different cell types. Stimulation of phosphatidylinositol 4,5-bisphosphate hydrolysis in LtK^- fibroblasts, hyperpolarization, and cytosolic-free Ca^{+2} concentration decrease in GH_4C_1 Cells, *J. Biol.*

Chem. 265, 10320.

Van Dop, C., Tsubokawa, M., Bourne, H.R. and Ramachandran, J. (1984) Amino acid sequence of retinal transducin at the site ADP-ribosylated by cholera toxin. *J. Biol. Chem.* **259**, 696.

Van Tol, H.H.M., Bunzow, J.R., Guan, H-C., Sunahara, R.K., Seeman, P., Niznik, H.B. and Civelli, O.(1991) Cloning of the gene for a human dopamine D4 receptor with high affinity for the antipsychotic clozapine. *Nature* **350**, 610.

Van Tol, H.H.M., Wu, C.M., Guan, H-C., Ohara, K., Bunzow, J.R., Civelli, O., Kennedy, J., Seeman, P., Niznik, H.B. and Jovanovic, V. (1992) Multiple dopamine D4 receptor variants in the human population. *Nature* **358**, 149.

Vasudevan, S., Premkumar, L, Stowe, S., Gage, P.W., Reilander, H., Chung, S.H. (1992) Muscarinic acetylcholine receptor produced in recombinant baculovirus infected Sf9 insect cells couples with endogenous G-proteins to activate ion channels. *FEBS* **311**, 7.

Vassout, A., Bruinink, A., Krauss, J., Waldmeier, P., and Bischoff, S. (1993) Regulation of dopamine receptors by bupropion: comparison with antidepressants and CNS stimulants. *J. Receptor Res.* **13**, 341.

Venter, J.C., and Fraser, C.M. (1983) Beta-adrenergic receptor isolation and characterization with immobilized drugs and monoclonal antibodies. *FEBS* **42**, 273.

Vialard, J., M. Lalumiere, T. Vernet, D. Briedis, G. Alkhatib, D. Henning, D. Levin and C. Richardson, (1990) Secretion of functional papain precursor from insect cells. Requirement for N-glycosylation of the pro-region. *J. Biol. Chem.* **265**, 16661.

Von Zastrow, M.V. and B.K. Kobilka (1992) Ligand-regulated internalization and recycling of human adrenergic receptors between the plasma membrane and endosomes containing

transferring receptors. *J. Biol. Chem.* **267**, 3530.

Waldo, G.L., Northup, J.K., Perkins, J.P., Harden, T.K. (1983) Characterization of an altered membrane form of the β_2-adrenergic receptor produced during agonist induced desensitization. *J. Biol. Chem.* **258**, 13900.

Walters, J.R., Bergstrom, D.A., Carlson, J.H., Chase, T.N. and Braun, A.R. (1987) D1 dopamine receptor activation required for postsynaptic expression of D2 agonist effects, *Science* 236, 719.

Wamsley, J.K., Gehlert, D.R., Filloux, F.M., Dawson, T.M. (1989) Comparison of the distribution of D1 and D2 dopamine receptors in the rat brain. *J. Comp. Neuroanat.* **2**, 119.

Wang, H.Y., Berrios, M., and Malbon, C.C. (1989) Indirect immunofluorescence localization of beta-adrenergic receptors and G-proteins in human A431 cells. *Biochem. J.* **263**, 519.

Wiese, R.J., Uhland-Smith, a., Ross, T.K., Prahl, J.M., and Deluca, h.F. (1992) Up-regulation of the vitamin D receptor in response to 1,25-dihydroxyvitamin D3 results from ligand-induced stabilization. *J. Biol. Chem.* **267**, 20082.

Wong, D.F., Tune, L., Shaya, E., Pearlson, G., Yung, B., Dannais, R.F., Wilson, A.A., Ravert, H.T., Wagner, H.N. Jr., Gjedde, A. (1993) *Schizophrenia Res.* **8**, 212.

Wong, S.KF., E.M. Parker, and E.M. Ross (1990) Chimeric muscarinic cholinergic: β-adrenergic receptors that activate Gs in response to muscarinic agonists. *J. Biol. Chem.* **265**, 6219.

Wreggett, K.A., and Wells, J.W. (1995) cooperativity manifest in the binding properties of purified muscarinic receptors. *J. Biol. Chem.* **270**, 22488.

Yamamoto, T., Davis, C.G., Brown, M.S., Chneider, W.J., Casey, M.L., Goldstein, J.L., and Russell,

D.W. (1984) The human LDL receptor: a cysteine-rich protein with multiple Alu sequences in its mRNA. *Cell* **39**, 27.

Yu, S.S., Lefkowitz, R.J. and Hausdorff, W.P. (1993) Beta-adrenergic receptor sequestration. A potential mechanism of receptor resensitization. *J. Biol. Chem.* **268**, 337.

Zhang, L.-J., Lachowicz, J.E., and Sibley, D.R. (1994) The D2S and D2L dopamine receptor isoforms are differentially regulated in chinese hamster ovary cells, *Mol. Pharmacol.* **45**, 878.

Zastrow, M.V. and Kobilka, B.K. (1992) ligand-regulated internalization and recycling of human beta 2-adrenergic receptors between the plasma membrane and endosomes containing transferrin receptors. *J. Biol. Chem.* **267**, 3530.

10. APPENDIX

Biochemical Characterization of the Serotonin 5-HT_{1B} Receptor in Sf9 Cells: Phosphorylation, Palmitoylation and Adenylyl Cyclase Inhibition

Parts of this appendix have been reprinted with permission, from Ng et al., Human serotonin1B receptor expression in Sf9 cells: Phosphorylation, palmitoylation and adenylyl cyclase inhibition, Biochemistry 32, 11727-11733, 1993, American Chemical Society.

10.1 Summary

The baculovirus/Sf9 cell system was critically evaluated for its suitability to express GPCRs for detailed functional studies using the human serotonin$_{1B}$ (5-HT_{1B}) receptor as a model for other GPCRs. This was done by expressing a c-myc epitope tagged 5-HT_{1B} receptor (m5-HT_{1B}) in the Sf9 cells whereby the biology of the 5-HT_{1B} receptor was investigated. This strategy held the potential that other c-myc epitope-tagged GPCRs could be detected by immunoblot analysis and purified by immunoprecipitation using a monoclonal antibody, 9E10, specific for the c-myc epitope. Agonist radioligand [^{3}H]5-HT binding studies showed that m5-HT_{1B} displayed the characteristic pharmacological profile of the human 5-HT_{1B} receptor indicating that pharmacological properties of the receptor were unaltered by the presence of the epitope. Further, expressed receptors displayed both high and low affinity states for [^{3}H]5-HT, suggesting that they were coupled to endogenous G-proteins. Indeed, agonist binding to the high affinity receptor state was regulated in the presence of GTPγS, Gpp(NH)p and pertussis toxin as shown for receptors expressed in native tissues. [^{32}P]ADP-ribosylation experiments identified a major ~41 kDa ADP-ribosylated protein present in

Sf9 membranes that co-migrated with partially purified bovine brain $G_{i\alpha}/G_{o\alpha}$ subunits suggesting intact effector pathways in this cell line. Indeed, measurements of adenylyl cyclase activity in membranes from cells expressing m5-HT_{1B} showed that serotonergic agonists mediated the inhibition of adenylyl cyclase activity with a rank order of potency comparable to their affinity constants. Immunoblot analysis of membranes prepared from cells expressing m5-HT_{1B} and photoaffinity labelling of immunoprecipitated m5-HT_{1B} receptors revealed ligand binding species at ~95 kDa and at ~42 kDa. Immunoprecipitated material migrating with the ~95 kDa and ~42 kDa species were shown to be post-translationally modified following whole cell metabolic labelling with [$^{32}P_i$]phosphate or [^{3}H]palmitic acid, and provides the first evidence that a member of the serotonin receptor family is phosphorylated and palmitoylated. Additionally, these studies constituted direct evidence validating the suitability of this model system for the detailed pharmacological and biochemical studies of other GPCRs.

10.2 Introduction

The neurotransmitter, 5-hydroxytryptamine (5-HT) is a monoamine like the neurotransmitter dopamine. Whereas dopamine has been associated with neuropsychiatric disorders such as schizophrenia, serotonin is postulated to have an important role in affective disorders such as depression, anxiety and substance abuse (Peroutka, 1990, Sellers et al, 1992). The functional diversity of 5-HT action is reflected in the multiplicity of 5-HT receptors which like dopamine receptors belong to the superfamily of G protein-coupled receptors. Distinct genes for fifteen 5-HT receptors have been categorized into seven families, 5-HT_1 - 5-HT_7, according to pharmacological and biochemical criteria (Hartig et al, 1990, Smith and Parker, 1995). To date, cloning studies have identified 5-$HT_{1A,1B,1C,1D,1E,1F}$ receptors belonging to the 5-HT_1 class (Fargin et al, 1988, Jin et al, 1992, Julius et al, 1988, Hamblin et al, 1991, Adham et al, 1993). The 5-HT_1 class of receptors all bind 5-HT with high affinity but are distinguished from each other by their unique rank order of affinities for typical serotonergic ligands. Each receptor appears to have a unique distribution and possibly a distinct function in the central nervous system. The biological studies of each receptor have been limited by the nonavailability of highly selective ligands or antisera. Our recently cloned 5-HT_{1B} receptor has been characterized by binding assays (Jin et al, 1991), recently reviewed by Peroutka 1993, and classified as coupling to and inhibiting adenylyl cyclase (Julius et al, 1991). However, none of the serotonin receptors have been purified and there is no information regarding the post-translational modification of any of the serotonin 5-HT_{1B} receptor, although important functional roles for post-translational modifications such as phosphorylation and palmitoylation have been documented for other G-protein coupled receptors (Bouvier et al, 1988; O'Dowd et al, 1989).

Amino acid sequence analysis of the 5-HT_{1B} receptor revealed consensus serine and

threonine residues in the third intracellular loop for phosphorylation by cyclic AMP-dependent protein kinase (PKA), and protein kinase C (PKC) shown in other GPCRs such as dopamine. A putative site for palmitoylation is present at the cysteine residue in the small carboxy tail of the 5-HT_{1B} receptor (Fig. 33) shown to be the determinant of palmitoylation for the β-AR (O'Dowd et al, 1989). The similarities between serotonin and dopamine systems make it appropriate that the 5-HT_{1B} receptor be chosen at the onset of the thesis research as a model for other GPCRs like dopamine for the validation of the expression system.

The baculovirus/Sf9 cell system was selected for receptor expression for the principal reason that other GPCRs expressed in these cells appear to be biochemically, pharmacologically, and functionally similar to those in native membranes (George et al, 1989, Parker et al, 1991). The strategy chosen was to express a recombinant c-myc epitope tagged 5-HT_{1B} (m5-HT_{1B}) receptor so that specific antibodies directed against the c-myc epitope in the amino terminal domain of m5-HT_{1B} enabled receptor identification by immunoblotting and purification by immunoprecipitation. In addition, this strategy also allows us in future studies to rapidly express, purify and characterize other GPCRs. The data show that 5-HT_{1B} receptors expressed in Sf9 cells are pharmacologically similar to the human neuronal 5-HT_{1B} receptor and are coupled to pertussis toxin-sensitive G-proteins that mediate the inhibition of adenylyl cyclase. Moreover, in this report we show for the first time that the serotonin 5-HT_{1B} receptor is phosphorylated and palmitoylated. Additionally, these data confirmed in our hands the suitability of the model for the study of other GPCRs.

Fig. 35. Proposed model illustrating only the intracellular domains of the human 5-HT_{1B} receptor. The seven transmembrane-spanning regions (1-7), the intracellular loops (C1-C4), and three PKC and two PKA sites are indicated. The small arrow indicates a possible palmitoylation site. Circles with letters represent amino acids in the single-letter code. *Reprinted with permission, from Ng et al., Human serotonin1B receptor expression in Sf9 cells: Phosphorylation, palmitoylation and adenylyl cyclase inhibition, Biochemistry 32, 11727-11733, 1993, American Chemical Society.*

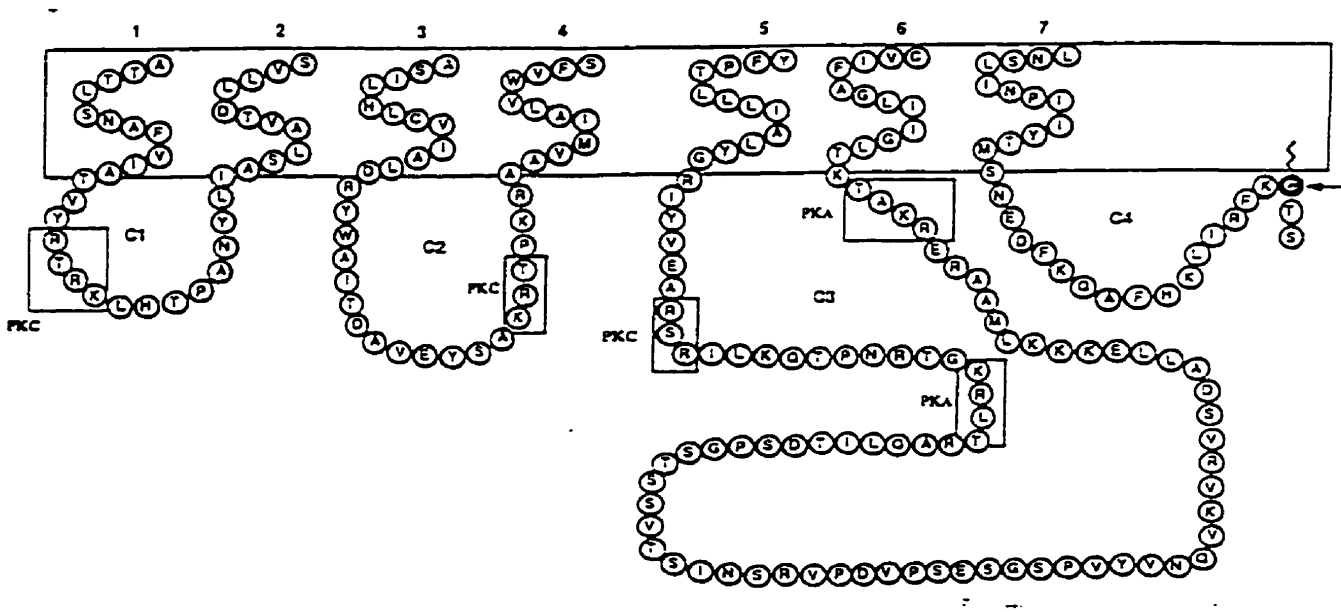
1
2
3
4
5
6
7
C1
C2
C3
C4
PKC
PKC
PKC
PKA
PKA

10.3 Results

10.3.1 Pharmacological Characterization of Expressed 5-HT_{1B} Receptors

[^{3}H]5-HT bound in a specific and saturable manner to 5-HT_{1B} and m5-HT_{1B} receptors expressed in Sf9 cells with receptor densities ranging from 1 to 5 pmol/mg of protein at 72 hours post infection (Fig. 34). [^{3}H]5-HT binding to 5-HT_{1B} and m5-HT_{1B} receptors was not significantly different and saturation data analyzed by LIGAND was best fitted to a two-site model ($p<0.05$) similar to wild type 5-HT_{1B} receptors in neuronal tissue (Peroutka, 1993). The mean Kd values for the expressed receptors and proportions for high- and low- affinity states were 24±2 nM and 62% (n=4) and 104±17 nM and 38% (n=4) respectively. The identification of two agonist-detected affinity states of the receptor supports an interaction of expressed receptors with endogenous G-proteins in Sf9 cells. Indeed, the [^{3}H]5-HT binding to the high-affinity state of m5-HT_{1B} receptors decreased in a concentration dependent manner in the presence of GTPγS or Gpp(NH)p (Fig. 35) with Ki values of 3.1 ± 0.1 nM (n=3) and 38.8 ± 1.9 nM (n=2), respectively.

Displacement of [^{3}H]5-HT binding to the high-affinity state of m5-HT_{1B} receptors by competing drugs was in the appropriate rank order of potency for serotonergic ligands, consistent with the human brain 5-HT_{1B} receptor profile. The 5-HT_{1B} pharmacological profile is defined by higher affinity for 5-CT (Frazer et al, 1990) and a lower affinity for 8-OH-DPAT (Heuring and Peroutka, 1987). In membranes prepared at 72 hours post-infection, the following rank order of potency was observed: 5-CT > 5-HT ≥ methiothepin > methysergide > sumatriptan > 8-OH-DPAT and binding constants are indicated in Table 8. SCH-23390 displaced [^{3}H]5-HT binding at concentrations > 1μM (data not shown). As shown in Table 8, the Ki values for the competing drugs are in good agreement with the values we have obtained for the 5-HT_{1B} receptor expressed in

mammalian cells (Jin et al, 1991). Collectively, these data indicate that serotonin and likely other GPCRs expressed in Sf9 cells are pharmacologically indistinguishable from native receptors.

Table 8. Dissociation constants for [^{3}H]5-HT in cells expressing m5-HT$_{1B}$. Membranes prepared from Sf9 cells at 72 hour post-infection were incubated with varying concentrations (10^{-11} - 10^{-3} M) of competitors in the presence of ~5 nM [^{3}H]5-HT as described in methods. Nonspecific binding was defined by 20 μM methiothepin. Data was analyzed by LIGAND.

	Sf9 cells K_i, nM	Human 5-HT$_{1B}$ 293 cells* $K_{i,nM}$	CHO cells# K_i, nM
Drug			
5-CT	0.55	5.1±0.3	0.9±0.1
methiothepin	1.53	17.0±2.0	3.1±1.0
5-HT	3.66	16.0±1.0	4.0±1.9
methysergide	18.44		7.6±0.6
sumatriptan	64.15	61.0±5.0	11.0±0.7
8-OH-DPAT	106.9	2600±100	634.0±11

Fig. 36. Saturation isotherms of [^{3}H]5-HT specific binding to membranes from cells expressing 5-HT$_{1B}$ and m5-HT$_{1B}$. Bmax (pmol/mg protein) and Ki (nM) values for [^{3}H]5-HT binding were determined by the nonlinear, least square curve fitting program, LIGAND and fitted statistically for one or two site models at $p<0.05$. (A) Saturation curve of [^{3}H]5-HT binding to membranes prepared at 72 hours post-infection. Results shown are from one of three independent experiments and in this experiment Bmax and Kd values were: 5-HT$_{1B}$ (o--o) Bmax = 0.5, K_h = 10, Bmax = 0.5, K_l = 100; m5-HT$_{1B}$ (o-o) Bmax = 0.4, K_h = 9, Bmax =0.7, K_l = 120. (B) Inset, double rectangular hyperbola plot of saturation data as bound (%)/free [^{3}H]5-HT versus bound (%). Specific [^{3}H]5-HT binding was defined as binding inhibited by 20 μM methiothepin. [^{3}H]5-HT binding in the presence of 20 μM methiothepin was detected in cells infected with the wild type baculovirus but represented <10% of specific binding in cells infected with recombinant virus. *Reprinted with permission, from Ng et al., Human serotonin1B receptor expression in Sf9 cells: Phosphorylation, palmitoylation and adenylyl cyclase inhibition, Biochemistry 32, 11727-11733, 1993, American Chemical Society.*

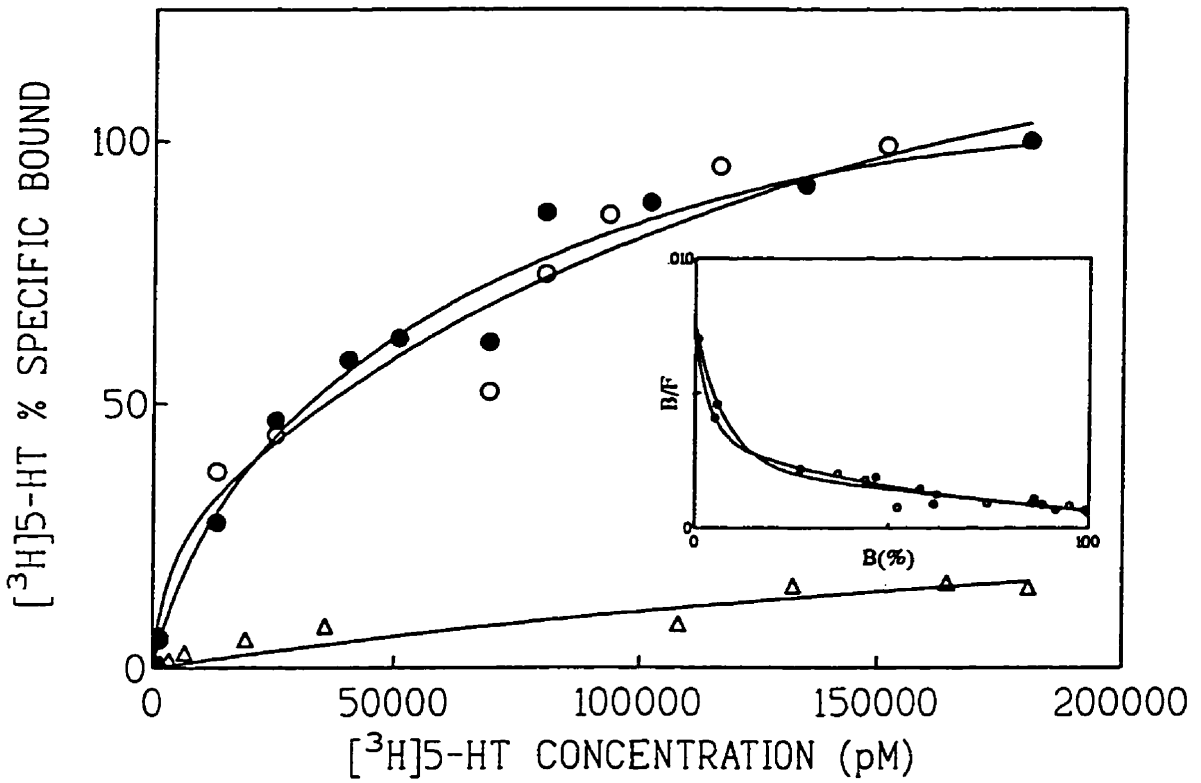
[3H]5-HT % SPECIFIC BOUND
100
50
0
0
50000
100000
150000
200000
[3H]5-HT CONCENTRATION (pM)
B/F
.010
0
B(%)
100

Fig. 37. Effect of guanine nucleotide regulation on [^{3}H]5-HT binding. (A) membranes from cells expressing m5-HT_{1B} at 72 hours post-infection were incubated with ~5 nM [^{3}H]5-HT and increasing concentrations (10^{-12} - 10^{-3} M) of Gpp(NH)p (o-o) or GTPs ($\wedge$--$\wedge$) in the presence and absence of 20 μM methiothepin as described in methods. The data were analyzed by LIGAND and K_i values are listed in Table 1. The results shown are representative of two independent experiments. (B) Membranes from cells expressing m5-HT_{1B} at 72 hours post-infection were incubated with increasing concentrations of [^{3}H]5-HT as described in methods. Specific binding isotherm in the absence (o-o) and presence (o-o) of 150 uM Gpp(NH)p. Specific binding was defined as that displaced by 20 uM methiothepin and is expressed as % specific for comparison. Shown is a representative of two independent experiments. *Reprinted with permission, from Ng et al., Human serotonin1B receptor expression in Sf9 cells: Phosphorylation, palmitoylation and adenylyl cyclase inhibition, Biochemistry 32, 11727-11733, 1993, American Chemical Society.*

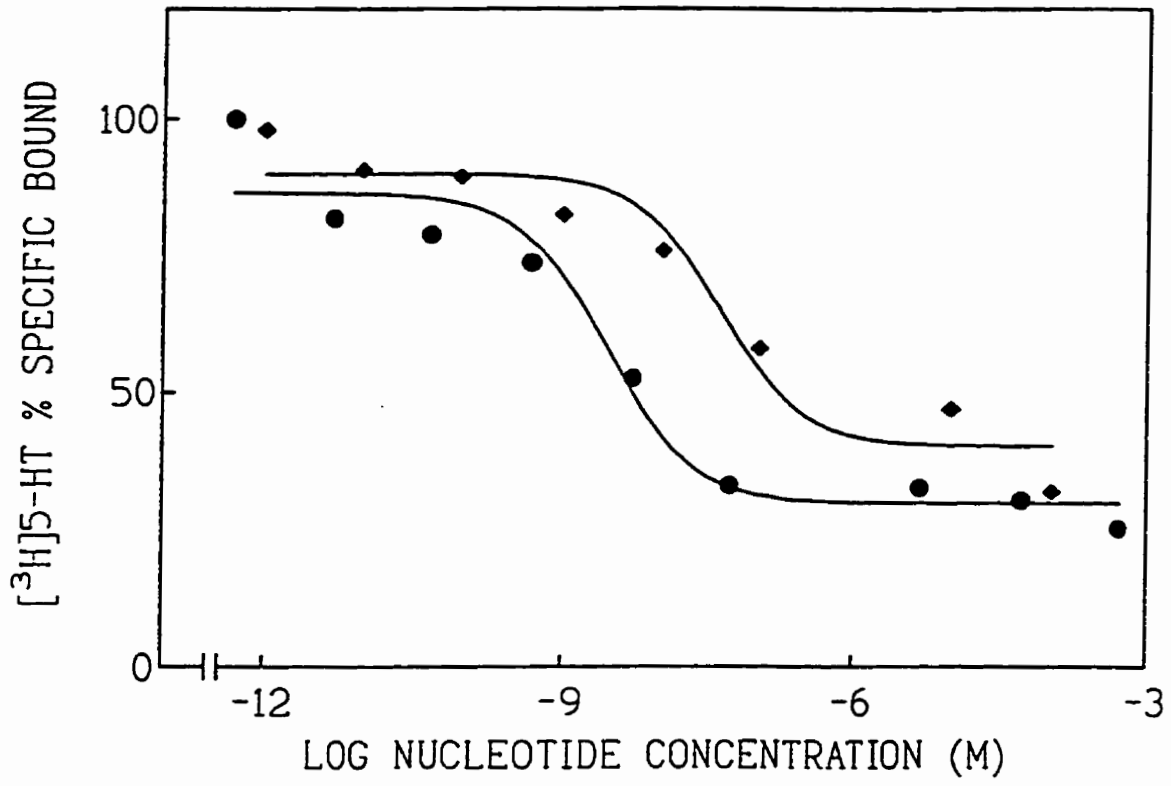
[3H]5-HT % SPECIFIC BOUND
100
50
0
-12
-9
-6
-3
LOG NUCLEOTIDE CONCENTRATION (M)

10.3.2 Pertussis toxin-mediated [^{32}P]ADP-ribosylation of membrane components from Sf9 cells

To demonstrate the presence of pertussis toxin-sensitive proteins in Sf9 cells, toxin-mediated [^{32}P]ADP-ribosylation was studied. Fig. 36A shows an autoradiograph of pertussis toxin-mediated [^{32}P]ADP-ribosylation of membrane components resolved on SDS-PAGE. A phosphorylated protein band at ~41 kDa was present in membrane from wild-type baculovirus-infected cells and in membranes from cells expressing m5-HT1B receptors. This band migrated identically with the ~41 kDa bovine brain G_i/G_o standard, which was also [^{32}P]ADP-ribosylated by pertussis toxin under the same reaction conditions. No labelling was observed in Sf9 membranes in the absence of pertussis toxin (data not shown). Bands were excised, and liquid scintillation counting determined the presence of 6.5 $\pm$ 0.15 pmol (n=3) of ADP-ribosylated protein/mg of Sf9 membrane protein.

10.3.3 Pertussis toxin sensitivity of Sf9 cells and effect on [^{32}P]ADP-ribosylation

To determine whether intact Sf9 cells were pertussis toxin-sensitive, cells were incubated with different concentrations of pertussis toxin prior to toxin-catalyzed [^{32}P]ADP-ribosylation experiments on membrane preparations (Fig. 36B). Autoradiographs of the pertussis toxin-mediated [^{32}P]ADP-ribosylated proteins resolved on SDS-PAGE show that pretreatment of intact cells with the toxin resulted in a dose-dependent decrease in labelling of the ~ 41 kDa substrate present in untreated cells. These results show that Sf9 cells are pertussis toxin sensitive and preincubation of 1 μg/mL toxin is required to inactivate endogenous pertussis toxin substrates. Collectively, the results clearly indicate the presence of a pertussis toxin substrate in Sf9 membranes suggesting it to be highly suitable for expression of other G_i/G_o coupled receptors.

Fig. 36. Pertussis Toxin Assays. (A) Autoradiographs of [^{32}P]ADP-ribosylated Sf9 membrane proteins resolved by SDS-PAGE analysis. In lane (1) 100 ug of Sf9 membrane, lane (2) 100 μg of membrane protein from Sf9 cells expressing m5-HT_{1B}, lane (3) 2.5 pmol bovine brain G_i/G_o. Under our assay conditions, no other pertussis toxin substrate could be resolved. Lane 1 and 2 are autoradiographs from a 2 hour exposure and lane 3 is from an autoradiograph from a 15 minute exposure. The data shown is representative of 3 independent experiments. (B) Sf9 cells expressing m5-HT_{1B} were incubated with 1.5 μg/ml (lane 1), 1.0 μg/ml (lane 2) , 0.5 μg/ml (lane 3) pertussis toxin or left untreated (lane 4) prior to further toxin mediated [^{32}P]ADP-ribosylation. ADP-ribosylation reactions were done as described under methods and proteins were resolved in 12% SDA-PAGE gels under constant current for 18 hours. *Reprinted with permission, from Ng et al., Human serotonin1B receptor expression in Sf9 cells: Phosphorylation, palmitoylation and adenylyl cyclase inhibition, Biochemistry 32, 11727-11733, 1993, American Chemical Society.*

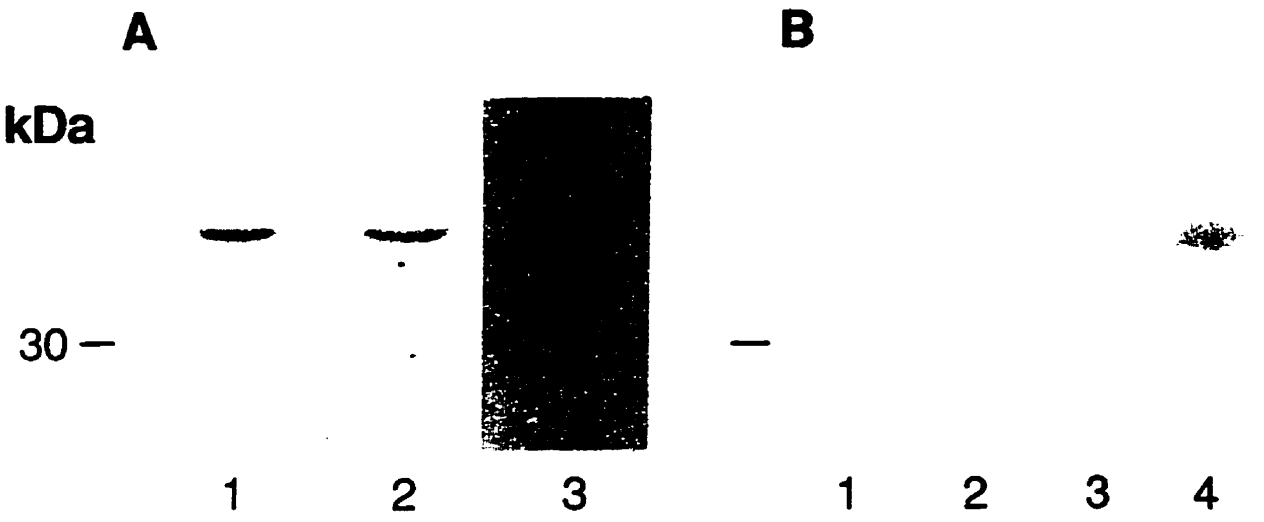
A
B
kDa
30
1
2
3
1
2
3
4

10.3.4 Effect of Pertussis Toxin on the Binding of [^{3}H]5-HT

The [^{3}H]5-HT binding isotherm in nontreated Sf9 cells expressing m5-HT$_{1B}$ is best fitted by LIGAND to a two-site model ($p < 0.05$) with mean Kd values and proportion of receptors in high- and low-affinity states of 40 $\pm$ 14 nM and 2%, and 106 $\pm$ 6 nM and 38% (n=2), respectively. In contrast, the [^{3}H]5-HT binding isotherm in membranes from Sf9 cells expressing m5-HT$_{1B}$ treated with pertussis toxin for 20 hours was shifted toward the right and best fitted by LIGAND to a single affinity site with Kd 185 $\pm$ 9 nM (n=2). These results suggest that m5-HT$_{1B}$ is coupled to a pertussis toxin sensitive G-protein in Sf9 cells.

10.3.5 m5-HT$_{1B}$ Receptor Coupling to Endogenous Adenylyl Cyclase

Agonist binding to G protein-coupled receptors, in most cases, results in the activation of G proteins that initiates down-stream signalling pathways. Although agonist-detected m5-HT$_{1B}$ receptor high affinity state was sensitive to both guanine nucleotides and pertussis toxin suggesting that receptors are coupled to endogenous guanine nucleotide-binding proteins, direct evidence for functional coupling of expressed receptors was sought. As seen in Fig. 37, m5-HT$_{1B}$ receptor activation mediated a 30% inhibition of adenylyl cyclase activity, with a rank order of potency highest for 5-HT followed by 8-OH-DPAT. The IC$_{50}$ values for 5-HT and 8-OH-DPAT inhibition of adenylyl cyclase activity by m5-HT$_{1B}$ receptors were (expressed as an average $\pm$SD) at 1 $\pm$ 8 nM (n=2) and 12 $\pm$ 3 μM (n=2), respectively. Adenylyl cyclase activity was not affected by increasing concentrations of 5-HT in cells infected with the wild type baculovirus (Fig. 37). Interestingly, basal adenylyl cyclase activity in membranes from cells expressing the 5-HT1B receptor was 26% lower than in membranes from wild-type baculovirus-infected cells (Fig. 37). Thus, the expressed receptors appeared to be fully functional and interacted with an endogenous G-proteins.

Collectively the radioligand binding, toxin experiments and adenylyl cyclase data show that Sf9 cells possess the complement of G proteins and effector components necessary for the study of serotonin and other related GPCRs.

10.3.6 Biochemical characterization of the m5-HT_{1B} receptor

Immunoblot analysis of membranes prepared from cells expressing m5-HT_{1B} receptor, using the anti-c-myc 9E10 monoclonal antibody, specifically identified immunoreactive species of ~42 and ~95 kDa (Fig. 38A); similar patterns have been identified for other G-protein receptors expressed in Sf9 cells (Parker et al, 1991, Mouillac et al, 1992). Since the molecular weight of the 5-HT_{1B} receptor from the deduced amino acid sequence is ~ 40 kDa (Jin et al, 1992), it is possible that the immunoreactive species at approximately twice the molecular mass of ~40 kDa represents receptor dimers. Receptor dimer formation has also been suggested for the M1 and M2 receptors expressed in Sf9 cells (Parker et al, 1991), and for the cloned metabotropic glutamate receptor expressed in hamster kidney cells (Pickering et al., 1993). Specific immunoreactive material was absent in membranes prepared from cells infected with the wild-type baculovirus or with the untagged 5-HT_{1B} (Fig. 38A).

The specificity of the 9E10 monoclonal antibody for c-myc in Sf9 cells has been well characterized by in biochemical and desensitization studies utilizing a c-myc epitope tagged β-adrenergic receptor (Mouillac et al, 1992). These studies showed that the 9E10 antibody specifically recognized and immunoprecipitated over 70% of the ligand-bound c-myc tagged receptors. Taken together with our findings, the 9E10 antibody appears to be highly specific for c-myc with no detectable cross-reactivity with endogenous Sf9 proteins, and confirms the appropriateness of the epitope-tagging strategy for the study of m5-HT_{1B} and other GPCRs. Indeed,

immunoprecipitated material from cells expressing m5-HT_{1B} was shown to be specifically and reversibly photoaffinity labelled with the benzazepine [^{125}I]MAB, [3methyl-2-(4'-azidophenyl)-2,3,4,5-tetrahydro-2H-3-benzazepine] (Fig. 38B). Upon exposure to UV light, [^{125}I]MAB was specifically photoincorporated into two major protein species at ~42 and ~95 kilodaltons (lane 2, Fig. 38) as resolved under reducing conditions using SDS-PAGE. Receptor labelling was prevented by incubation with 1 mM 5-HT and was absent in immunoprecipitated material from cells infected with the wild-type baculovirus. Thus, both the ~95 and ~42 kDa proteins were capable of binding ligand supporting the notion that m5-HT_{1B} exist as receptor monomers and dimers.

Following metabolic labelling of the cells with $^{32}P_i$, m5-HT_{1B} was immunoprecipitated using the 9E10 antibody. As shown in Fig. 38C, autoradiography of an SDS-PAGE of the immunoprecipitated material revealed a major phosphorylated species of ~42 kDa and a lesser phosphorylated species at ~95 kDa, corresponding to the mobility and size of the photolabelled receptor monomer and dimer. No phosphorylated immunoreactive proteins were immunoprecipitated from cells infected with the wild-type baculovirus processed in parallel.

Following metabolic labelling with [^{3}H]palmitic acid of Sf9 cells expressing m5-HT_{1B}, immunoprecipitated material was electrophoresed on SDS-PAGE, and subsequent fluorography revealed the presence of ~42 and ~95 kDa radiolabelled bands migrating at equivalent size to that of the photolabelled receptor monomer and dimer (Fig. 38D).

Fig. 37. m5-HT_{1B} receptor mediated agonist inhibition of adenylyl cyclase activity. (A) Effect of increasing concentrations of 5-HT (o-o) and 8-OH-DPAT (o--o) to inhibit forskolin stimulation of adenylyl cyclase in cells infected with recombinant m5-HT_{1B} baculovirus at 72 hours post-infection. Adenlyly cyclase activity was measured as described in methods and is expressed as % maximal response for comparison. (B) Inset, basal and NaF and forskolin stimulated adenlyly cyclase activities at 36 and 72 hours post-infection. The data were analyzed using nonlinear least squares regression. The results shown are representative of 2 independent experiments. *Reprinted with permission, from Ng et al., Human serotonin1B receptor expression in Sf9 cells: Phosphorylation, palmitoylation and adenylyl cyclase inhibition, Biochemistry 32, 11727-11733, 1993, American Chemical Society.*

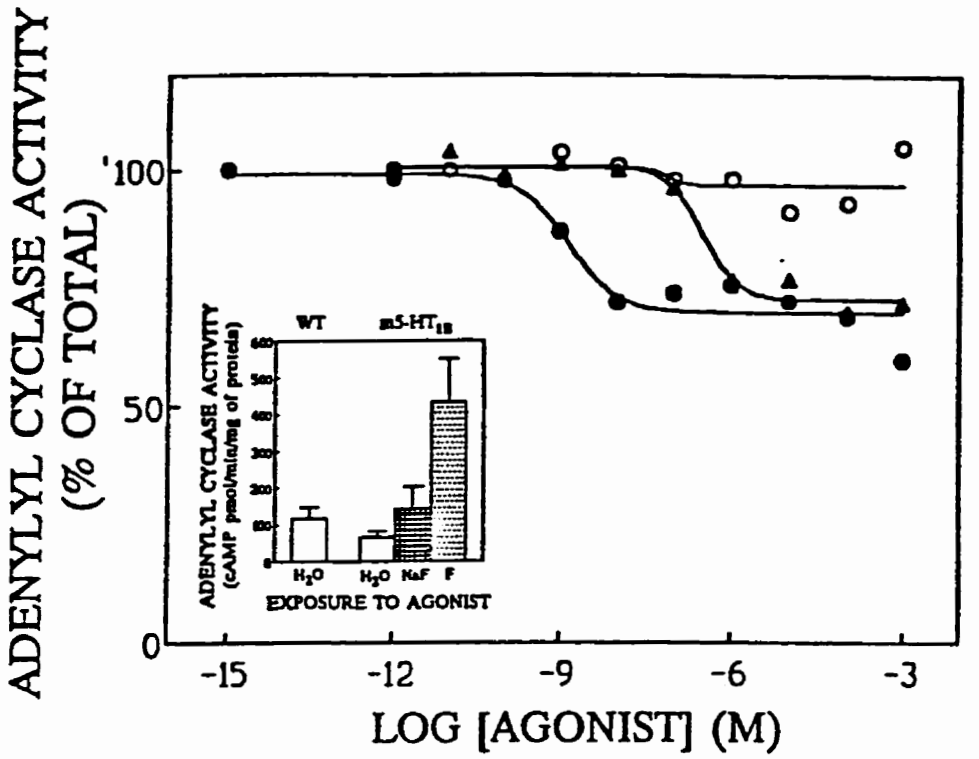
ADENYLYL CYCLASE ACTIVITY
(% OF TOTAL)
100
50
0
-15
-12
-9
-6
-3
LOG [AGONIST] (M)
WT
mS-HT1B
ADENYLYL CYCLASE ACTIVITY
(cAMP pmol/min/mg of protein)
H2O
H2O
NaF
F
EXPOSURE TO AGONIST

Fig. 38. Biochemical Characterization of m5-HT_{1B} receptor. A. 2 mg of protein was solubilized from membranes derived from wild type and m5-HT_{1B} baculovirus infected cells at 72 hours post-infection and immunoprecipitated as described. Immunoprecipitated material was photolabelled with [^{125}I]MAB and visualized by autoradiography. Lane 1, sample from cells infected with wild type baculovirus. Lane 2, sample from cells infected with m5-HT_{1B} in absence and lane 3 in presence of 1 mM 5-HT. The autoradiogram shown is from a 7-day exposure and is representative of 2 independent experiments. Mobility of protein molecular weight standards (Amersham) is indicated on left. B. Identification of Immunoreactive m5-HT_{1B} in Sf9 Membranes. Membranes (200 μg protein) were prepared at 72 hours post-infection from cells infected with wild type baculovirus (lane 1), and cells infected with m5-HT_{1B} baculovirus (lane 2), and cells infected with the untagged 5-HT_{1B} baculovirus (lane 3). Membranes were solubilized in SDS buffer, electrophoresed, and electroblotted onto nitrocellulose as described in methods. Immunoreactivity was revealed with a goat anti-mouse IgG conjugated to alkaline phosphatase. C. Phosphorylation of m5-HT_{1B}. The figure shows an autoradiogram (7 day exposure) of 9E10 immunoprecipitated m5-HT_{1B} solubilized from membranes prepared from Sf9 cells infected with m5-HT_{1B} (lane 2) or wild type baculovirus prelabelled with carrier free ^{32}P (lane 1). This figure is representative of two independent experiments. D. Palmitoylation of m5-HT_{1B}. Fluorograph (3 weeks exposure) following immunoprecipitation from cells prelabelled with [^{3}H]palmitic acid at 72 hours post-infection. Sample from cells infected with m5-HT_{1B} (lane 2) and sample from cells infected with wild type baculovirus (lane 1). Sample from cells infected with m5-HT_{1B} following hydroxylamine treatment as described in methods (lane 3). This figure is representative of 4 independent experiments. *Reprinted with permission, from Ng et al., Human serotonin1B receptor expression in Sf9 cells: Phosphorylation, palmitoylation and adenylyl cyclase inhibition, Biochemistry 32, 11727-11733, 1993, American Chemical Society.*

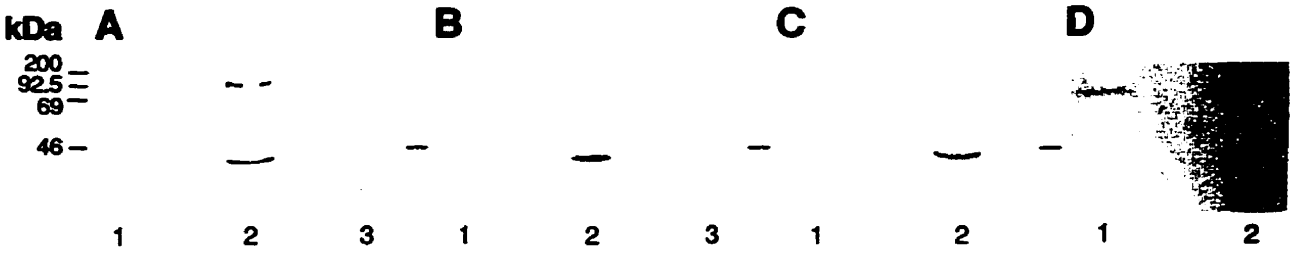
kDa
A
B
C
D
200
92.5
69
46
1
2
3
1
2
3
1
2
1
2

10.4 Discussion

We have employed the baculovirus/Sf9 cell system to successfully express and study the biology, function, and posttranslational modification of the human 5-HT_{1B} receptor using a c-myc epitope-tagged receptor expressed in the absence of the pharmacologically indistinguishable 5HT1D receptor. The strategy of epitope-tagging has provided an opportunity to thoroughly investigate the characteristics of the 5HT1B receptor for which no specific antibodies are available. Further, these studies using the 5-HT1B receptor as a model for other GPCRs enabled us to establish and validate the suitability of this model system for the study of GPCRs at the molecular level.

Saturation binding to expressed serotonin receptors showed advantageously high signal to noise ratio in the Sf9 cells promising similar quality of results for other GPCRs expressed in this cell line. Analysis of the saturation binding isotherm of [^{3}H]5-HT to membranes from Sf9 cells infected with recombinant virus fitted a two-site model, suggesting that the expressed m5-HT_{1B} receptor, detected in two affinity forms, interacted with endogenous G-proteins. This was suggested by the guanine nucleotide regulation of [^{3}H]5-HT binding to the high affinity state of the receptor. The binding of guanine nucleotides to G-proteins is thought to cause dissociation of the G-protein from the receptor, thus converting the receptor to a state with low agonist affinity. Similarly, guanine nucleotide sensitivity of agonist binding has been described for other GPCRs expressed in Sf9 cells (Kwatra et al., 1993, Mills et al., 1993).

Further confirmation of receptor-G protein interaction was provided by the decrease (loss) of [^{3}H]5-HT binding to the high affinity receptor state by pertussis toxin and suggested the presence of a pertussis toxin-sensitive G-proteins in Sf9 cells. Pertussis toxin has been shown to ADP-ribosylate and uncouple the α subunits of G_i and G_o from their respective cognate receptors

(Sternweis et al, 1984, Van Dop et al, 1984). A ~41 kDa substrate for pertussis toxin mediated ADP-ribosylation was identified in Sf9 cells that co-migrated with bovine G_i/G_o standards. The expressed m5-HT_{1B} appears then to be coupled to endogenous pertussis toxin-sensitive G-proteins of the G_i or G_o subtype to mediate a dose-dependent agonist inhibition of adenylyl cyclase activity in Sf9 cells.

A critical examination of the pharmacological profile (agonist and antagonist binding) of the expressed receptors was next conducted since any relevance of the proposed studies to physiological processes should require that expressed receptors were pharmacologically similar to neuronal counterparts. Of the ligands tested for the expressed 5-HT_{1B} receptor, 5-CT (a 5-HT_1 agonist) had the highest affinity, and 8-OH-DPAT (a 5-HT_{1A} subtype selective agonist) had the lowest affinity. The data indicated that the expressed 5-HT_{1B} receptors were pharmacologically similar to the cloned human neuronal 5-HT_{1B} (Jin et al, 1992). Additionally, an important finding of this study suggested that GPCRs expressed in Sf9 cells bind ligand and are biologically active and functionally coupled.

The next step was to discern whether Sf9 cells generated immunoreactive recombinant receptors, and whether antibodies were specific with a high signal to low noise background ratio. A monoclonal antibody directed against c-myc specifically identified the expressed c-myc epitope-tagged $5HT_{1B}$ receptors not present in wild type cells demonstrating the appropriateness of the epitope-tagging strategy for the immunological detection and purification of other GPCRs in this cell line.

Agonist-induced desensitization has been best characterized for the β_2-adrenergic receptor coupled adenylyl cyclase system and shown to involve post-translational processes such

as phosphorylation (reviewed by Perkins et al., 1991). Consensus sequences for PKA and PKC phosphorylation are present in the primary structure of 5-HT_{1B} (Jin et al, 1991), and immunoprecipitated material (co-migrating with photolabelled receptor species) from $^{32}P_i$ metabolically labelled Sf9 cells expressing m5-HT_{1B} was shown to be phosphorylated. Additionally, a cysteine residue in the carboxyl terminus of the β_2-adrenergic receptor has been shown to be a site for palmitoylation and shown to be important for functional coupling. We also show that the m5-HT_{1B} in Sf9 cells is post-translationally modified with palmitic acid. Palmitoylation may involve the cysteine residue (Cys^{348}) in the carboxy tail since we have previously shown that the Cys^{341} located in the carboxy tail of β2-AR is the site for palmitoylation (O'Dowd et al, 1989). According to the proposed model (Fig. 33), anchorage of a palmitate residue attached to Cys^{348} in the receptor would impose a loop structure of the amino terminal region of the carboxy tail forming a small 4th intracellular loop which may regulate GRK accessibility and receptor phosphorylation. Thus, the 5-HT_{1B} receptor is phosphorylated and palmitoylated suggesting that these posttranslatinal modifications may be involved in receptor processes such as desensitization. We have provided evidence that the m5-HT_{1B} receptors are coupled to a major pertussis toxin sensitive G-protein in Sf9 cells and mediate the inhibition of adenylyl cyclase. We have also provided the first evidence that this serotonin receptor has been purified by immunoprecipitation and post-translationally modified by phosphate and palmitate residues. Finally, these studies also indicate the usefulness of epitope-tagging strategy for the purification of GPCRs to which no specific receptor antisera is available and show that Sf9 cells are able to sustain posttranslational modifications. The results of this research indicate the suitability of the baculovirus/Sf9 model system for evaluating the pharmacological and biochemical properties of the important class of

G-protein coupled receptors.

IMAGE EVALUATION
TEST TARGET (QA-3)

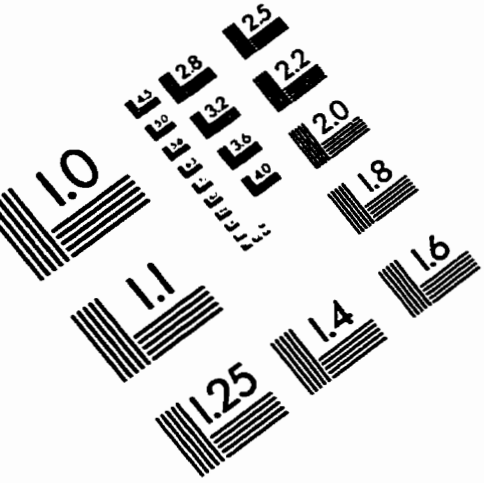

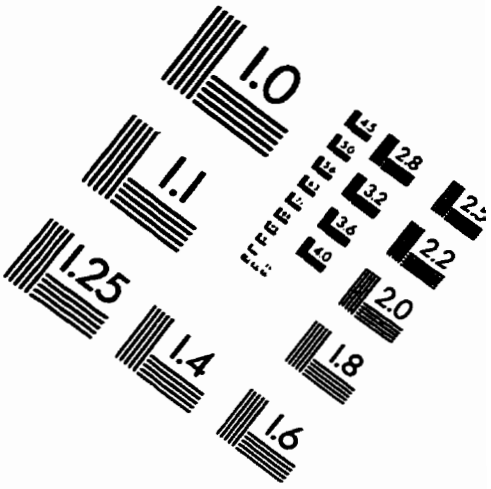

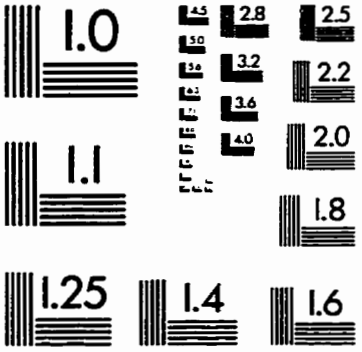

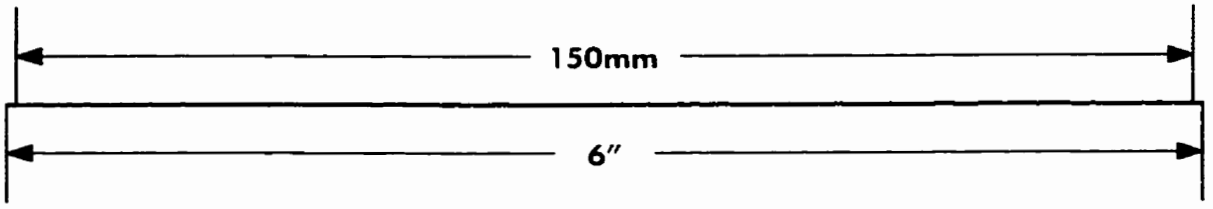

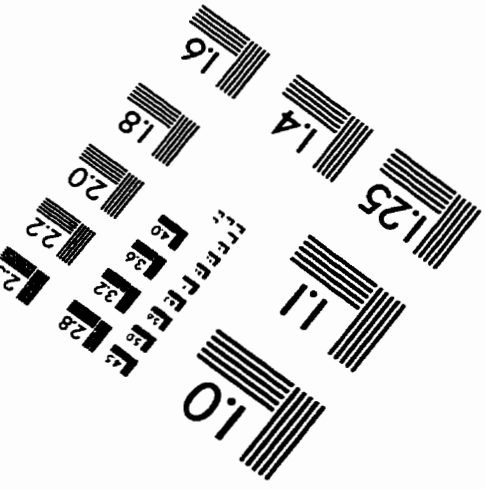

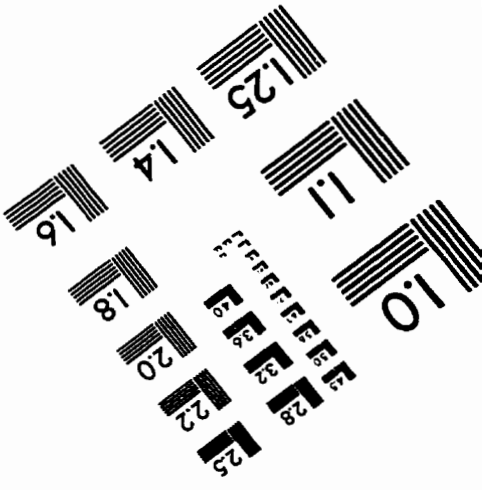

APPLIED IMAGE, Inc
1653 East Main Street
Rochester, NY 14609 USA
Phone: 716/482-0300
Fax: 716/288-5989